

<title>

Benjamin Yu Hang Bai

2020-05-11 15:10:52+01:00

Contents

List of Figures	vii
List of Tables	xi
1 Transcriptomic response to influenza A (H1N1)pdm09 vaccine	1
1.1 Introduction	1
1.1.1 Seasonal and pandemic influenza	1
1.1.2 Quantifying immune response to influenza vaccines	2
1.1.3 Systems vaccinology of influenza vaccines	2
1.1.4 The Human Immune Response Dynamics (HIRD) study	3
1.1.5 Chapter summary	4
1.2 Methods	4
1.2.1 Existing HIRD study data and additional data	4
1.2.2 Computing baseline-adjusted measures of antibody response	5
1.2.3 Genotype data generation	6
1.2.4 Genotype data preprocessing	6
1.2.5 Computing genotype principal components as covariates for ancestry	10
1.2.6 RNA-seq data generation	10
1.2.7 RNA-seq quantification and filtering	13
1.2.8 Array data preprocessing	15
1.2.9 Differential gene expression	15
1.2.9.1 Per-platform differential gene expression model	18
1.2.9.2 Choice of differential gene expression meta-analysis method	20

1.2.9.3	Prior for between-studies heterogeneity	21
1.2.9.4	Prior for effect size	21
1.2.9.5	Evaluation of priors	22
1.2.9.6	Multiple testing correction	22
1.2.10	Gene set enrichment analysis using blood transcription modules	22
1.3	Results	24
1.3.1	Extensive global changes in expression after vaccination	24
1.3.2	Innate immune response at day 1 post-vaccination . .	24
1.3.3	Adaptive immune response at day 7 post-vaccination .	26
1.3.4	Expression signatures associated with antibody response	26
1.3.5	Identifying expression signatures for predicting anti- body response [probably cut this section and just add to discussion]	30
1.4	Discussion	30
2	Genetic factors affecting Pandemrix vaccine response	35
2.1	Introduction	35
2.1.1	Genetic factors affecting influenza vaccine response . .	35
2.1.2	Response expression quantitative trait loci for seasonal influenza vaccination	36
2.1.3	Chapter summary	36
2.2	Methods	37
2.2.1	Genotype phasing and imputation	37
2.2.2	Overall strategy for detecting reQTLs	37
2.2.3	Controlling for population structure with linear mixed models	39
2.2.3.1	Estimation of kinship matrices	39
2.2.4	Additional eQTL-specific expression preprocessing . .	40
2.2.5	Estimation of cell type abundance from expression . .	41
2.2.6	Finding hidden confounders using factor analysis . .	47
2.2.7	eQTL mapping per timepoint	50
2.2.8	Joint eQTL analysis across timepoints	50
2.2.9	Defining shared and response eQTLs	53
2.2.10	Replication of eQTLs in a reference dataset	53
2.2.11	Genotype interactions with cell type abundance	54

2.2.12 TODO Statistical colocalisation	56
2.3 Results	56
2.3.1 Mapping reQTLs to Pandemix vaccination	56
2.3.2 Characterising reQTLs post-vaccination	58
2.3.3 Genotype by cell type interaction effects	58
2.3.4 TODO Genotype by platform interaction effects . . .	61
2.3.5 TODO Colocalisation of reQTLs with known <i>in vitro</i> condition-specific immune eQTLs	61
2.4 Discussion	62
A Supplementary Materials	67
A.1 Chapter 2	67
A.2 Chapter 3	67
A.3 Chapter 4	68
Bibliography	69
List of Abbreviations	85

CONTENTS

CONTENTS

List of Figures

1.1	Data types, timepoints, and sample sizes. Individuals were vaccinated after day 0 sampling. Antibodies to the vaccine strain were measured by haemagglutination inhibition (HAI) and microneutralisation (MN) assays. Array and RNA-sequencing (RNA-seq) gene expression measured in the peripheral blood mononuclear cell (PBMC) compartment.	5
1.2	Comparison of titre response index (TRI) to HAI (left column) and MN (right column) titres and binary responder/non-responder status (colored) in 166 Human Immune Response Dynamics (HIRD) individuals. Row 1: baseline titres are positively correlated to post-vaccination titres. Row 2: baseline titres are negatively correlated to fold change. Row 3: TRI regresses out the correlation between baseline titre and response. Row 4: TRI is still comparable in ordering to binary response status.	7
1.3	Distribution of TRI, stratified by platform used to measure expression.	8
1.4	Sample filters for missingness and heterozygosity rate. Samples outside the central rectangle were excluded.	9
1.5	HIRD samples (cyan) projected onto principal component (PC)1 and PC2 axes defined by principal component analysis (PCA) of HapMap 3 samples. The first two PCs separate European (CEU, upper-right) from Asian (CHB and JPT, lower-right) and African (YRI, lower-left) individuals.	11
1.6	FastQC sequence quality versus read position for HIRD RNA-seq samples.	11
1.7	FastQC sequence duplication levels for HIRD RNA-seq samples.	12

1.8	FastQC GC profile for HIRD RNA-seq samples.	12
1.9	Distributions of removed short ncRNA and globin counts as a proportion of total counts in RNA-seq samples.	14
1.10	Distribution of the proportion of samples in which genes were detected (non-zero expression). Many genes are not detected in any samples. Vertical line shows 5% threshold below which genes were discarded.	14
1.11	Distribution of gene expressions for RNA-seq samples before and after filtering no expression and low expression genes. Vertical line shown at counts per million (CPM) = 0.5 threshold.	15
1.12	Raw foreground intensities for 173 HIRD array samples. Colored by array processing batch.	16
1.13	Array intensity estimates after VSN normalisation and collapsing of probes to genes. Colored by array processing batch.	17
1.14	First four PCs in the HIRD expression data, colored by platform and batch (left), and timepoint (right).	19
1.15	Gamma prior for τ used for bayesmeta (blue), compared to the empirical distribution of per-gene frequentist metafor::rma estimates for τ , for the day 1 vs. baseline effect (small estimates of $\tau < 0.01$ excluded). Empirical log-normal fit also shown (red).	23
1.16	Normal prior for μ used for bayesmeta (blue), compared to the empirical distribution of per-gene frequentist metafor::rma estimates for τ , for the day 1 vs. baseline effect. The non-scaled normal fit is shown (black), as well as a Cauchy fit (red). . .	23
1.17	Normalised gene expression for genes differentially expressed between any pair of timepoints ($lfsr < 0.05$, absolute fold change > 1.5) across HIRD samples, clustered by gene (Manhattan distance metric).	25
1.18	Transcriptomic modules significantly up or downregulated post-vaccination. Size of circle indicates effect size. Color of circle indicates significance and direction of effect (red = upregulation, blue = downregulation).	27
1.19	DGE effect sizes estimated in array vs. RNA-seq. Significance colored by frequentist random effects meta-analysis FDR < 0.05 . Genes with day 7 expression associated with responder/non-responder status in ¹⁸ are circled for that contrast.	28

1.20 DGE effect sizes estimated in array vs RNA-seq. Significance colored by Bayesian random effects meta-analysis lfsr < 0.05. Genes with day 7 expression associated with responder/non-responder status in ¹⁸ are circled for that contrast.	28
1.21 Transcriptomic modules enriched in genes with expression associated with antibody response (TRI) at each day. Size of circle indicates effect size. Color of circle indicates significance and direction of effect (red = expression positively correlated with TRI, blue = negative).	29
2.1 Simulated log scale expression in two conditions for six genes (columns) representing six different scenarios: Scenario 0 has no expression quantitative trait locus (eQTL), scenario 1 is a shared eQTL ($\beta = 1$), scenario 2 is a response expression quantitative trait locus (reQTL) where β increases from 0 to 1, scenario 3 is a reQTL where β increases from 0 to 2, scenario 4 is a reQTL where β increases from 1 to 2, and scenario 6 is a reQTL where β increases from 1 to 4. Rows represent the effect of different expression transformations across samples, conducted both within condition, and including both conditions.	42
2.2 Standardised xCell enrichment scores for seven PBMC cell types in array samples.	44
2.3 Standardised xCell enrichment scores for seven PBMC cell types in RNA-seq samples.	45
2.4 Quality of representation (\cos^2) for each input variable in each PC dimension after PCA of xCell scores. Higher \cos^2 represents higher contribution of that variable to that dimension.	46
2.5 Correlation between standardised xCell scores and normalised fluorescence-activated cell sorting (FACS) measurements for a similar immune subset, in the subset of individuals with FACS data.	48
2.6 Correlation of PEER factors to known factors and other possible covariates. Note that PEER factors are not constrained to be orthogonal, so correlations to known factors are expected.	49

2.7	Number of significant eGenes detected on chromosome 1 (hierarchical Bonferroni-Benjamini-Hochberg (BH) FDR < 0.05) as a function of the number of PEER factors included as covariates k.	51
2.8	Clustering of within-timepoint Z scores in the strong mashr subset (random sample of 10000/45962 tests), confirming the presence of strong condition-specific effects.	52
2.9	Effect of HIRD lfsr threshold on GTEx whole blood replication rate (π_1), number of p values used to compute π_1 , and maximum p value among those p values; for shared and reQTL called from the array-only, RNA-seq-only and mega-analysis pipelines. Shaded region for π_1 represents the 5th-95th percentile range of 1000 bootstraps.	55
2.10	Summary of eQTL mapping results at 13570 genes-lead eQTL pairs, with intersections based on significance (lfsr < 0.05). Counts of shared eQTLs and reQTLs; and distribution of INFO score, min MAF across timepoints, and max PVE across timepoints for those lead variants are shown above each intersection.	57
2.11	Z score for difference in effect vs. day 0, of lead eQTLs for all eGenes significant at either day 1 or day 7; versus distance of the lead SNP to the TSS. Direction of effect is aligned so that the beta at day 0 is positive. Points with positive z score are magnified effects post-vaccination, points with negative z scores are dampening and opposite sign effects.	59
2.12	<i>ADCY3</i> , strongest reQTL at day 1.	60
2.13	<i>SH2D4A</i> , strongest reQTL at day 7. Top: Array and RNA-seq expression before merging with ComBat for mega-analysis. Bottom: eQTL effects at each timepoint condition in the mega-analysis.	60
2.14	Multi-trait colocalisation of HIRD reQTL signal at <i>ADCY3</i> (500 Kb window), with QTL studies from IHEC, BLUEPRINT, eQTL Catalogue, and GWAS Catalogue. Plots are colored by colocalised cluster. Black indicates non-colocalised datasets. .	63

List of Tables

1.1	Sample descriptive statistics	33
1.2	HIRD batch balance	34

Chapter 1

Transcriptomic response to influenza A (H1N1)pdm09 vaccine

1.1 Introduction

1.1.1 Seasonal and pandemic influenza

Influenza is an infectious disease, generally seasonal, caused by the influenza A and influenza B viruses in humans. Influenza A viruses circulate not only in humans, but also in a variety of other birds and mammal hosts. They are classified into antigenically-distinct subtypes by the combination of two surface proteins: haemagglutinin (HA) and neuraminidase (NA)¹.

There are three classes of influenza vaccine against seasonal strains in use: inactivated vaccines, live attenuated influenza vaccines (LAIVs), and recombinant HA vaccines. These vaccines confer a degree of strain-specific protection, primarily by raising serum antibodies against the HA and/or NA proteins. Antigenic drift, the accumulation of mutations in these surface proteins over time, necessitates the annual reformulation of seasonal influenza vaccines to reflect circulating strains^{2,3}. On occasion, a novel subtype against which the majority of the population is immunologically naive can arise suddenly (antigenic shift), often from zoonotic origins. A recent example occurred in 2009, when an outbreak of a novel swine-origin strain, eventually termed influenza A (H1N1)pdm09, resulted in a global

why? for diff groups of people

CHAPTER 1. TRANSCRIPTOMIC RESPONSE TO INFLUENZA A

1.1. INTRODUCTION

(H1N1)PDM09 VACCINE

add a point that
2009h1n1 is now circu-
lating seasonally, this is a
common trend

pandemic, the fourth to occur in the last 100 years¹.

1.1.2 Quantifying immune response to influenza vaccines

Add specific section about
pandemrix, it's correlates
of protection, it's durabil-
ity? or maybe in methods

Here, add few points
about the immunological
response to adjuvanted
TIVs i.e. what happens af-
ter Pandemrix admin?
Involve the innate ->
B/CD4T response. Goto
plotkins

The 2009 pandemic motivated the rapid development, trialing, and licensing of several novel vaccines⁴. Immune response to influenza vaccines in clinical trials is evaluated by assays that measure levels of antibodies specific to the vaccine strain(s). The **haemagglutination inhibition (HAI)** assay measures the levels of serum antibodies specific to the **HA** surface protein. The related **microneutralisation (MN)** assay measures levels of antibodies (which may or may not be anti-**HA**) that neutralise the infectivity of the virus in cell culture⁵. Values from these assays can be compared against thresholds for known correlates of protection: markers that associate with whether an individual is protected from the disease. For example, **HAI** titres are regarded as the primary correlate of protection for inactivated influenza vaccines. Targets that regulatory agencies expect a licensed vaccine to meet are based on thresholds such as the proportion of trial individuals achieving **HAI** titres ≥ 40 and seroconversion (≥ 4 -fold increase in titres)^{6,7}.

1.1.3 Systems vaccinology of influenza vaccines

is there a more recent
review?

Although **HAI** titres are accepted as established correlates for inactivated seasonal influenza vaccines, they fail to account for alternate mechanisms such as T cell-mediated protection, and correlates for **LAI** and pandemic influenza vaccines are less reliable². For novel and emerging diseases, there may be no prior knowledge of robust correlates to use in the vaccine development process. In response, the last decade has seen the rise of systems vaccinology studies: the analysis of high-dimensional data measured using multiple technologies in vaccinated individuals, in order to characterise response to vaccination at multiple levels of the biological system⁸. Such information helps elucidate a vaccine's mode of action, discover "molecular signatures" predictive of vaccine safety and efficacy, and has become an increasingly important part of the modern vaccine development chain^{9,10}.

Various systems vaccinology studies of seasonal influenza vaccines have been conducted, taking longitudinal measurements pre-vaccination, and commonly at some subset of days 1, 3, 7, and 28 post-vaccination. These measurements can be correlated to changes in antibody titres after vacci-

nation to define signatures of antibody response with potential utility as correlates of protection. One of the earliest such studies by Zhu et al.¹¹ found that expression of type 1 interferon-modulated genes was a signature of response to **LAIV**. An expression signature including *STAT1*, *CD74*, and *E2F2* correlated with serum antibody titres after vaccination with trivalent inactivated influenza vaccine¹²; kinase CaMKIV expression is also a strong predictor¹³, as are genes related to B cell proliferation¹⁴.

For these studies of seasonal influenza vaccines in adults, responses tend to be biased by recall from past vaccination or infection^{12,15}. There have also been few studies of adjuvanted influenza vaccines, despite their superior efficacy in comparison to non-adjuvanted counterparts^{16,17}.

1.1.4 The Human Immune Response Dynamics (HIRD) study

The **Human Immune Response Dynamics (HIRD)** study conducted by Sobolev *et al.* [18] was conceived with the above limitations in mind. The vaccine studied was Pandemrix, an AS03-adjuvanted, split-virion, inactivated vaccine against the influenza A (H1N1)pdm09 strain, for which the majority of the cohort at the time would be unlikely to have immunological memory. A total of 178 individuals were vaccinated with a single dose of Pandemrix, and longitudinal transcriptomic, cellular, antibody titre, and adverse event phenotypes were collected. Gene expression was profiled using a microarray, and **differential gene expression (DGE)** analyses detected genes associated with both myeloid and lymphoid effector functions upregulated at day 1, most prominently for genes associated with interferon responses. These early myeloid responses were consistent with studies of unadjuvanted seasonal influenza vaccines, but the interferon gamma-associated lymphoid response was unique to this adjuvanted vaccine.

Genes related to plasma cell development and antibody production were more highly expressed in 23 vaccine responders compared to 18 non-responders at day 7 post-vaccination. However, due to high variability among the vaccine non-responders in variables such as baseline antibody titres, a consensus predictive model that segregated the two groups could not be built, even considering other measures such as frequencies of immune cell subsets and serum cytokine levels, suggesting there was no single contributing factor that led to vaccine failure. This is in contrast to several studies of seasonal influenza vaccines, where certain expression signatures are able to predict

make sure gap and how it
is filled is empded enough

vaccine response even pre-vaccination^{19–22}.

1.1.5 Chapter summary

Transcriptomic measurements in the original **HIRD** study were restricted to a relatively small number (46/178) of individuals, potentially limiting power to detect expression signatures associated with antibody response. In addition, the responder vs. non-responder phenotype definition used does not account for variation in pre-existing baseline titres, and the binary definition can result in loss of statistical power^{23–25}.

In this chapter, I integrate the original microarray data from **HIRD** with **RNA-sequencing (RNA-seq)** data on a larger subset (75) of newly sequenced individuals from the same cohort using Bayesian random-effects meta-analysis. The overall pattern of expression over time from my meta-analysis agrees with the patterns from the original study¹⁸, with transient innate immune response at day 1 post-vaccination, progressing to adaptive immune response by day 7.

needs 1 more punchline
sentence here

From existing **HAI** and **MN** data, I compute a baseline-adjusted, continuous measure of antibody response to vaccination, the **titre response index (TRI)**¹². Effect sizes of genes with expression that correlated with **TRI** were very dependent on measurement platform (array or **RNA-seq**), and no robust hits were detected in the meta-analysis. Leveraging the greater power that rank-based gene set enrichment analyses affords, I find modules of coexpressed genes that correlate with antibody response, with the strongest effects observed for adaptive immune modules at day 7, but also in inflammatory modules at baseline.

1.2 Methods

1.2.1 Existing HIRD study data and additional data

The design of the **HIRD** study is described in¹⁸. In brief, the study enrolled 178 healthy adult volunteers in the UK. The vaccine dose was administered after blood sampling on day 0; five other longitudinal blood samples were taken on days -7, 0, 1, 7, 14 and 63. Serological responses were measured on days -7 and 63 using the **HAI** and **MN** assays, and various subsets of the cohort were also profiled for serum cytokine levels (Luminex panel, days -7,

0, 1 and 7), immune cell subset counts (fluorescence-activated cell sorting (**FACS**) panels, all days), and peripheral blood mononuclear cell (**PBMC**) gene expression (microarray, days -7, 0, 1 and 7). The gene expression microarrays were performed in two batches.

In addition to the existing data, array genotypes were generated for 169 individuals; and **RNA-seq** data for 75 individuals at days 0, 1, and 7. The sets of individuals with gene expression assayed by microarray and **RNA-seq** is disjoint, as no biological material for RNA extraction remained for the microarray individuals. An overview of datasets is shown in Fig. 1.1.

1.2.2 Computing baseline-adjusted measures of antibody response

In¹⁸, Pandemrix responders were defined as individuals with ≥ 4 -fold titre increases in either the **HAI** or **MN** assays. This is a threshold for seroconversion set out by the U.S. Food and Drug Administration²⁶, and is used in many studies of seasonal influenza vaccines⁹. The responder status for 166 individuals with both **HAI** and **MN** titres available at baseline (day -7) and post-vaccination (day 63) were computed according to this definition. However,¹⁸ noted there was heterogeneity in the baseline titres of non-responders, citing “glass ceiling” non-responders whose high baseline titres made the fixed 4-fold threshold hard to achieve. Dichotomisation of continuous response variables can also result in loss of statistical power^{23,25}.

atm I'm not using R/NR.
wording here implies I am

cite appropriate subfigures here

To address these concerns, I computed the **TRI** as defined in Bucasas *et al.* [12]. For each assay, a linear regression was fit with the \log_2 day 63/day -7

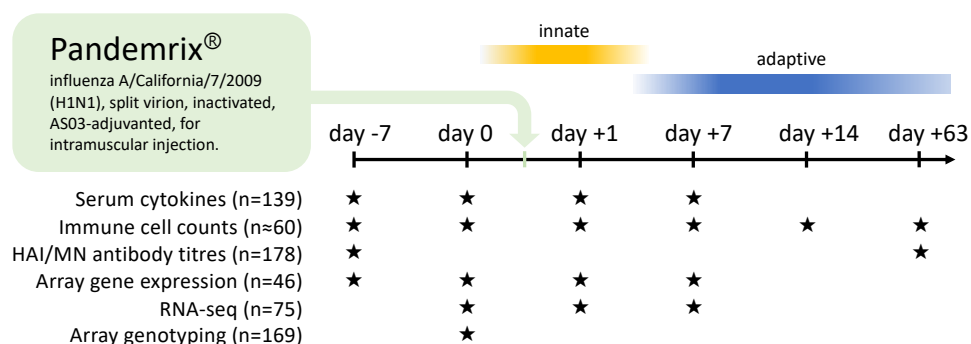


Figure 1.1: Data types, timepoints, and sample sizes. Individuals were vaccinated after day 0 sampling. Antibodies to the vaccine strain were measured by **HAI** and **MN** assays. Array and **RNA-seq** gene expression measured in the **PBMC** compartment.

titre fold change as the response, and the \log_2 day -7 baseline titre as the predictor. The residuals from the two regressions were each standardized to zero mean and unit variance, then averaged. The **TRI** expresses a continuous measure of change in antibody titres across both assays post-vaccination, compared to individuals with a similar baseline titre, and remains comparable to the binary 4-fold change definition ([Fig. 1.2](#)).

cite appropriate subfigures here, after adding proper subfigure labels

Descriptive statistics for the 114 individuals with both gene expression and antibody titre data are presented in [Table 1.1](#). Although the proportion of responders between array (32/44) and **RNA-seq** (59/70) individuals is similar ($p = 0.1551$, Fisher's exact test), the variance of **TRI** in array individuals is higher ($p = 0.0002098$, Levene's test), suggesting more extreme antibody response phenotypes are present ([Fig. 1.3](#)). The cause of this is unknown, there is a possibility that individuals with more extreme phenotypes were prioritised for array transcriptomics in the original **HIRD** study*.

Add to collab note that extractions were done at KCL

1.2.3 Genotype data generation

DNA was extracted from frozen blood using the Blood and Tissue DNeasy kit (Qiagen), and genotyping was performed using the Infinium CoreExome-24 BeadChip (Illumina). In total, 192 samples from 176 individuals in the HIRD cohort were genotyped at 550601 markers, including replicate samples submitted for individuals where extracted DNA concentrations were low.

1.2.4 Genotype data preprocessing

Using PLINK (v1.90b3w), genotype data underwent the following quality control procedures to remove poorly genotyped samples and markers: max marker missingness across samples < 5%, max sample missingness across markers < 1%, max marker heterozygosity rate within 3 standard deviations of the mean (threshold selected visually to exclude outliers, [Fig. 1.4](#)), removal of markers that deviate from Hardy–Weinberg equilibrium (–hwe option, $p < 0.00001$).

To exclude highly-related individuals and deduplicate replicate samples, pairwise kinship coefficients were computed on **minor allele frequency (MAF)** < 0.05 pruned genotypes using KING (v1.4). For each pair of samples with

*Personal communication with authors.

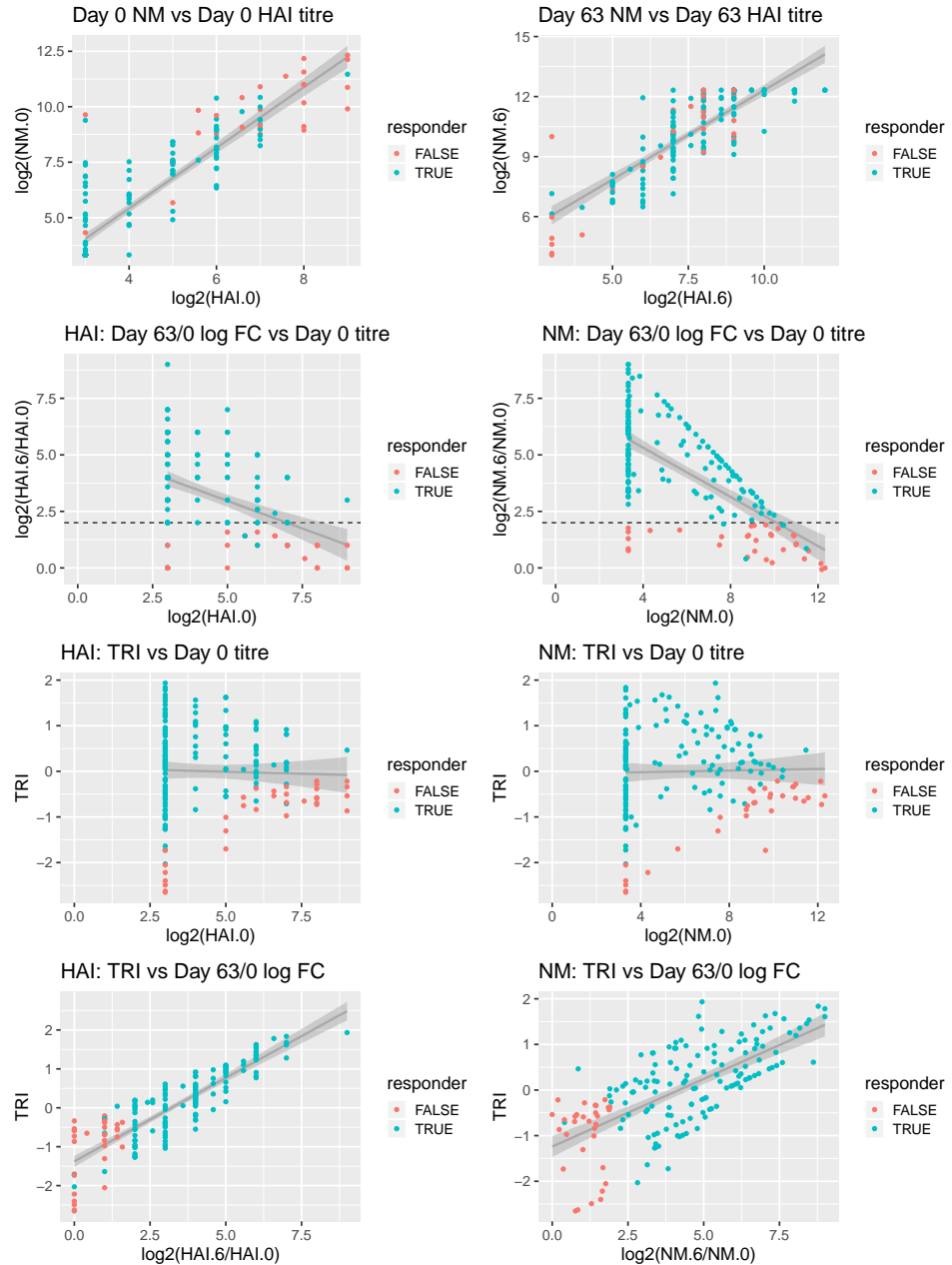


Figure 1.2: Comparison of **TRI** to **HAI** (left column) and **MN** (right column) titres and binary responder/non-responder status (colored) in 166 **HIRD** individuals. Row 1: baseline titres are positively correlated to post-vaccination titres. Row 2: baseline titres are negatively correlated to fold change. Row 3: **TRI** regresses out the correlation between baseline titre and response. Row 4: **TRI** is still comparable in ordering to binary response status.

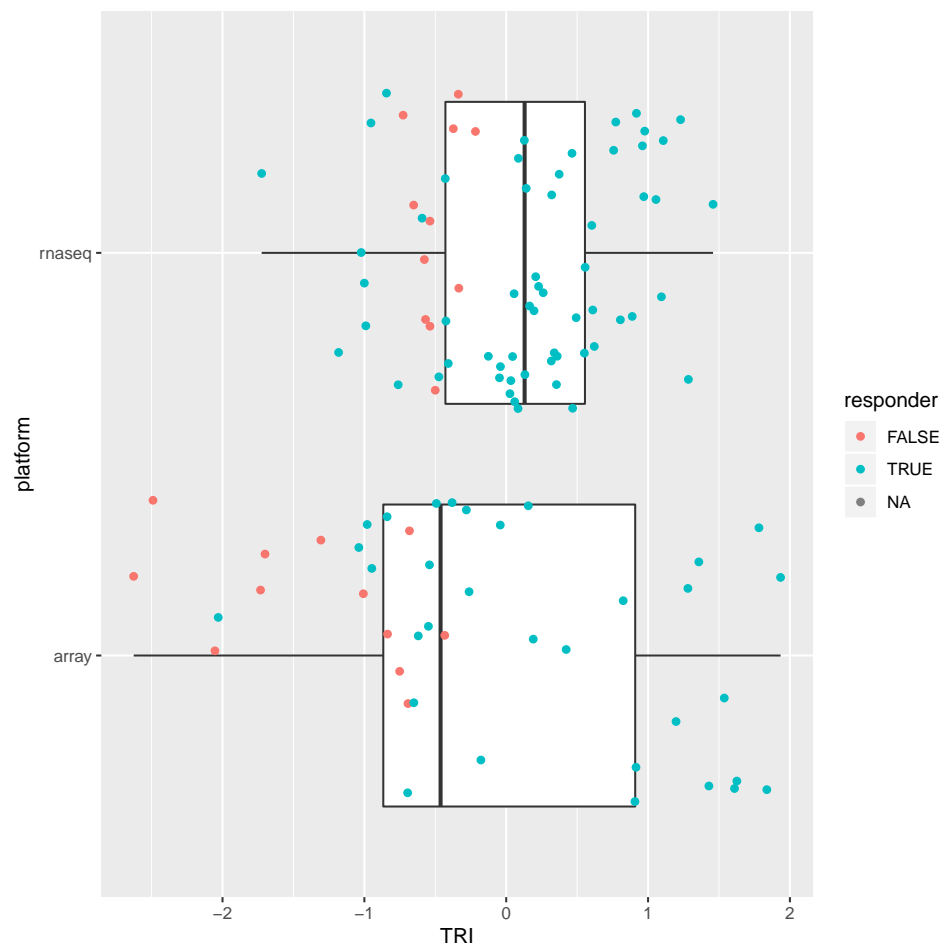


Figure 1.3: Distribution of TRI, stratified by platform used to measure expression.

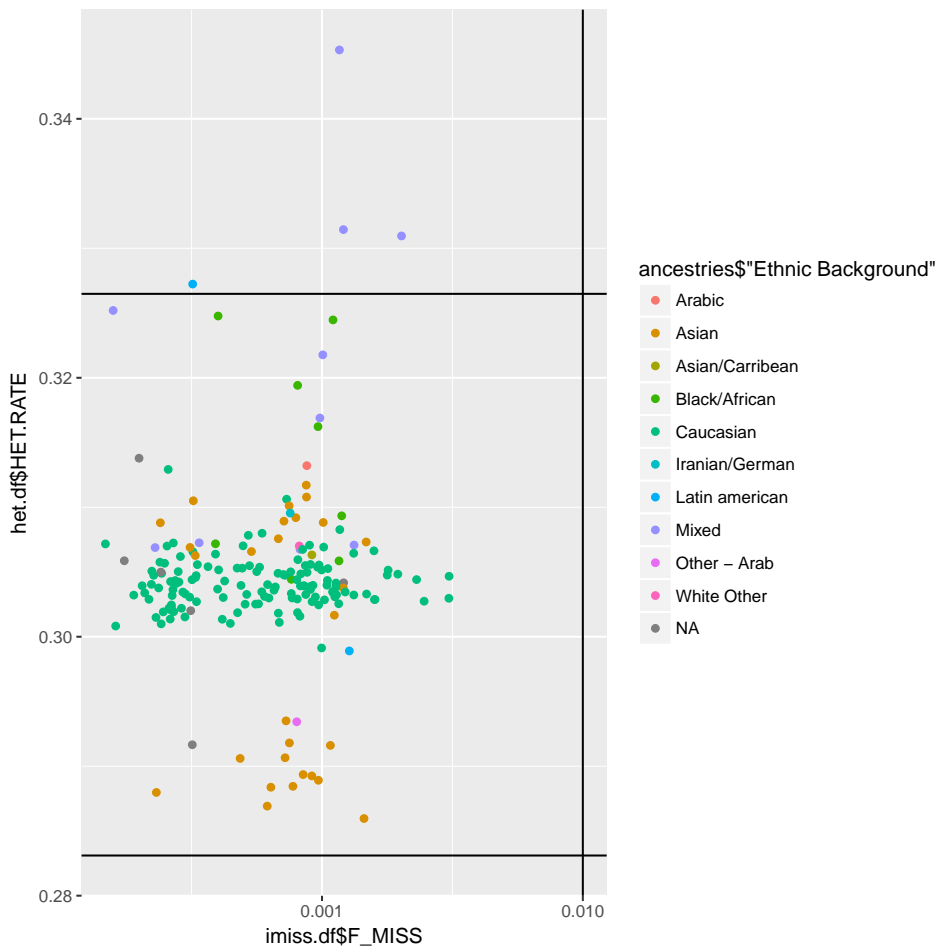


Figure 1.4: Sample filters for missingness and heterozygosity rate. Samples outside the central rectangle were excluded.

pairwise kinship coefficient > 0.177 (first-degree relatives or closer), the sample with lower marker missingness was selected.

After filtering, 169 samples and 549414 markers remained.

1.2.5 Computing genotype principal components as covariates for ancestry

As shown in [Table 1.1](#), the **HIRD** cohort is multi-ethnic, hence there is potential for confounding by population structure (sample structure due to genetic ancestry) in expression and genetic association studies^{27–29}. Treating HapMap 3 samples as a reference population where the major axes of variation in genotypes are likely to be ancestry, **principal component analysis (PCA)** was performed using smartpca (v8000) on **linkage disequilibrium (LD)-pruned** genotypes (PLINK --indep-pairwise 50 5 0.2). **HIRD** sample **principal components (PCs)** were computed by projection onto the HapMap 3 **PCA** eigenvectors. For non-genotyped individuals, **PC** values were imputed as the mean value for all genotyped individuals with the same self-reported ancestry. The top **PCs** separate samples of European, African and Asian ancestry ([Fig. 1.5](#)), hence these **PCs** can be used as covariates for ancestry downstream.

Add Tracy-Widom statistics for PCs to justify later choice of 4 PCs for covariates

nicer version, copy the peer code, facet the hird and hapmap samples

Can add other fastqc plots e.g. kmers, overrepresented seqs, seq length

1.2.6 RNA-seq data generation

Total RNA was extracted from **PBMCs** using the Qiagen RNeasy Mini kit, with on-column DNase treatment. RNA integrity was checked on the Agilent Bioanalyzer and mRNA libraries were prepared with the KAPA Stranded mRNA-Seq Kit (KK8421), which uses poly(A) selection. To avoid confounding of timepoint and batch effects from pooling, samples were pooled by library prep plate, ensuring libraries from all timepoints of an individual were in the same pool, and then sequenced across multiple lanes as technical replicates (HiSeq 4000, 75bp paired-end).

RNA-seq quality metrics were assessed using FASTQC* and Qualimap³⁰, then visualised with MultiQC³¹. Sequence quality was high ([Fig. 1.6](#)), and duplication levels were low ([Fig. 1.7](#)). The unimodal GC-content distribution suggested negligible levels of non-human contamination ([Fig. 1.8](#)).

*<https://www.bioinformatics.babraham.ac.uk/projects/fastqc/>

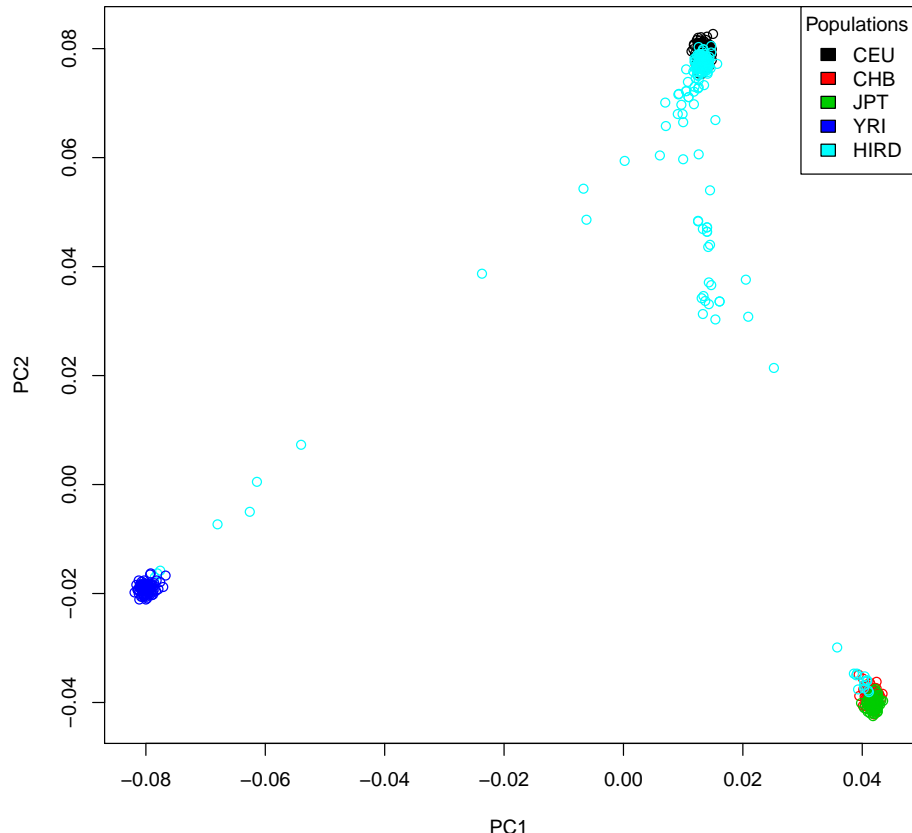


Figure 1.5: HIRD samples (cyan) projected onto PC1 and PC2 axes defined by PCA of HapMap 3 samples. The first two PCs separate European (CEU, upper-right) from Asian (CHB and JPT, lower-right) and African (YRI, lower-left) individuals.



Figure 1.6: FastQC sequence quality versus read position for HIRD RNA-seq samples.

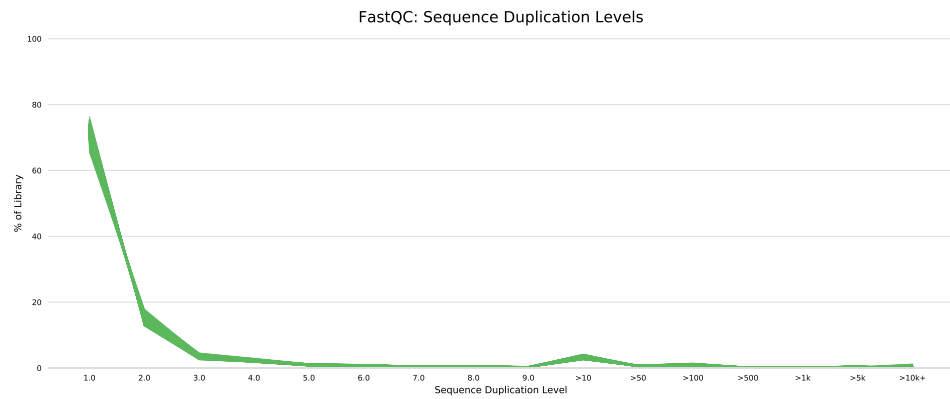


Figure 1.7: FastQC sequence duplication levels for HIRD RNA-seq samples.

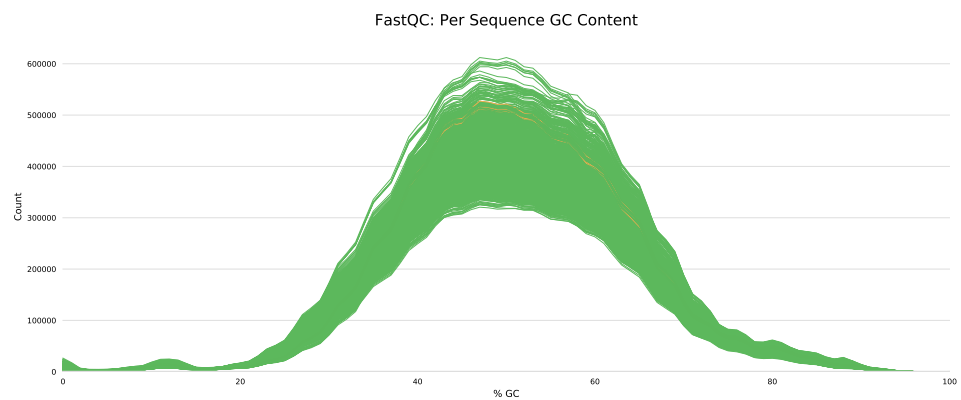


Figure 1.8: FastQC GC profile for HIRD RNA-seq samples.

1.2.7 RNA-seq quantification and filtering

[add software versions](#)

Reads were quantified against the Ensembl reference transcriptome (GRCh38) using Salmon³² in quasi-mapping-based mode, which internally accounts for transcript length and GC composition. To combine technical replicates, as the sum of Poisson distributions remains Poisson-distributed, counts for technical replicates were summed for each sample. The mean number of mapped read pairs per sample after summing was 27.09 million read pairs (range 20.24-39.14 million), representing a mean mapping rate of 80.73% (range 75.57-90.10%), comfortably within sequencing depth recommendations for DGE experiments³³. Relative transcript abundances were summarised to Ensembl gene-level count estimates using tximport (scaledTPM method) to improve statistical robustness and interpretability³⁴.

Genes with short noncoding RNA biotypes* were removed, as they are generally not polyadenylated, and expression estimates can be biased by misassignment of counts from overlapping protein-coding or lncRNA genes³⁵. Globin genes, which are highly expressed in erythrocytes and reticulocytes, cell types expected to be depleted in PBMC³⁶, were also removed. Given the proportion of removed counts at this stage was low for most samples (Fig. 1.9), poly(A) selection and PBMC isolation procedures were deemed to have been efficient.

Many of the genes in the reference transcriptome are not expressed in PBMC (Fig. 1.10), and many genes are expressed at counts too low for statistical analysis of DGE. Genes were further filtered to require detection (non-zero expression) in at least 95% of samples, and a minimum of 0.5 counts per million (CPM) in at least 20% of samples. The 0.5 CPM threshold was chosen to correspond to approximately 10 counts in the smallest library, where 10-15 counts is a rule of thumb for considering a gene to be robustly expressed³⁷. The change in the distribution of gene expressions among samples before and after filtering shows a substantial number of low expression genes are removed (Fig. 1.11).

After the application of all filters, expression values were available for 21626 genes over 223 samples (75/75 individuals on day 0, 73/75 on day 1, and 75/75 on day 7).

*miRNA, miRNA_pseudogene, miscRNA, miscRNA_pseudogene, Mt rRNA, Mt tRNA, rRNA, scRNA, snlRNA, snoRNA, snRNA, tRNA, tRNA_pseudogene. List from <https://www.ensembl.org/Help/Faq?id=468>

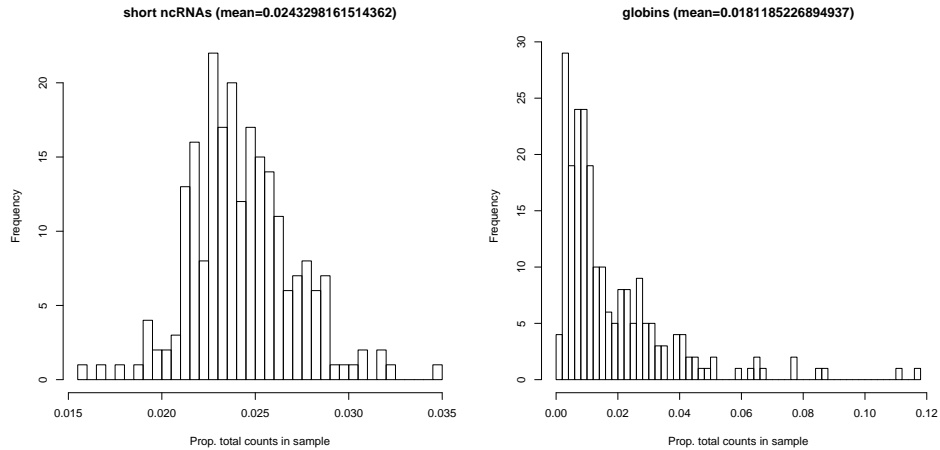


Figure 1.9: Distributions of removed short ncRNA and globin counts as a proportion of total counts in RNA-seq samples.

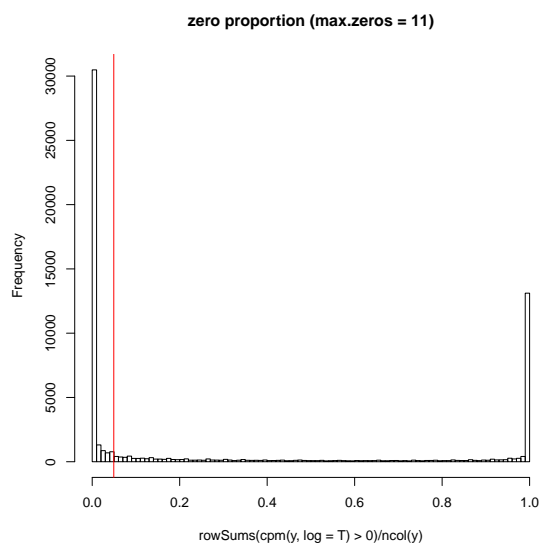


Figure 1.10: Distribution of the proportion of samples in which genes were detected (non-zero expression). Many genes are not detected in any samples. Vertical line shows 5% threshold below which genes were discarded.

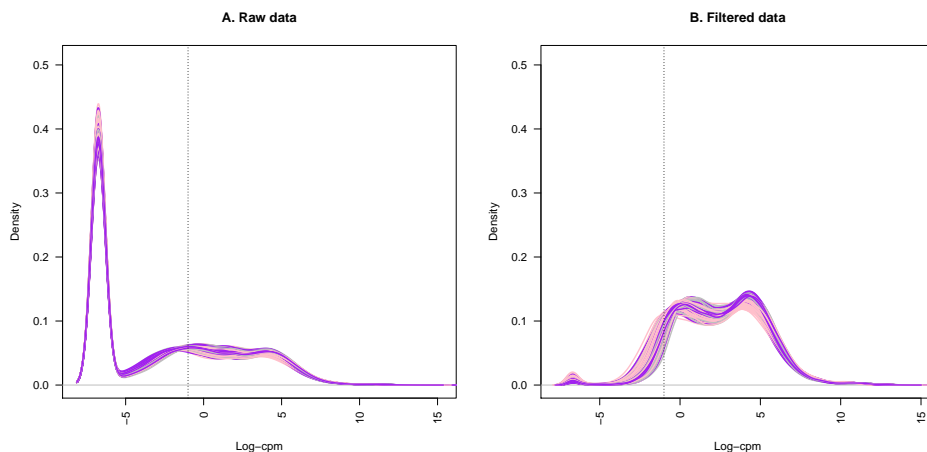


Figure 1.11: Distribution of gene expressions for RNA-seq samples before and after filtering no expression and low expression genes. Vertical line shown at CPM = 0.5 threshold.

1.2.8 Array data preprocessing

Single-channel Agilent 4x44K microarray (G4112F) data for 173 samples from¹⁸ were downloaded from ArrayExpress*. These arrays were originally processed in two batches, the effect of which is seen in the raw foreground intensities (Fig. 1.12).

VSN³⁸ was used to perform background correction, between-array normalisation, and variance-stabilisation of intensity values, resulting in expression values on a log₂ scale.

Most genes are targetted by multiple array probes; 31208 probes were collapsed into 18216 Ensembl genes using by selecting the probe with the highest mean intensity for each gene (`WGCNA::collapseRows(method=MaxMean)`, recommended for probe to gene collapsing³⁹). While it would be optimal to select a collapsing method to maximise the concordance between array and RNA-seq expression values, there were no samples assayed by both platforms in the HIRD dataset. The final normalised log₂ intensity values for these 18216 genes over 173 samples is shown in Fig. 1.13.

1.2.9 Differential gene expression

PCA of the expression data reveals although samples separate by experimental timepoint along PC3 (Fig. 1.14d), measurement platform is by far the

*<https://www.ebi.ac.uk/arrayexpress/experiments/E-MTAB-2313/>

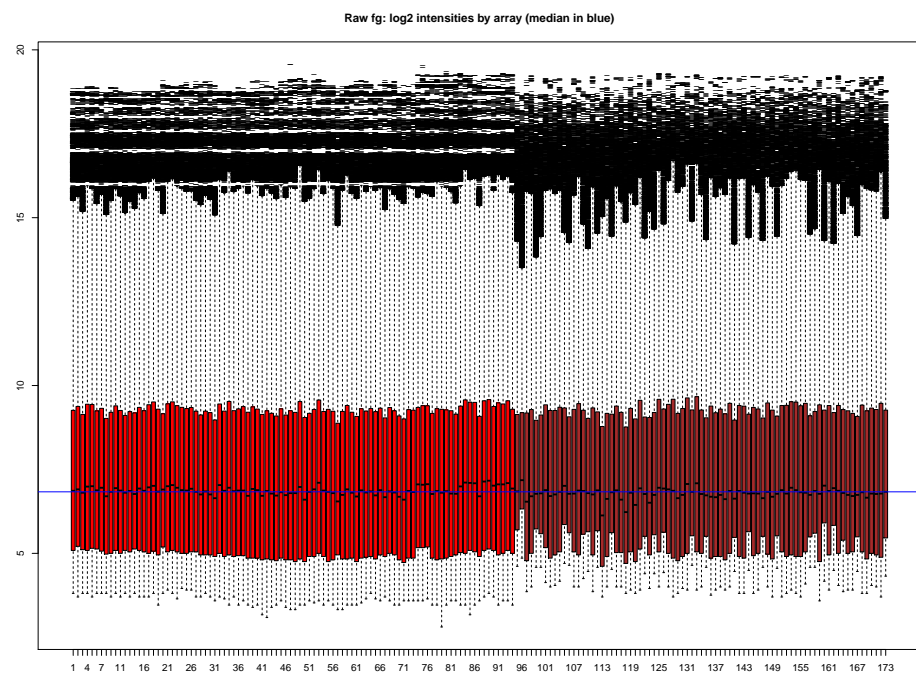


Figure 1.12: Raw foreground intensities for 173 HIRD array samples. Colored by array processing batch.

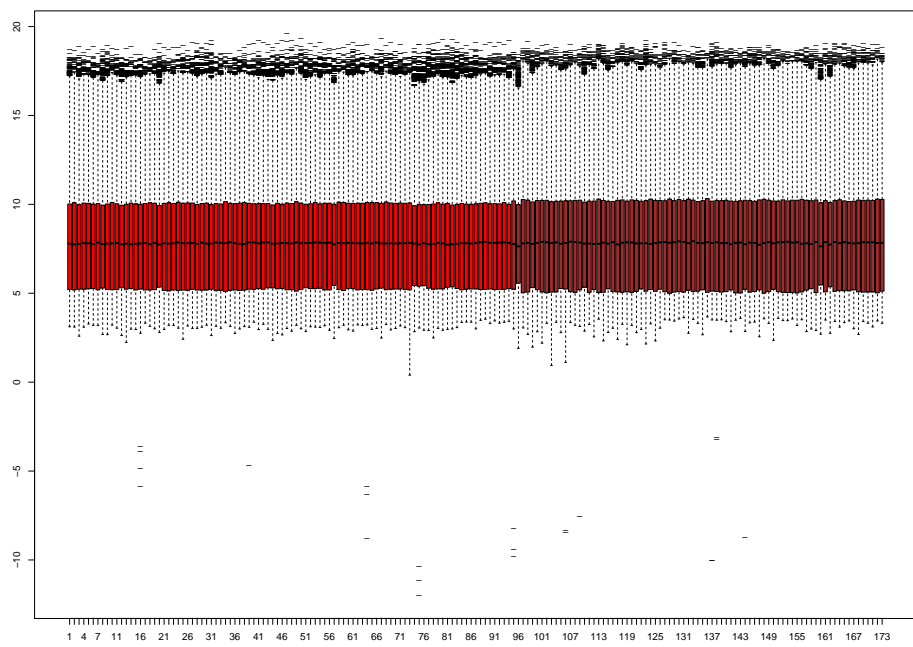


Figure 1.13: Array intensity estimates after VSN normalisation and collapsing of probes to genes. Colored by array processing batch.

largest source of variation. Normalisation was also not able to completely remove the batch effect within the array data (Fig. 1.14a). The large platform effect likely stems from systematic technological differences in how each platform measures expression. For example, arrays suffer from ratio compression due to cross-hybridisation⁴⁰. RNA-seq has a higher dynamic range, resulting less bias at low expression levels, but estimates are more sensitive to changes in depth than array estimates are to changes in intensity⁴¹. There are also differences in the statistical models behind expression quantification and normalisation, as described above.

orange box: cite relevant preprocessing sections

Despite the shortcomings of array data detailed above, the array dataset tends to contain individuals with more extreme antibody response phenotypes (Fig. 1.3), and hence the data should not be excluded. Given the magnitude of the platform effect, I concluded that the appropriate approach should be a two-stage approach that integrates per-platform DGE effect estimates while explicitly accounting for between-platform heterogeneity.

orange box: combat does have a pro in that it can do per gene scaling, that fixed fx won't do

Regarding the batch effect within the array data, a popular adjustment method is ComBat⁴², which estimates centering and scaling parameters by pooling information across all genes using empirical Bayes. ComBat is the method used in¹⁸. In comparisons of microarray batch effect adjustment methods, ComBat performs favourably (vs. five other adjustment packages)⁴³ or comparably (vs. batch as a fixed or random effect in the linear model)⁴⁴. However, where batches are unbalanced in terms of sample size⁴⁵ or distribution of study groups that have an impact on expression⁴⁶, ComBat can overcorrect batch differences or bias estimates of group differences respectively. In our data, sample size and timepoint groups are fairly balanced between the two array batches, but the proportion of responders is not Table 1.2, hence I elect not to use ComBat to pre-adjust the array expression data, and model the batches as fixed effects. In practice, results from the DGE analysis were not substantially affected by the choice of whether to use a ComBat pre-adjustment or a fixed effect.

orange box: this is not a very precise justification. actually, if I were to color R/NR in the PCA plot, R/NR doesn't really explain a lot of var in global gene expression. that's probably why the results don't change much.

orange box: weaken this. combat is used multiple times in ch3

orange box: be more specific about how combat works i.e. estimates factors per gene per batch?

1.2.9.1 Per-platform differential gene expression model

For the array data, as¹⁸ demonstrated no significant global differences in expression between day -7 and day 0, I likewise merge these two timepoints into a single “day 0” baseline timepoint in the following DGE models.

For the RNA-seq data, between-sample normalisation was performed

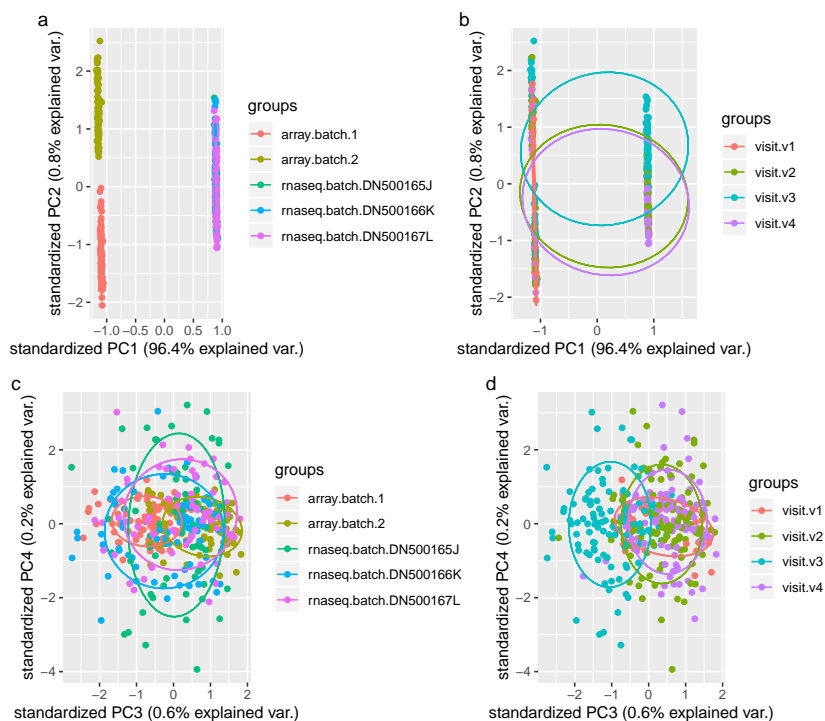


Figure 1.14: First four PCs in the HIRD expression data, colored by platform and batch (left), and timepoint (right).

using the trimmed mean of M-values (TMM) method⁴⁷ from edgeR⁴⁸; then variance-stabilisation was performed using voom⁴⁹, resulting in expression values with units of $\log_2 \text{CPM}$.

this is DGE specific normalisation, which is why it goes here, not in the preprocessing section

Linear models were fit using limma⁵⁰, which is computationally fast, and performs well for sufficiently large ($n \geq 3$ per group) sample sizes⁵¹. For each gene, I fit a model (model 1) with expression as the response variable; with timepoint (baseline, day 1, day 7), TRI, batch, sex, age, and the first 4 genotype PCs as fixed-effect predictors; and individual as a random-effect predictor. Within-individual correlations for the random effect were estimated using limma::duplicateCorrelation. A second model (model 2) was also fit, including 3 additional terms for the interactions between each timepoint and TRI. From model 1, I defined contrasts for day 1 vs. baseline, day 7 vs. baseline, day 7 vs. day 1, TRI, sex, and age. From model 2, I defined contrasts for the TRI specifically at each of the three timepoints. Corresponding coefficients and standard errors for the contrasts were extracted from the linear models, which represent effect size in units of \log_2 expression fold change per unit change in predictor value.

link to papers justifying sex, age, ancestry as significant effects on immune gene expression

1.2.9.2 Choice of differential gene expression meta-analysis method

add section labels

In the section, I concluded that a two-stage meta-analysis approach would be appropriate. This meta-analysis is restricted to 13593 genes assayed by both the array and RNA-seq platforms.

add label

make all the notation in this section consistent with, and add the equation 2.1. The normal-normal hierarchical model.⁵⁴

Two popular frameworks for effect size meta-analysis are fixed-effect and random-effects^{52,53}. Given k studies, the fixed-effect model assumes a common population effect size shared across all studies, with observed variation explained only by sampling error. The random-effects model assumes the k study-specific effect sizes are drawn from some distribution with variance τ^2 (standard deviation (SD) τ), representing an additional source of variation termed the between-studies heterogeneity, reducing to the fixed-effect model when $\tau = 0$. In the HIRD data, there are $k = 2$ 'studies' (array and RNA-seq), where the platform differences described in section contribute to considerable between-studies heterogeneity. The assumption of $\tau = 0$ is unrealistic, hence a random-effects model is more appropriate.

Unfortunately, there is no optimal solution for directly estimating τ in random-effects meta-analyses with small k ⁵⁵, in the case of $k = 2$ especially⁵⁶. Many estimators are available⁵⁷, but lack of information with small k causes

estimation to be imprecise, and often results in boundary values of $\tau = 0$ that are incompatible with the assumed positive heterogeneity^{58,59}. In such circumstances, the most sensible choice may be to incorporate prior information about model hyperparameters in a Bayesian random-effects framework^{57–60}. For this study, I use the implementation in `bayesmeta`⁵⁴, which requires priors for both effect size and between-studies heterogeneity.

1.2.9.3 Prior for between-studies heterogeneity

The choice of prior for between-studies heterogeneity is influential when k is small⁶⁰. Gelman [61] considers the case of $k = 3$, showing that a flat prior places too much weight on implausibly large estimates of τ , and recommends a weakly informative prior that acts to regularise the posterior distribution. Since I assumed zero estimates for τ are unrealistic, I use a weakly-informative gamma prior recommended by⁵⁸, which has zero density at $\tau = 0$, increasing gently as τ increases. This constrains τ to be positive, but still permits estimates close to zero if the data support it. This is in contrast to priors used in other studies from the log-normal (e.g.^{62,63}) or inverse-gamma (e.g.⁶⁴) families that have derivatives or zero close to zero, thus ruling out small values of τ no matter what the data suggest; and in contrast to half-t family priors (e.g.^{60,61}), which have their mode at zero, and do not rule out $\tau = 0$.

To estimate the appropriate shape and scale parameters for the gamma empirically, a frequentist random-effects model using the **restricted maximum likelihood (REML)** estimator for τ (recommended for continuous effects⁵⁷) was first for each gene using `metafor::rma`. Genes with small estimates of $\tau < 0.01$ were excluded, and a gamma distribution was fit to the remaining estimates using `fitdistrplus`.

1.2.9.4 Prior for effect size

While the choice of prior on τ is influential when k is small, there is usually enough data to estimate the effect size μ such that any reasonable non-informative prior can be used^{59,61}. `bayesmeta` implements both flat and normal priors for μ . Assuming that most genes are not differentially expressed with effect sizes distributed randomly around zero, I selected a normal prior with $N(\mu = 0, \sigma^2)$, over a flat prior. As in the section above, to determine an appropriate scale, a normal distribution with mean $\mu = 0$ was fit to the

why is this? is it having well powered studies? gelman is vague

distribution of effect sizes from the gene-wise frequentist models to empirically estimate σ .

Heavy-tailed Cauchy priors have been proposed for effect size distributions in DGE experiments to avoid over-shrinkage of true large effects in the tails⁶⁵. Since `bayesmeta` does not implement a Cauchy prior, to avoid over-shrinkage, I flatten the normal prior considerably by scaling up the variance to $N(0, 100\sigma^2)$. This is equivalent to assuming placing a 95% prior probability that effects are less extreme than approximately 20σ .

the derivation here is
 $qnorm(0.975, \text{mean}=0, \text{sd}=1*10) = 1*19.59964$,
 bit iffy, double check this
 is correct

could also include a table
 of all sets of parameters
 here?

1.2.9.5 Evaluation of priors

An example of the empirically estimated hyperparameters for the priors for the day 1 vs. baseline contrast are shown in Fig. 1.15 (for τ) and Fig. 1.16 (for μ). For τ , the final prior used was $\text{Gamma}(\text{shape} = 1.5693, \text{scale} = 0.0641)$. This is comparable to⁵⁸'s default recommendation of a $\text{Gamma}(\text{shape} = 2, \text{scale} = \lambda)$ prior where λ is small. For μ , the final prior used was $N(0, (0.3240 * 10)^2)$. The tails of the non-scaled normal fit (black) are light compared to the Cauchy fit (red), which may lead to over-shrinkage, especially since there are many genes with high positive fold changes for the day 1 vs. baseline effect.

1.2.9.6 Multiple testing correction

For the frequentist random-effects meta-analysis, nominal gene-wise p values are converted to **false discovery rate (FDR)** estimates using the **Benjamini-Hochberg (BH)** procedure (`p.adjust` in R). For the Bayesian random-effects meta-analysis, posterior effect sizes and standard errors are supplied to `ashr`, which estimates the **local false sign rates (lfsrs)**, which are analogous to **FDR**, but quantifies the probability of calling the wrong sign for an effect rather than than the confidence of a non-zero effect⁶⁶.

add comment on symmetry

1.2.10 Gene set enrichment analysis using blood transcription modules

Gene set enrichment analyses were conducted using `tmod::tmodCERN0test`⁶⁷, which assesses the enrichment of small ranks within specific sets of genes compared to all genes, when the genes are ranked by some metric—here I used effect sizes from `bayesmeta`. The gene sets used were **blood transcription modules (BTMs)** from⁶⁸, which are annotated sets of coexpressed genes

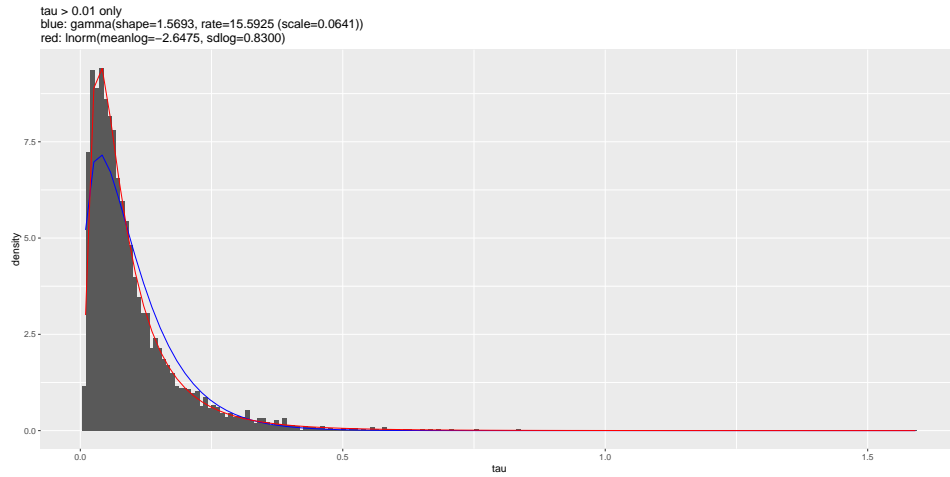


Figure 1.15: Gamma prior for τ used for `bayesmeta` (blue), compared to the empirical distribution of per-gene frequentist `metafor::rma` estimates for τ , for the day 1 vs. baseline effect (small estimates of $\tau < 0.01$ excluded). Empirical log-normal fit also shown (red).

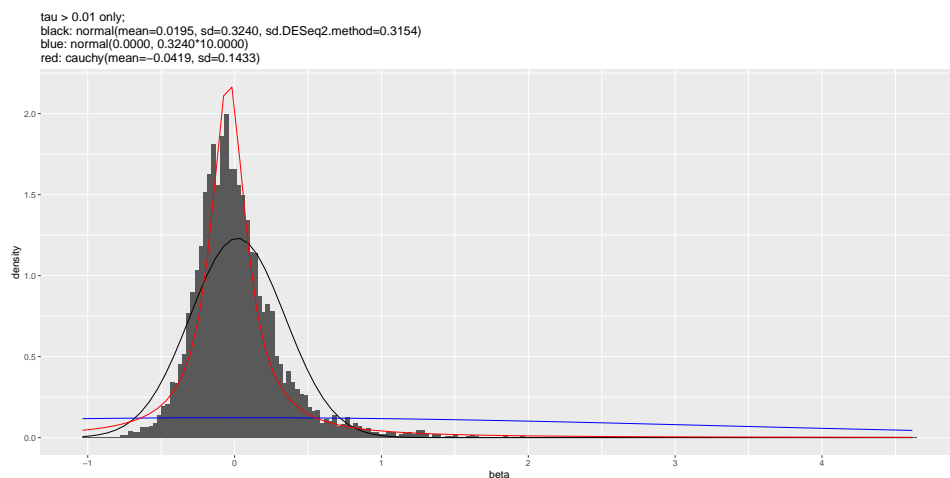


Figure 1.16: Normal prior for μ used for `bayesmeta` (blue), compared to the empirical distribution of per-gene frequentist `metafor::rma` estimates for τ , for the day 1 vs. baseline effect. The non-scaled normal fit is shown (black), as well as a Cauchy fit (red).

mined from publicly available human blood transcriptomic data, and provide sets tailored for enrichment analyses in blood cells.

1.3 Results

1.3.1 Extensive global changes in expression after vaccination

To gain an overview of how the transcriptome changes after vaccination, linear models were fit to identify genes differentially expressed at day 1 or day 7 compared to baseline (day -7 and day 0) in the HIRD array and RNA-seq expression data, accounting for covariates such as batch effects, sex, age, TRI, and ancestry. At 13593 genes with expression measured by both platforms, models were fit within each platform, then effect sizes were combined using Bayesian random-effects meta-analysis.

At a $\text{lfsr} < 0.05$ and absolute $\text{FC} > 1.5$ cutoff, 857/13593 genes were differentially expressed between any pair of timepoints, with their expression clustering into three main clusters (Fig. 1.17).

1.3.2 Innate immune response at day 1 post-vaccination

Consistent with global expression at day 1 being markedly different from expression at other timepoints (Fig. 1.14), the highest numbers of differentially expressed genes are observed at day 1, with 644 genes differentially expressed vs. baseline. The majority of these (580/644) were upregulated. The gene with the highest FC increase at day 1 compared to baseline was *ANKRD22* ($\log_2 \text{FC} = 4.49$), an interferon-induced gene in monocytes and dendritic cells (DCs) involved in antiviral innate immune pathways⁶⁹. Other key genes in the interferon signalling pathway⁷⁰ such as *STAT1* ($\log_2 \text{FC} = 2.1693060$), *STAT2* ($\log_2 \text{FC} = 0.9489341$), and *IRF9* ($\log_2 \text{FC} = 0.8153674$) are also upregulated at day 1. Gene set enrichment analysis using tmod revealed that genes with the high FC increases at day 1 were enriched in modules associated with activated DCs, monocytes, toll-like receptor and inflammatory signalling (Fig. 1.18), confirming that day 1 responses are dominated by signatures of innate immunity. 64 genes were downregulated at day 1, enriched in modules associated with T cells and natural killer (NK) cells, with the largest absolute fold change observed for *FGFBP2* ($\log_2 \text{FC} = -0.9141547$). For both up and

can also add MSigDB hallmark sets, which include interferon sets; and of course gene ontology sets

not sure of interpretation at FGFBP2, it is indeed highly expressed in NKs through <https://dice-database.org/genes/FGFBP2>

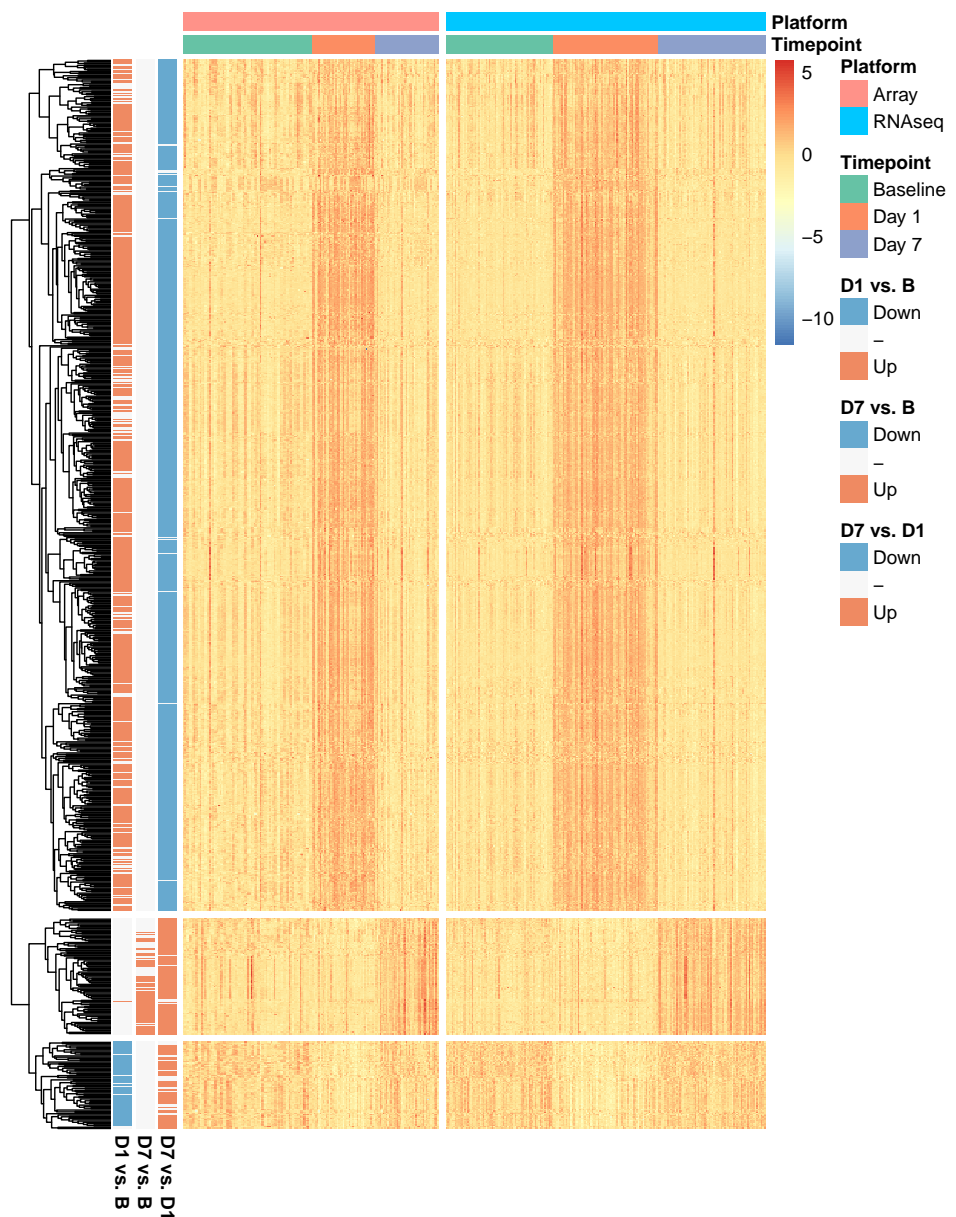


Figure 1.17: Normalised gene expression for genes differentially expressed between any pair of timepoints ($\text{lfsr} < 0.05$, absolute fold change > 1.5) across HIRD samples, clustered by gene (Manhattan distance metric).

any point in a table of e.g.
top 20 DE genes, or is the
gene set analysis already
enough?

change x axis labels to
baseline, specify top 10
procedure in figure cap-
tion

finish citing

downregulated genes, there was a tendency to return to baseline expression levels by day 7.

1.3.3 Adaptive immune response at day 7 post-vaccination

59 genes were differentially expressed at day 7 vs. baseline, with expression fold changes more modest than those at day 1. The genes with the highest up-regulation were the B cell-associated genes *TNFRSF17* ($\log_2 \text{FC} = 1.7538617$) and *MZB1* ($\log_2 \text{FC} = 1.7369668$). Plasma cell-specific genes including *SDC1* (encodes CD138 <https://www.ncbi.nlm.nih.gov/pmc/articles/PMC5437827/>) ($\log_2 \text{FC} = 1.3673081$) and *ELL2* (<https://www.nature.com/articles/ni.1786>) ($\log_2 \text{FC} = 0.8679659$) were also prominently upregulated.

Strongly enriched modules at day 7 were related to mitosis and cell proliferation, particularly in CD4^+ T cells (Fig. 1.18). Both the CD4^+ T cell and plasma cell response are indications of an adaptive immune response at day 7.

1.3.4 Expression signatures associated with antibody response

I also looked for genes which have expression associated with baseline-adjusted antibody response, as quantified by **TRI**. At the initial frequentist meta-analysis stage, with a significance threshold of **FDR** < 0.05, 6 genes had expression associated with **TRI** at baseline, 55 at day 7, and 11 pooling samples across timepoints (Fig. 1.19).¹⁸ also identified genes with day 7 expression associated with antibody response, where response was defined

add label

as a binary phenotype based on 4-fold change (described in section). They reported 62 significant associations at **FDR** < 0.05, of which 58/62 fall into the 13593 genes considered in my meta-analysis (circled, Fig. 1.19), and 15/58 replicated, all with the same positive direction of effect (high expression with high **TRI**). In the Bayesian meta-analysis, no single gene was detected as significantly associated with **TRI** at **lfsr** < 0.05 at any timepoint, or when pooling samples across all timepoints (Fig. 1.20).

Significant enrichments were detected at the gene set level; the strongest effects are seen at day 7, where expression of cell cycle, CD4^+ T cells, and plasma cells are associated with high **TRI**. At day 0, modules related with inflammatory response in myeloid cells are also associated with high **TRI** (Fig. 1.21).

figure x labels here should
be **TRI**, not R.vs.NR

CHAPTER 1. TRANSCRIPTOMIC RESPONSE TO INFLUENZA A (H1N1)PDM09 VACCINE

1.3. RESULTS

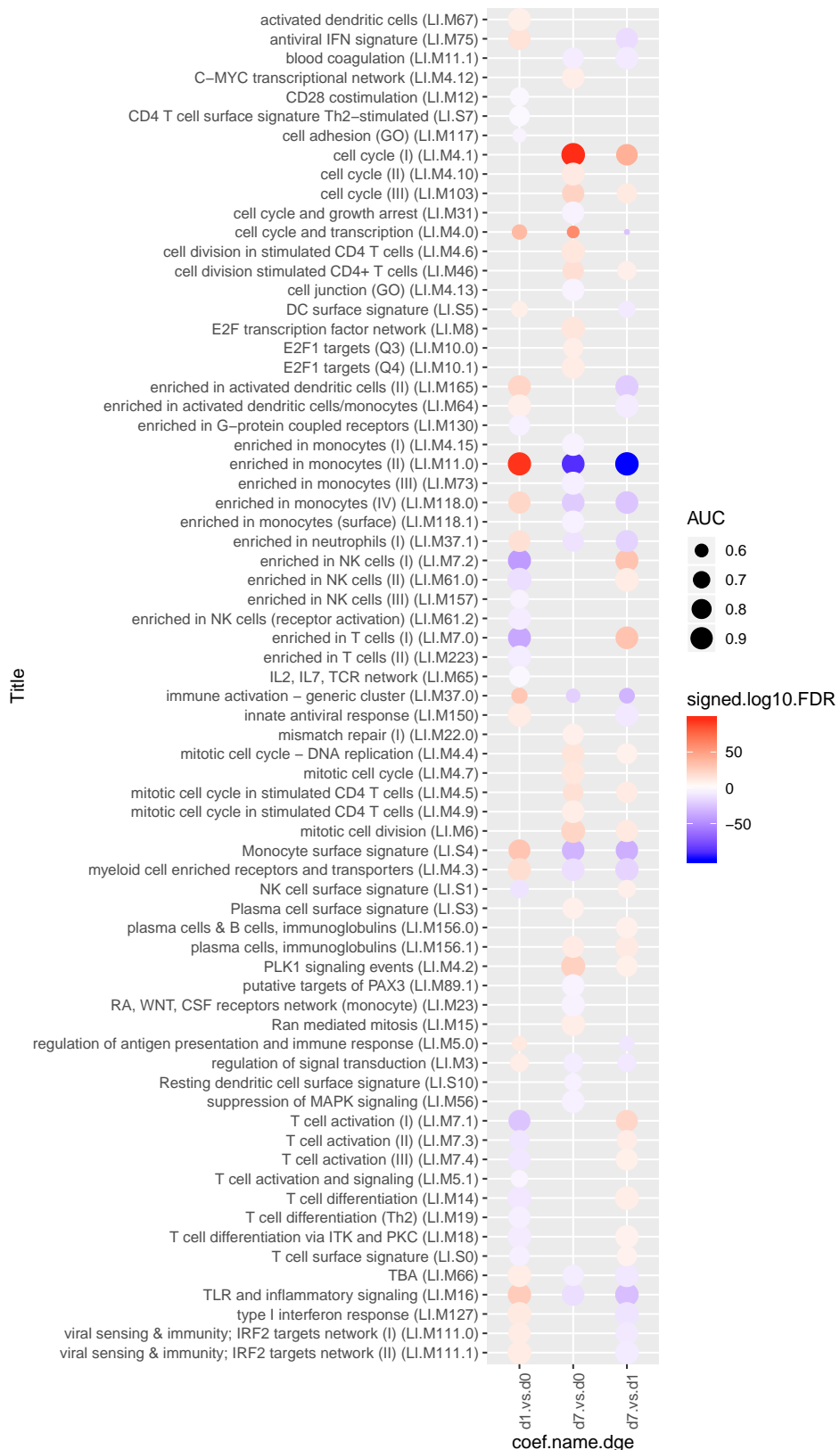


Figure 1.18: Transcriptomic modules significantly up or downregulated post-vaccination. Size of circle indicates effect size. Color of circle indicates significance and direction of effect (red = upregulation, blue = downregulation).

CHAPTER 1. TRANSCRIPTOMIC RESPONSE TO INFLUENZA A
1.3. RESULTS (H1N1)PDM09 VACCINE

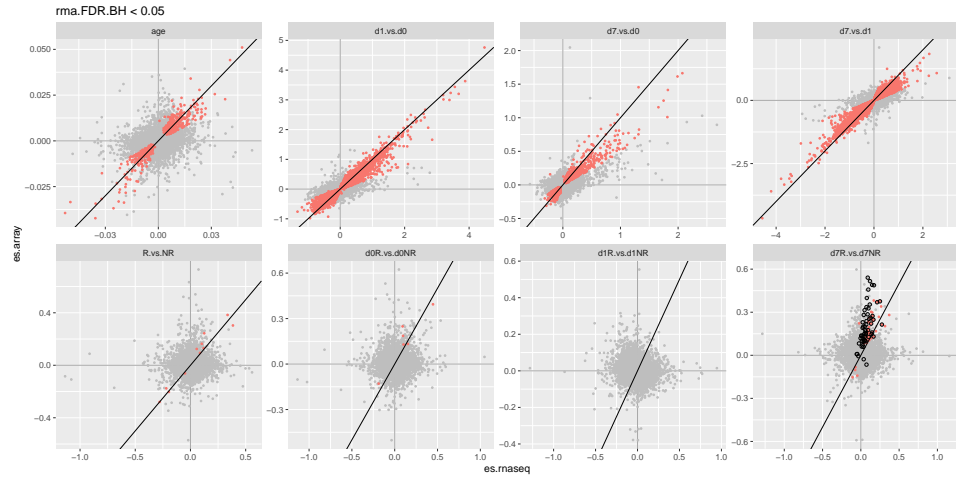


Figure 1.19: DGE effect sizes estimated in array vs. **RNA-seq**. Significance colored by frequentist random effects meta-analysis FDR < 0.05 . Genes with day 7 expression associated with responder/non-responder status in¹⁸ are circled for that contrast.

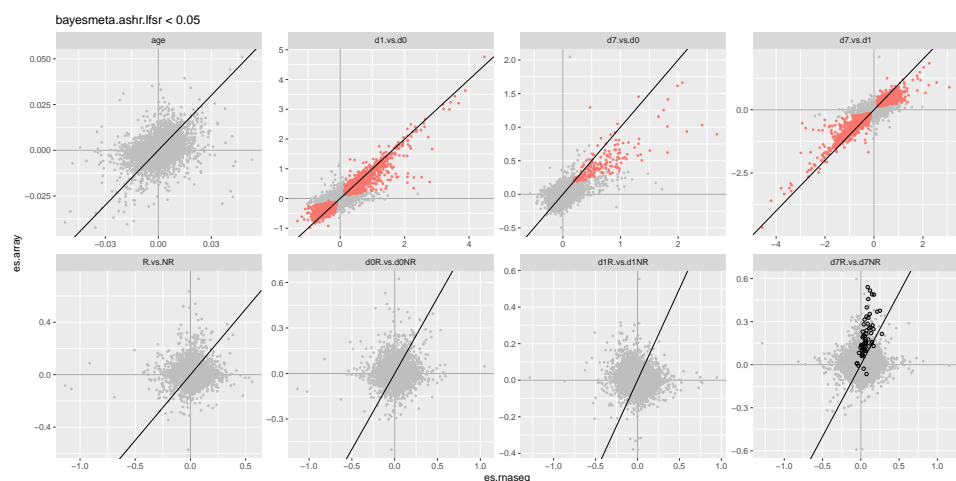


Figure 1.20: DGE effect sizes estimated in array vs **RNA-seq**. Significance colored by Bayesian random effects meta-analysis lfsr < 0.05 . Genes with day 7 expression associated with responder/non-responder status in¹⁸ are circled for that contrast.

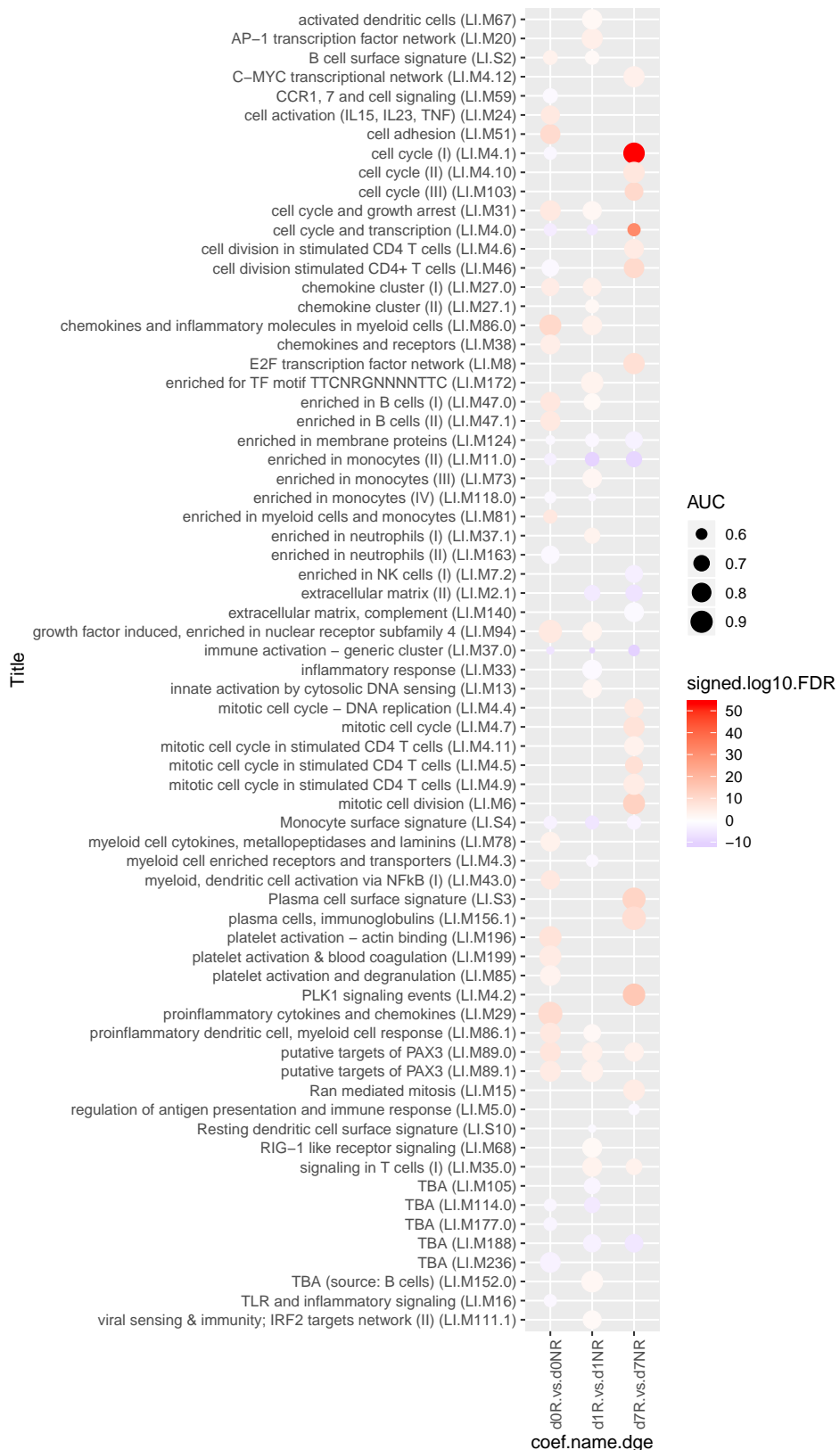


Figure 1.21: Transcriptomic modules enriched in genes with expression associated with antibody response (TRI) at each day. Size of circle indicates effect size. Color of circle indicates significance and direction of effect (red = expression positively correlated with TRI, blue = negative).

1.3.5 Identifying expression signatures for predicting antibody response [probably cut this section and just add to discussion]

1.4 Discussion

There is extensive transcriptomic response to Pandemrix vaccination in the **HIRD** cohort. Upregulation of genes and modules related to the interferon signalling pathway, monocytes, inflammatory response, and other aspects of innate immunity were detected at day 1. This response is transient, with most such genes returning to baseline expression by day 7. Upregulation of cell cycle/proliferation, activated CD4⁺ T cell, and B (plasma) cell genes and modules were detected at day 7. This is likely a signature indicating the shift to an adaptive immune response, involving CD4⁺ T cell-supported differentiation and proliferation of antibody-secreting plasmablasts and plasma cells⁷². These patterns of expression change between timepoints in the **RNA-seq** data are consistent with the patterns in the array data in the original study¹⁸, and with expansions of monocyte and plasma cell populations seen in the **FACS** data at days 1 and 7 respectively in the original **HIRD** study¹⁸.

In contrast, I was not able to fully replicate the originally reported single gene-level associations between day 7 expression and antibody response in the **RNA-seq** data and subsequent and meta-analyses. In¹⁸, 62 genes were reported as differentially expressed between vaccine responders and non-responders. Although¹⁸ encodes responder status as a binary phenotype, whereas my analysis uses **TRI**, this is not the primary difference, as 51/62 genes replicated (**FDR** < 0.05) using **TRI** when considering just the array data. The same analysis using only the **RNA-seq** data replicated 0/62 genes.

The majority of the effects for these genes were simply much stronger in the array dataset than in the RNAseq dataset (Fig. 1.19). Given that the range of **TRI** is higher in the array individuals (Table 1.1), this does not seem unusual that stronger **TRI**-associated effects are observed there.

58/62 reported hits were measured by both platforms and assessed in the meta-analysis. Only 15/58 signals replicated using frequentist random-effects meta-analysis to combine per-platform estimates. I do not consider these hits as robust, as the **REML** estimate of between-platform heterogeneity was zero for 8563/13593 for the day 7 **TRI** contrast overall, and zero for

Not sure if there is a biological interpretation of downreg of T cells and NK cells gene sets at day 1, since it could be due to increase in other cell types in the sample. similar findings in⁷¹ though

lit search for downregulation interpretation paper, and downreg T cell paper

might have to rerun everything using the original binary R/NR if this line of reasoning isn't strong enough

move numbers to results?

all 15 of these signals. None of these signals replicated in the Bayesian random-effects meta-analysis. The Bayesian meta-analysis is in general more conservative, calling fewer differentially expressed genes compared to the frequentist analysis for all contrasts (Fig. 1.20). Prior information about τ is incorporated, discouraging unrealistic estimates of zero heterogeneity. Given the between-platform heterogeneity coming from both platform-specific technical differences and **TRI** phenotype differences, relative to the modest effect size distributions compared to between-timepoint **DGE** comparisons, the data are not well-positioned to identify significant single-gene associations with antibody response.

Expression signatures of antibody response were, however, observed at the gene set level, for modules of coexpressed genes that are associated with **TRI** as a whole. The strongest effects were observed at day 7, where expression of adaptive immune response modules (cell cycle, stimulated CD4⁺ cell, plasma cell modules) were positively associated with **TRI**. These are the same modules observed to be upregulated at day 7 compared to baseline; it seems that those individuals with the greatest antibody response to vaccination are most able to upregulate these gene sets by day 7 post-vaccination.

Module associations were also observed pre-vaccination (cell adhesion, enriched in B cells, proinflammatory cytokines, platelet activation), suggesting baseline immune state has some influence on long-term antibody response to Pandemrix. Over the years, a diverse range of gene sets have been found to be baseline predictors of serological response to influenza vaccination: apoptosis¹⁹; Fc γ receptor-mediated phagocytosis, TREM1 signaling²⁰; enriched in B cells, T cell activation²¹; B cell receptor signalling, inflammatory response, platelet activation²²; several of which I also observe. It should be noted that comparisons with these signatures from existing influenza systems vaccinology studies should be caveated, as most existing studies are for non-adjuvanted influenza vaccines. Adjuvanted influenza vaccines are considerably more immunogenic, and post-vaccination expression patterns differ to those of non-adjuvanted vaccines^{16,18}. Hence, it is particularly important that the robustness of these observed baseline expression signatures be validated in an independent cohort for a comparable AS03-adjuvanted influenza vaccine.

could comment on phenotype differences too, i.e. HIRD measure antibodies at d63, much later than is popular in the field: d28 usually

In conclusion, Chapter 2 characterises the expansive changes in **PBMC** gene expression that follow vaccination with Pandemrix. The dominant trend

should probably emphasize sobolev didn't find pre-vacc signatures, and we did. But it's not exactly fair, as sobolev didn't use gene set enrichment as far as I can tell

for all individuals is transient upregulation of the innate immune response at day 1, transitioning into adaptive immunity by day 7. Baseline-adjusted antibody response is correlated with expression of gene sets, particularly adaptive immunity modules at day 7, but also for some modules pre-vaccination. Unfortunately, between-platform variation in expression impedes identification of specific genes that contribute. The fundamental question of why gene expression and antibody responses vary between HIRD individuals remains. Chapter 3 will examine one hypothesis: the impact of common human genetic variation on Pandemrix expression response.

found signatures, but so what? Feels like chapter lacks a punchline?

why blood? ready easy supply of immune cells

Table 1.1: Sample descriptive statistics.

	Total n = 114	array n = 44	platform rnaseq n = 70
Gender			
F	72 (63.2%)	27 (61.4%)	45 (64.3%)
M	42 (36.8%)	17 (38.6%)	25 (35.7%)
Age at vaccination years			
	29.2 (11.8)	32.9 (14.1)	26.8 (9.4)
Ethnic Background			
Asian	14 (12.3%)	5 (11.4%)	9 (12.9%)
Black/African	9 (7.9%)	4 (9.1%)	5 (7.1%)
Caucasian	82 (71.9%)	33 (75%)	49 (70%)
Latin american	2 (1.8%)	1 (2.3%)	1 (1.4%)
Mixed	5 (4.4%)	1 (2.3%)	4 (5.7%)
Other - Arab	1 (0.9%)	0 (0%)	1 (1.4%)
White Other	1 (0.9%)	0 (0%)	1 (1.4%)
log2 HAI 0	4.4 (1.8)	4.2 (1.6)	4.5 (1.9)
log2 HAI 6	7.6 (1.8)	7.4 (2.2)	7.6 (1.5)
log2 HAI ratio	3.2 (1.9)	3.2 (2.4)	3.1 (1.6)
log2 MN 0	6.2 (2.8)	5.4 (2.4)	6.6 (3.0)
log2 MN 6	10.4 (2.0)	9.5 (2.2)	10.9 (1.6)
log2 MN ratio	4.2 (2.3)	4.1 (2.6)	4.3 (2.1)
responder			
FALSE	23 (20.2%)	12 (27.3%)	11 (15.7%)
TRUE	91 (79.8%)	32 (72.7%)	59 (84.3%)
TRI	-0.0 (0.9)	-0.2 (1.2)	0.1 (0.7)

CHAPTER 1. TRANSCRIPTOMIC RESPONSE TO INFLUENZA A
1.4. DISCUSSION *(H1N1)PDM09 VACCINE*

Table 1.2: HIRD batch balance

	Total n = 374	1 n = 87	2 n = 79	batch DN500165J n = 70	DN500166K n = 69	DN500167L n = 69
visit						
v1	40 (10.7%)	20 (23%)	20 (25.3%)	0 (0%)	0 (0%)	0 (0%)
v2	114 (30.5%)	24 (27.6%)	20 (25.3%)	24 (34.3%)	23 (33.3%)	23 (33.3%)
v3	109 (29.1%)	21 (24.1%)	20 (25.3%)	22 (31.4%)	23 (33.3%)	23 (33.3%)
v4	111 (29.7%)	22 (25.3%)	19 (24.1%)	24 (34.3%)	23 (33.3%)	23 (33.3%)
responder						
FALSE	80 (21.4%)	12 (13.8%)	36 (45.6%)	11 (15.7%)	9 (13%)	12 (17.4%)
TRUE	294 (78.6%)	75 (86.2%)	43 (54.4%)	59 (84.3%)	60 (87%)	57 (82.6%)
TRI	-0.1 (1.0)	-0.1 (1.0)	-0.4 (1.4)	0.1 (0.6)	-0.0 (0.8)	0.2 (0.6)

Chapter 2

Genetic factors affecting Pandemrix vaccine response

2.1 Introduction

2.1.1 Genetic factors affecting influenza vaccine response

Vaccination is the most effective way by which seasonal influenza is controlled², and the mechanism by which influenza vaccines are efficacious is by raising strain-specific antibodies protective against future infection⁷³. Humoral responses are influenced by vaccine-associated factors (e.g. type, dose, adjuvants), but are also a complex trait influenced by host genetics^{74,75}. Genetic variants associated with antibody response have been detected for vaccines such as hepatitis B, influenza, measles, rubella, and smallpox^{74,76}. For antibody response to seasonal influenza vaccines, studies have implicated genetic variation within cytokine genes, cytokine receptors⁷⁷; antigen processing and intracellular trafficking genes⁷⁸; immunoglobulin heavy-chain variable region loci⁷⁹; and specific **human leukocyte antigen (HLA)** alleles^{77,80}.

A potential mechanism through which genetic variation can play a causal role in influenza vaccine response is through altering the expression of genes as **expression quantitative trait loci (eQTLs)**. eQTL can have condition-specificity: an interaction between their effect on expression and different environmental contexts such as tissue or cell type^{81,82}. The mechanisms by which eQTLs interact with environment are of great interest; for example, cell type specificity can inform us about how expression is regulated in a cell type specific manner⁸³. In a vaccination context, an important subset of

pull in citations from intro

environment-interacting eQTLs are **response expression quantitative trait loci (reQTLs)**, defined as an eQTL whose effect interacts with external stimulation or perturbation. reQTL have been observed in many human cell types *in vitro*, or in the whole organism *in vivo*. As the pre- and post-stimulation environments are separated in time, a possible mechanism that leads to the observation of reQTL is a genotype-dependent change in gene expression between timepoints, which may underly genotype-dependent differences in antibody phenotypes.

2.1.2 Response expression quantitative trait loci for seasonal influenza vaccination

reQTL can be mapped considering a vaccine as an *in vivo* immune stimulation, looking for genotype-dependent changes in gene expression in immune cells. Little work has been done on vaccine-stimulated reQTLs, except one study conducted for the seasonal **trivalent inactivated influenza vaccine (TIV)**.⁷⁸ collected longitudinal data in 247 European adults: peripheral whole blood gene expression measured at four timepoints (day 0, 1, 3, 14), and antibody titres measured at three timepoints (day 0, 14, 28). They identified 20 genes with a cis-eQTL effect, expression correlation with antibody response, and either post-vaccination differential expression *or* a reQTL effect at that cis-eQTL. Genes involved in intracellular antigen transport and processing were enriched among those 20 genes.

2.1.3 Chapter summary

The HIRD cohort represents a unique opportunity for detecting genetic contributions to influenza vaccine response. In chapter 1, we observed global changes in gene expression after Pandemrix vaccination, as well as expression signatures correlated to degree of antibody response. For seasonal influenza vaccines, the contribution is small: antibody responses in adults are largely driven by non-genetic influences such as previous influenza vaccination or infection⁸⁴. As the Pandemrix vaccine is against the pdm09 pandemic strain that was not in seasonal circulation at the time the **Human Immune Response Dynamics (HIRD)** cohort was recruited (2010-11), with individuals mounting an expression response that was not recall-dominated¹⁸, the relative contribution of genetic factors to Pandemrix response may be greater.

distinction between expression/ab response is blurry here

straighten out tenses

In this chapter, I model the influence of common host genetic variation on longitudinal *in vivo* expression response to Pandemrix. I map cis-eQTL within each timepoint, accounting for ancestry, cell type abundance and unmeasured confounders, then call shared and reQTL effects from a joint model, looking for genes where the lead eQTL has a different effect size pre- and post-vaccination. Many of the strongest reQTL effects involve opposite signed effects on expression for the same variant at different timepoints. I detect a strong day 1 specific reQTL effect at *ADCY3*. Through modelling interaction of reQTL with cell type abundance estimates and statistical colocalisation with cell type specific QTL datasets, the reQTL signal was determined to be a monocyte-specific effect likely driven by increase monocyte abundance at day 1.

1 more sentence to round off context

2.2 Methods

2.2.1 Genotype phasing and imputation

Prior to imputation, 213277 monomorphic variants that provide no information for imputation were removed. Imputation for the autosomes and X chromosome was conducted using the Sanger Imputation Service*, which involves pre-phasing with EAGLE2 (v2.4), then imputation with PBWT (v3.1) using the Haplotype Reference Consortium (r1.1) panel. variants were lifted-over from GRCh37 to GRCh38 coordinates using CrossMap. Poorly-imputed variants with INFO < 0.4 or post-imputation missingness > 5% were removed, leaving 40290981 variants.

2.2.2 Overall strategy for detecting reQTLs

Since the aim of this chapter is to identify genetic variation that affects expression response to vaccination, it may seem most direct to model the change in each individual's expression after vaccination as the response variable. This approach has been applied for identification of condition-specific eQTL, typically with the response taking units of log fold change between conditions (e.g.^{85–87}). Although potentially powerful if eQTL effects are small and opposite between conditions⁸⁶, it is analogous to the “change score” approach, which can suffer from regression to the mean, and increased

*<https://imputation.sanger.ac.uk/>

CHAPTER 2. GENETIC FACTORS AFFECTING PANDEMIX

2.2. METHODS

VACCINE RESPONSE

Can this really demonstrate genotype-dependent change in gene expression between timepoints? i.e. need understand how the change score/ANCOVA approaches differ from repeated measures ANOVA differ from the interaction/stratified approach I take?

why I didn't just do a mega-analysis in chapter 2 then, given I haven't any evidence if it's better or worse than Bayesian meta-analysis in that context.

uncertainty from the variance sum law if effects between conditions have positive covariance^{88,89}. Instead, I map **eQTLs** within each of three timepoint conditions (day 0 pre-vaccination, day 1, and day 7), and find **reQTLs** by looking for **eQTLs** that have different effects between conditions.

Within each timepoint, recall the the **HIRD** dataset includes expression measured by both array and **RNA-sequencing (RNA-seq)**. As discussed in [subsubsection 1.2.9.2](#), it is difficult to directly estimate the between-studies heterogeneity when the number of studies is small, and Bayesian meta-analysis was preferred for combining array and **RNA-seq differential gene expression (DGE) estimates**. That method does not scale to **eQTL** analysis, where the number of tests is large, in the order of thousands of tests per gene, versus the handful **DGE** contrasts per gene performed in [chapter 1](#). Instead, I perform a mega-analysis within each timepoint, first merging array and **RNA-seq** expression estimates into a single matrix with **ComBat**⁴². For comparison purposes, analyses were also run using in the array and **RNA-seq** samples separately.

Defining whether an **eQTL** is shared between conditions can be a tricky business. Naively, one can map **eQTLs** separately in each condition, then assess the overlap of significant associations between conditions. This underestimates sharing due to the difficulty of distinguishing true lack of sharing from missed discoveries from incomplete power within each condition. Condition-by-condition analysis also makes no attempt to borrow information across conditions for mapping shared associations^{90–92}. Counterintuitively, a joint multivariate analysis may be more powerful even when associations are not shared across all conditions⁹³.

A variety of models have been employed for joint **eQTL** mapping, including the use of classical multivariate methods such as **multivariate analysis of variance (MANOVA)**⁹⁴, frequentist meta-analyses (e.g. **Meta-Tissue**⁹⁵, **METASOFT**), and Bayesian models (e.g. **eQtlBma**⁹⁰, **MT-HESS**, **MT-eQTL**). Joint mapping has been repeatedly demonstrated to be more powerful than condition-by-condition analysis, and recent methods are now computationally efficient when scaling to large numbers of conditions and variants tested (e.g. **RECOV**⁹⁶, **mashr**⁹¹, **HT-eQTL**⁹²). In this chapter, I apply **mashr**⁹¹ for the estimation of **eQTL** effects across my three timepoints. **mashr** learns patterns of correlation among multiple conditions empirically from condition-by-condition summary statistics, then applies shrinkage to provide improved

posterior effect size estimates, and compute measures of significance per condition.

2.2.3 Controlling for population structure with linear mixed models

There is population structure due to ancestry in the **HIRD** cohort, which was addressed in **DGE** analyses by treating the top **principal components (PCs)** of the genotype matrix as covariates for large-scale population structure ([subsection 1.2.5](#)). In the context of **eQTL** mapping, where the aim is to assess the marginal effect of a single genetic variant on expression, it is even more important that the confounding effect of population structure is properly controlled, or test statistics may be inflated. An efficient approach is the **linear mixed model (LMM)** with a random effect that incorporates genetic correlation between individuals, usually in the form of a kinship matrix, into the covariance of that random effect^{28,97,98}. The **LMM** approach has the advantage of not only modelling large-scale population structure, but also cryptic relatedness (the presence of closely related individuals in a sample assumed to consist of unrelated individuals⁹⁹) due to finer-scale effects such as family structure⁹⁸.

add some indication of how much inflation can be reduced by LMMs

2.2.3.1 Estimation of kinship matrices

When testing a variant for association using **LMMs**, to avoid loss of power from “proximal contamination”, the kinship matrix used should not include that variant¹⁰⁰. A simple way to avoid this is to compute a **leave-one-chromosome-out (LOCO)** kinship matrix using all variants on chromosomes other than the tested variant’s chromosome¹⁰¹.

I estimated kinship in the **HIRD** data from common autosomal variants, using **LDAK** (5.0), which computes kinship matrices adjusted for bias caused by **linkage disequilibrium (LD)**¹⁰². Filtered, pre-imputation sample genotypes from [subsection 2.2.1](#) were pruned to **MAF** > 0.05. A kinship matrix was computed for each autosome, then combined into a single genome-wide matrix using **LDAK --join-kins**. To obtain a **LOCO** kinship matrix for each autosome, each autosome’s kinship matrix was then subtracted from this genome-wide matrix (**LDAK --sub-grm**).

add chr1 loco kinship matrix as example, note the estimates for self-relatedness on the diagonals are not constrained to be 1

2.2.4 Additional eQTL-specific expression preprocessing

There are a number of transformations often applied to expression data before **eQTL** mapping, such as the rank-based **inverse normal transformation (INT)** (e.g. GTEx v8¹⁰³), which conforms often non-normal expression data to an approximately normal distribution, and reduces the impact of expression outliers. In the context of genetic association studies, the practice of applying rank-based **INT** to phenotypes has been criticised for only guaranteeing approximate normality of residuals when effect sizes are small, and potential inflation of type I error, especially in linear models that include interactions¹⁰⁴. In multi-condition datasets, these transformations are also typically applied within conditions (e.g. within each tissue individually in GTEx v8¹⁰³). Another common transform is standardising (centering and scaling to zero mean and unit variance) (e.g. eQTLGen Consortium¹⁰⁵), often done so that effects across genes and studies can be comparably interpreted in units of standard deviation expression¹⁰⁶.

I performed simulations to evaluate the effect of these transformations on reQTL detection between a hypothetical baseline and day 1 post-vaccination condition. Expression values on the log scale were simulated with the **eQTL** slope (beta) set to specific values corresponding to six scenarios for six gene-variant pairs (Fig. 2.1). The simulated scenarios were subjected to rank-based **INT** (Blom method¹⁰⁴), standardisation (both centering and scaling), scaling-only, and centering-only transformations. Transformations were applied both within each condition and without separating conditions.

The boxed facets in Fig. 2.1 represent undesirable effects of transformations on **reQTL** calls. For example, rank-based **INT** induces false shared **eQTL** effects in scenarios 4 and 5. In general, transformations that scale within condition are not appropriate, as different variance between conditions can be what drives a **reQTL** effect. Scaling without separating conditions can also be problematic, since the total variance also contributes to the **reQTL** effect size. For example, scenarios 2 and 4 have the same 1 unit increase in slope pre-transformation (the same fold-change between conditions), but after scaling-only the beta increases are $0.75 - 0 = 0.75$ and $0.8 - 0.4 = 0.4$ respectively—eQTL 4 now looks like a weaker effect.

In light of these simulations, I decided that neither rank-based **INT** nor standardisation were appropriate given my intent of detecting **reQTLs** between conditions. Only the centering-only transformation avoided both false

shared effects and preserves relative **reQTL** effect sizes between genes. The simple inclusion of an intercept term in the **eQTL** model already achieves this. Not performing any rank-based transform does lose the advantage of reining in outliers. The expression data have already been preprocessed to remove low-expression outliers in subsection 1.2.7, but automatic outlier exclusion based on **standard deviation (SD)** thresholds at the **eQTL** mapping step could be considered in future implementations¹⁰⁵. Note that many preprocessing steps done prior to this stage in the pipeline (e.g. variance-stabilisation, ComBat batch effect correction) are also expression transformations, but I only consider the preservation of **reQTL** effects defined from expression values post-adjustment for those technical effects to be important.

add sample sizes and
model for expression sim

2.2.5 Estimation of cell type abundance from expression

Peripheral blood mononuclear cell (PBMC) samples are a mixture of immune cells, and a fixed input of RNA extracted from that mixture is used to estimate expression, so estimates for genes that have cell type specific expression depend on the relative proportions of each cell type in each sample. These proportions shift after Pandemrix vaccination¹⁸, and **eQTL** effects can also be cell type specific. As genotype can be assumed to stay constant, it is valid to compare the effect of genotype on expression between multiple timepoints to call **reQTLs**, but changes in cell type abundance confound this by modifying both expression and the effect of genotype on expression. Immune cell abundance also varies naturally between healthy individuals^{84,107}, so it is important to model these effects even at baseline.

determine appropriate
citations from existing
refs in intro

Cell type abundance directly measured via **fluorescence-activated cell sorting (FACS)** are only available for a small subset of **HIRD** individuals (subsection 1.2.1), so I derived cell type abundance estimates from the expression data as an alternative. Such estimates have previously been used in **eQTL** analyses from bulk samples where cell type specific effects are expected^{83,108,109}. As the estimates are based on the expression of multiple genes, is not entirely circular to use them as covariates in this way for genewise **eQTL** models. I selected **xCell**¹¹⁰, which previously been shown to outperform other deconvolution methods for cell type specific **eQTL** mapping in blood⁸³. **xCell** computes enrichment scores based on the expression ranks of approximately 10000 signature genes derived from purified cell types, works for both array and **RNA-seq** expression data, and implements

CHAPTER 2. GENETIC FACTORS AFFECTING PANDEMIX
2.2. METHODS

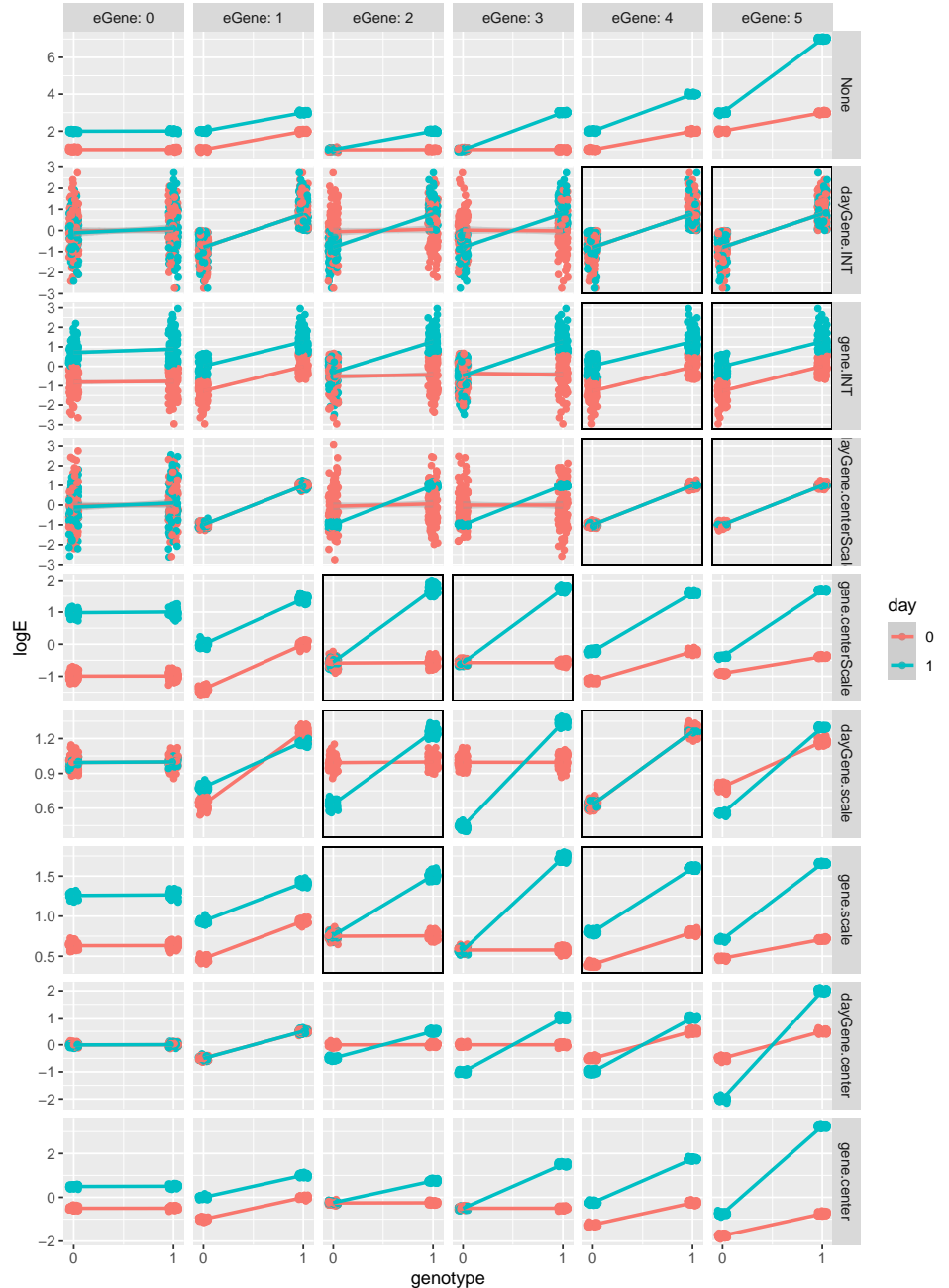


Figure 2.1: Simulated log scale expression in two conditions for six genes (columns) representing six different scenarios: Scenario 0 has no **eQTL**, scenario 1 is a shared eQTL ($\beta = 1$), scenario 2 is a **reQTL** where β increases from 0 to 1, scenario 3 is a **reQTL** where β increases from 0 to 2, scenario 4 is a **reQTL** where β increases from 1 to 2, and scenario 6 is a **reQTL** where β increases from 1 to 4. Rows represent the effect of different expression transformations across samples, conducted both within condition, and including both conditions.

“spillover compensation” to reduce dependency of estimates between related cell types¹¹⁰. xCell was originally developed for tumor samples, so many of the built-in cell types are not expected in PBMC. Reviewing the literature to find which broad classes of peripheral blood cell types are commonly-expected in the PBMC compartment^{109,111,112}, I selected 7/64 of the built-in cell types: CD4⁺ T cells, CD8⁺ T cells, B cells, plasma cells, natural killer (NK) cells, monocytes, and dendritic cells (DCs). Array and RNA-seq data from subsection 1.2.8 and subsection 1.2.7 were processed through xCell separately. The large batch effect present in the array expression was first removed using ComBat. Finally, enrichment scores were standardised, so that a score of zero estimates the average abundance of that cell type across all timepoints (Fig. 2.2 and Fig. 2.3).

As with actual cell type abundances, the enrichment scores are correlated. Multicollinearity will be a problem for interpreting effect size estimates when these scores are used as predictors downstream. To prune the number of scores, I performed a principal component analysis (PCA) of the cell type scores across samples, determined the number of principal components that exceed the eigenvalues-greater-than-one rule of thumb¹¹³, then selected only the one cell type with the highest contribution for each of those components. In both array and RNA-seq datasets, the number of components retained was three, and the selected cell types were monocytes, NK cells, and plasma cells (Fig. 2.4). The choice to use the actual cell type scores over principal components directly as covariates is a sacrifice of orthogonality for interpretability.

add comment on existence of chosen cell types in samples, and clustering by visit

Scores were validated against FACS measurements in the subset of individuals that had them. Depending on each panel’s gating strategy for each cell subset, the FACS data were in units of either absolute counts, or percentage of the previously gated population. A rank-based INT was applied within each panel and cell subset, so that the transformed measure could be compared between individuals for each subset (¹¹⁴ takes a similar approach for cell abundance data using a quantile-based INT). Missing values were imputed with missForest, a random forest imputation method suitable for high-dimensional data where $p \gg n$. Although the increase in xCell score for monocytes at day 1 and plasma cells at day 7 reflect the increases in these cell types observed by¹⁸, overall correlation between xCell and FACS was weak (Fig. 2.5). Weighing the downside of having imperfect estimates of cell

no need for both size and color, use one for contribution percent

add info on the markers used for the chosen FACS counterparts

CHAPTER 2. GENETIC FACTORS AFFECTING PANDEMRIX
2.2. METHODS VACCINE RESPONSE

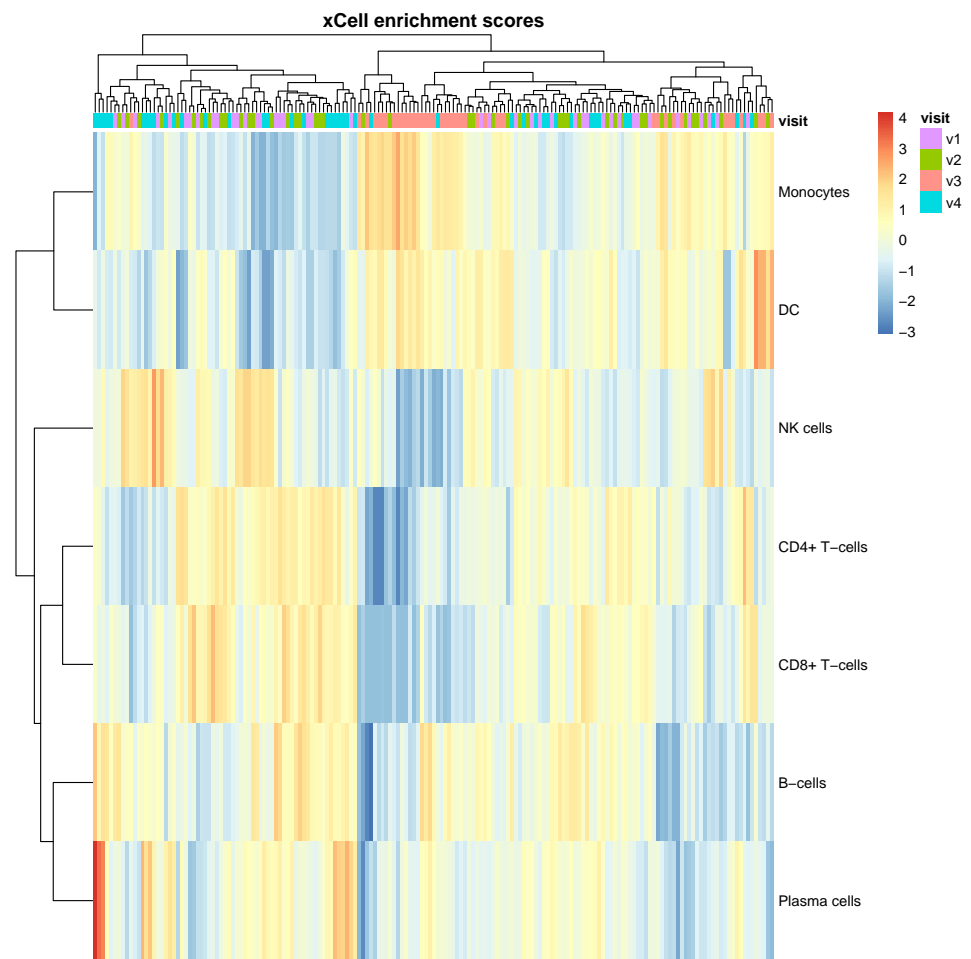


Figure 2.2: Standardised xCell enrichment scores for seven **PBMC** cell types in array samples.

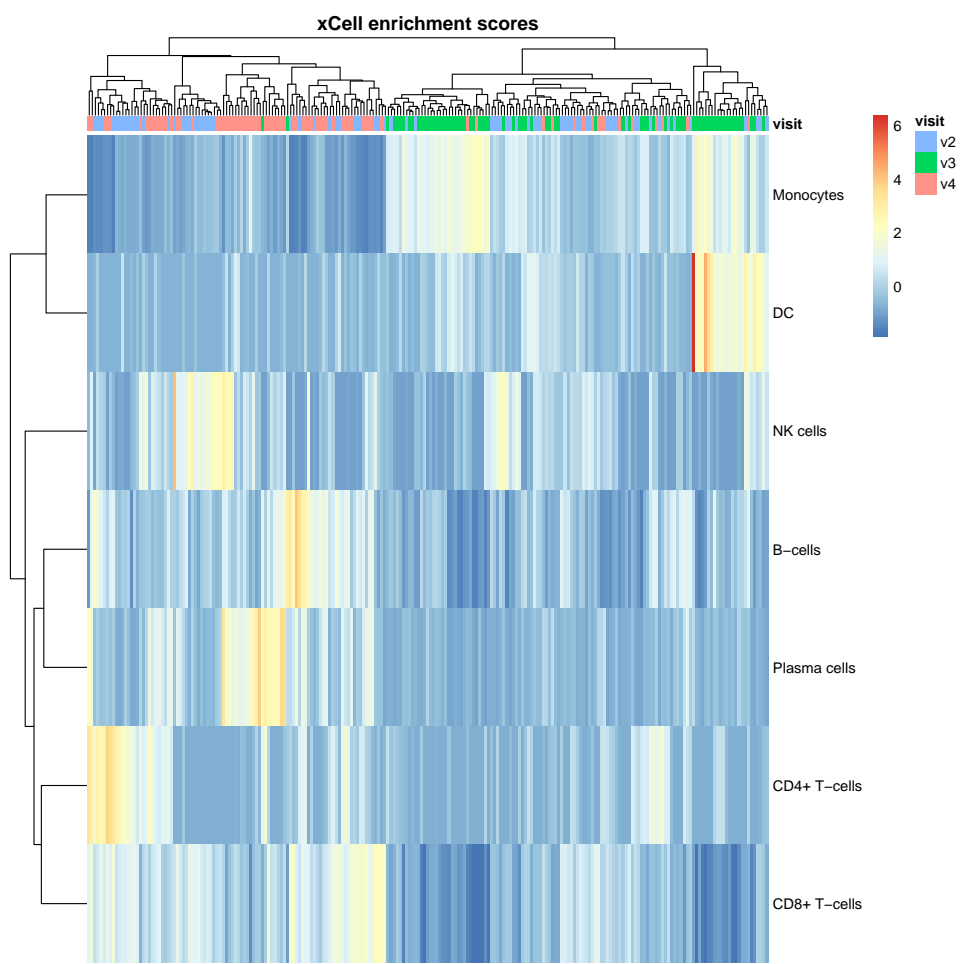
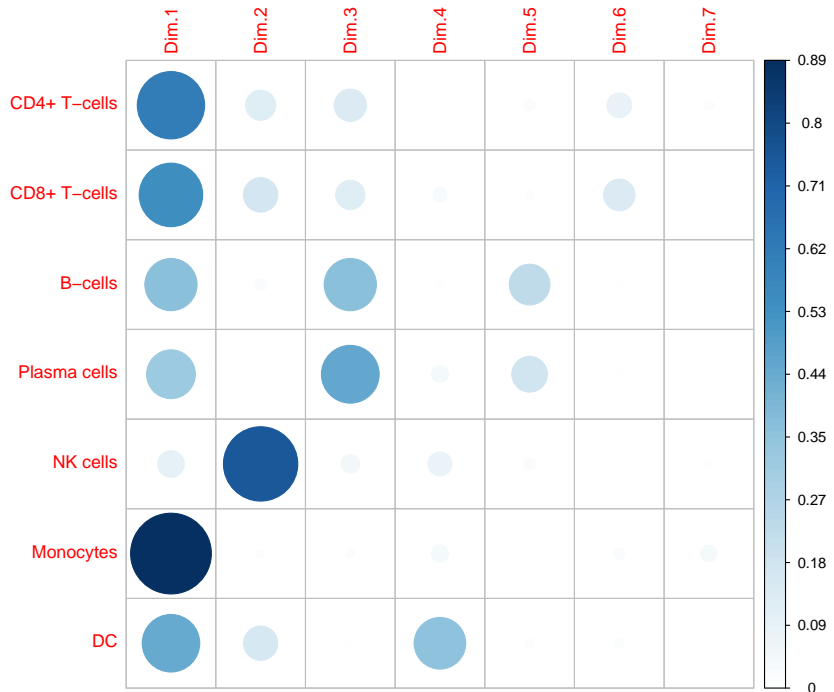
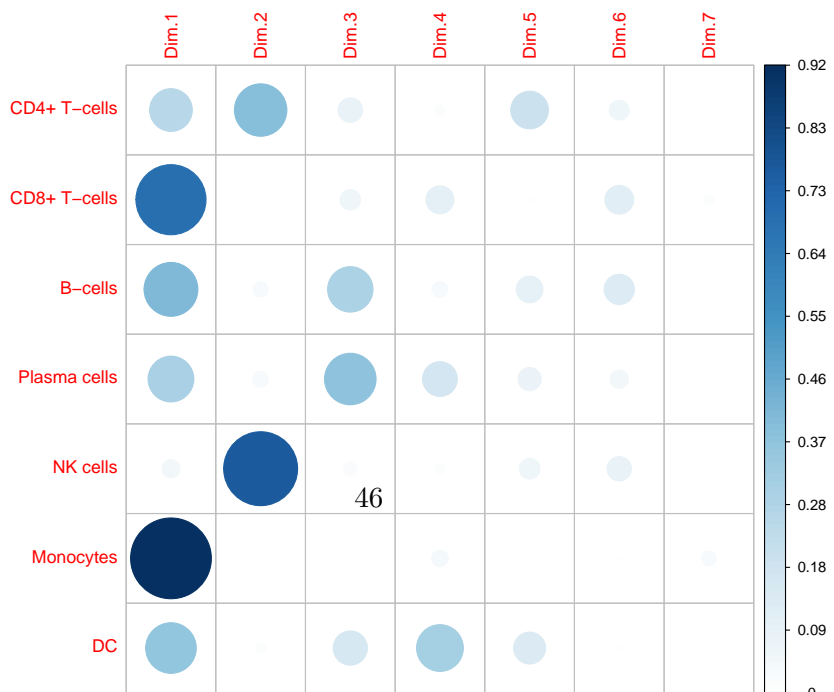


Figure 2.3: Standardised xCell enrichment scores for seven **PBMC** cell types in **RNA-seq** samples.

CHAPTER 2. GENETIC FACTORS AFFECTING PANDEMRIX
2.2. METHODS VACCINE RESPONSE



(a) Array estimates.



type abundance against the downsides of not accounting for abundance, or excluding samples without **FACS** measures, I chose to continue the analysis using the xCell scores.

get subset size

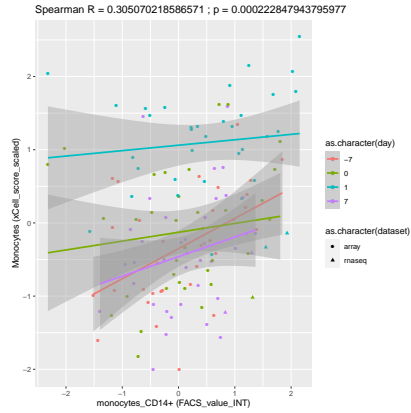
2.2.6 Finding hidden confounders using factor analysis

Apart from cell type abundance, a myriad of other unmeasured variables contribute to expression variation. Hidden determinants of expression variation were learnt using PEER¹¹⁵. As recommended by¹¹⁵, between-sample normalisation and variance stabilisation **RNA-seq** data was performed using **DESeq2::vsn**. ComBat was applied to first merge array and **RNA-seq** data into a single log scale expression matrix per timepoint, treating the largest global effects on expression—the two array batches and three **RNA-seq** library prep pools (Fig. 1.14)—as known batch effects. Given known covariates (intercept, sex, four genotype PCs from subsection 1.2.5 representing ancestry, and the three xCell scores estimated above), PEER was used to estimate additional hidden factors that explain variation in expression matrix. Factors are assumed to be unmeasured confounders that have global effects on a large fraction of genes, whereas a **cis-eQTL** will typically only have local effects, so including factors as covariates should not introduce dependence with the genotype term, but should soak up some of residual variation, improving power to detect **cis-eQTLs**. The analysis was run per timepoint, otherwise global changes in expression between timepoints induced by the vaccine would be recapitulated as factors.

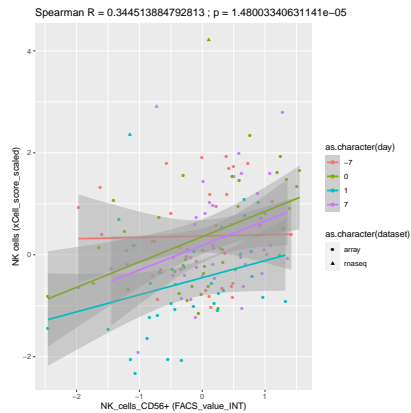
Correlating the estimated factors to a larger set of known covariates reveals many correlations with xCell estimates, indicating that cell type abundance does indeed have substantial global effects on the expression matrix. There is little correlation with known array or **RNA-seq** batch effects, indicating ComBat did an adequate job of removing batch- and platform-dependent global effects on expression (Fig. 2.6). Note that I did not leave this adjustment for PEER to perform, as ComBat estimates centering and scaling factors per gene to adjust for batch effects, whereas the use of PEER factors represent a mean-only adjustment. Given the severity of the batch effect in this dataset, especially between platforms, mean-only adjustment may be insufficient⁴⁵.

remake this with only top k factors, and prune the possible covariates

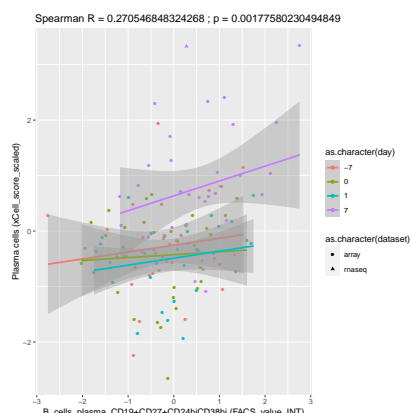
CHAPTER 2. GENETIC FACTORS AFFECTING PANDEMIX
2.2. METHODS VACCINE RESPONSE



(a) Monocytes.



(b) NK cells.



(c) Plasma cells.

Figure 2.5: Correlation between standardised xCell scores and normalised FACS measurements for a similar immune subset, in the subset of individuals with FACS data.

**CHAPTER 2. GENETIC FACTORS AFFECTING PANDEMRIX
VACCINE RESPONSE**

2.2. METHODS

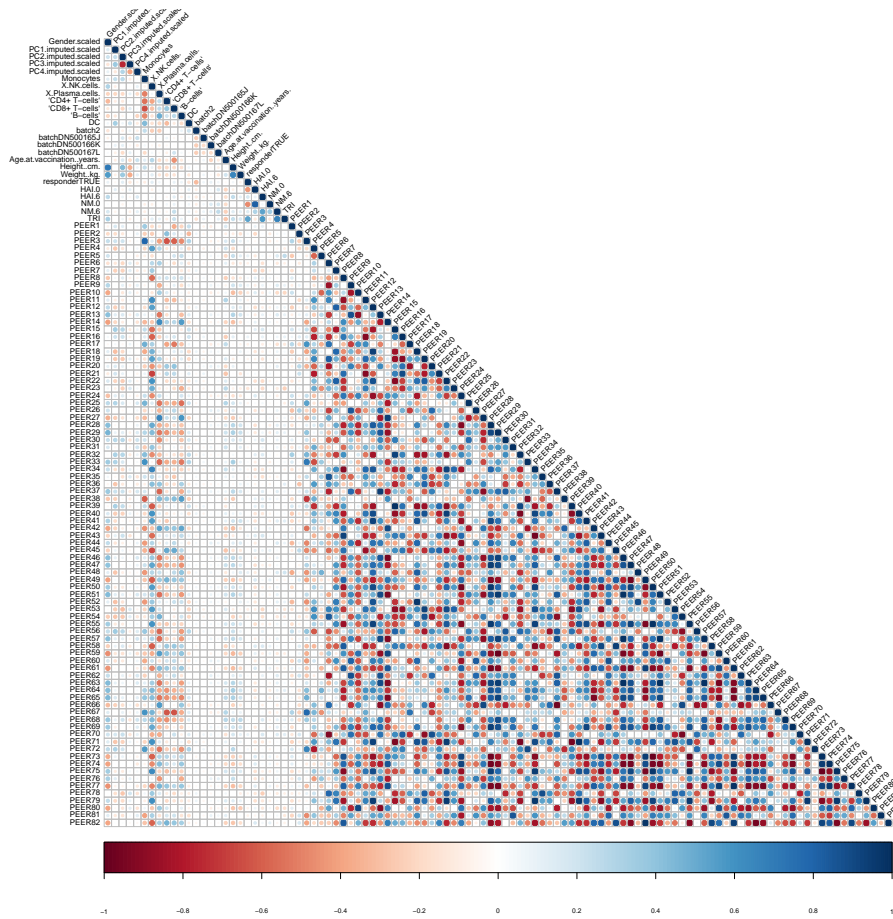


Figure 2.6: Correlation of PEER factors to known factors and other possible covariates. Note that PEER factors are not constrained to be orthogonal, so correlations to known factors are expected.

2.2.7 eQTL mapping per timepoint

The performance of various software implementations of LMMs specialised for genetic association studies are highly comparable; the specific choice of implementation can usually be made on the basis of computational efficiency²⁸. I map eQTLs within each timepoint using LIMIX¹¹⁶, which implements univariate and multivariate LMMs with one or more random effects.

Imputed genotype probabilities were converted to alternate allele dosages using bcftools (1.7-1-ge07034a). Variants with sample $\text{AC} < 15$ within each timepoint were excluded.

At each of 13570 genes, at all cis-variants within within $\pm 1\text{Mb}$ of the transcription start site (TSS), I fit the following model to map eQTL:

$$Y = 1 + \text{sex} + \sum_{i=1}^4 PC_i + \sum_{i=1}^3 xCell + \sum_{i=1}^k PC_i + \beta G + \mathbf{u} + \epsilon \quad (2.1)$$

where the eQTL effect size of interest is the slope of the genotype fixed effect β , and \mathbf{u} is a random effect with zero mean and covariance matrix proportional to the LOCO kinship matrix*.

PEER factors are automatically weighted such that the variance of factors tends to zero as more factors are estimated, hence continuing to add more and more factors as covariates will not continue to improve eQTL detection power, and eventually the model degrees of freedom will be depleted. To optimise k , the number of factors to include as covariates†, Per-timepoint eQTL mapping was performed in chromosome 1, iteratively increasing the number of factors until the number of eQTLs detected plateaus. I settled on a final choice of $k = 10$ factors for pre-vaccination, 5 factors for day 1, and 5 factors for day 7 (Fig. 2.7).

2.2.8 Joint eQTL analysis across timepoints

Joint analysis was conducted with mashr⁹¹, at 40197618 gene-variant pairs (mean of 2962 tests per gene) for which summary statistics from within timepoint mapping were available in all three timepoint conditions. The mashr

add approximate MAFs,
then cite hierarch paper

add note on treating x
chrom variants with cau-
tion

lift proper vector nota-
tion from limix, then redo
this with a timepoint sub-
script

add formulation of the
0-mean random effect to
show exactly how the kin-
ship matrix is used

recheck if did I do a SNPs
only filter

*For chromosome X variants, no LOCO matrix is available from LDAK, so the matrix for chromosome 1 is used.

†I avoid the commonly-performed two-stage approach of treating PEER residuals as expression phenotypes, as the degrees of freedom seen downstream will be incorrect, which can have a substantial effect on estimates at this modest sample size.

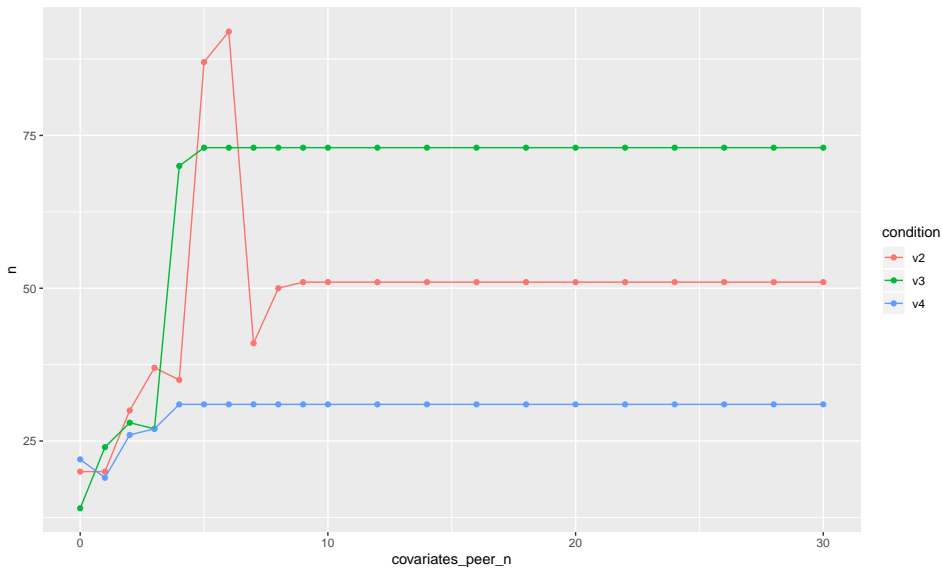


Figure 2.7: Number of significant eGenes detected on chromosome 1 (hierarchical Bonferroni-Benjamini-Hochberg (BH) FDR < 0.05) as a function of the number of PEER factors included as covariates k.

model incorporates multiple canonical (the identity matrix etc.) and data-driven covariance matrices to represent patterns of effects across conditions (in this case, 3×3 matrices). Data-driven covariance matrices are derived by dimension reduction of a strong subset of tests likely to have an effect in at least one condition. I took the most significant variant per gene per condition, which ensures strong condition-specific effects are included (Fig. 2.8), then further filtered to only nominally significant tests, resulting in a strong subset of 45962 tests.

The mash model was trained on a random subset of 200000 tests, using the Exchangeable Z-scores model⁹¹. The correlation of null tests between conditions, important to account for due to the repeated measures structure of the data, was estimated using `mashr::estimate_null_correlation`. The fitted model was used as a prior to compute posterior effects and standard errors for all tests through shrinkage. A condition-specific Bayesian measure of significance **local false sign rate (lfsr)** is returned, which can be interpreted as the probability given the data, that the declared sign of the effect is incorrect.

move lfsr explanation
prior to ashr in dge chapter

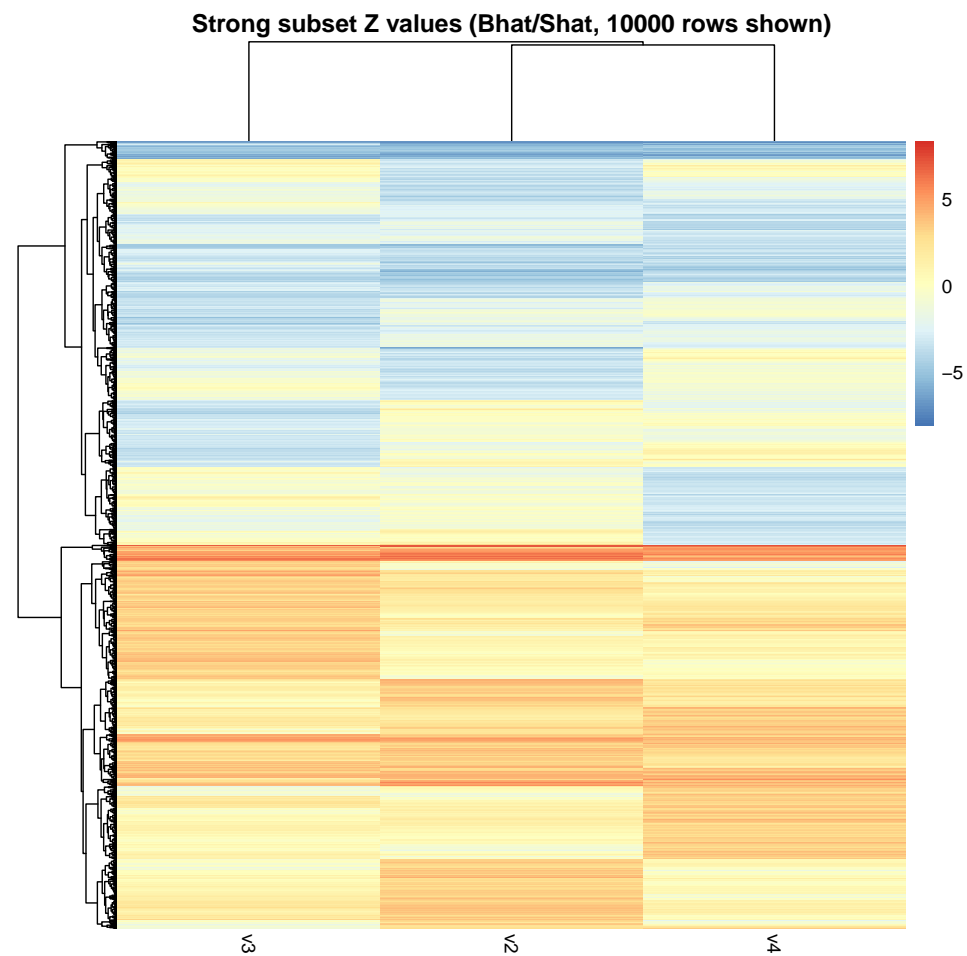


Figure 2.8: Clustering of within-timepoint Z scores in the strong mashr subset (random sample of 10000/45962 tests), confirming the presence of strong condition-specific effects.

2.2.9 Defining shared and response eQTLs

Many of the tested variants for each gene will be in high LD. To unambiguously select a lead eQTL variant per gene, I selected the variant with the lowest lfsr in any condition, breaking ties by highest imputation INFO, highest MAF, shortest distance to the TSS, and genomic coordinate. Sharing was then evaluated for that gene-variant pair across all three conditions.

Thresholding on the lfsr is not appropriate for determining sharing, as the difference between significant and non-significant effect estimates in two conditions is not necessarily significant^{117,91} provides a heuristic that two effects are shared by magnitude if they have the same sign, and are also within a factor of 2 of one another, but this does not consider the posterior standard error of the estimates. Between a pair of effects in two conditions, I compute a z score for the difference in effects^{118,119}:

$$z = \frac{\beta_x - \beta_y}{\sqrt{\sigma_x^2 + \sigma_y^2 - 2\sigma^2(x, y)}} \quad (2.2)$$

This strategy has been applied to call reQTLs by¹²⁰, assuming posterior pairwise covariance of effects is zero $\sigma^2(x, y)$. Unlike a test for difference implemented using a genotype-condition interaction term in a joint regression model, homoscedasticity of errors is not assumed for all conditions¹¹⁸. The z score can be compared to a standard normal to obtain a Wald test p value, the null hypothesis being a difference of zero. I use nominal p value < 0.05 as a heuristic threshold to define reQTL effects that are strong (like the mashr recommended 2-fold threshold), rather than a formal measure of significant difference. Effects are only compared if at least one of the two effects has lfsr < 0.05, to avoid sharing being driven by null effects.

not sure whether this is conservative or anti-conservative

2.2.10 Replication of eQTLs in a reference dataset

To validate the eQTL mapping approach, I estimate the replication of significant eQTLs in a large independent reference. Due to the lack of large sample size eQTL maps specific to PBMC, I use the GTEx v8 whole blood dataset as my reference dataset (n=670, 51.2% eGene rate). For lead variants called as significant in the HIRD dataset at a given lfsr threshold, I lookup the nominal p value for that variant in GTEx (where the variant exists in both datasets). I applied `qvalue::qvalue_truncp` to estimate the proportion of

those GTEx nominal p values that are null (π_0), the compute a measure of replication $\pi_1 = 1 - \pi_0$.

The mega-analysis has comparable replication rate to RNA-seq-only analysis for shared eQTLs at moderately stringent lfsr thresholds up to 10^{-5} (Fig. 2.9). Past this, as the π_1 procedure assumes a well-behaved p value distribution in $[0, 1]$, reliability declines due to the number of p values being too small*, or the maximum p value being too far from 1. The numbers of reQTLs were too low to assess replication using this method, and one might not expect them to replicate in a baseline dataset such as GTEx whole blood, especially for those reQTLs significant only at post-vaccination timepoints. As the mega-analysis has a higher eGene rate (50.75 % vs. 29.91 %) compared to the RNA-seq-only analysis, with similar replication, I assume this represents a power advantage from having larger a sample size, rather than technical effects from merging the expression data.

RNAseq does test about
7000 more genes though...

2.2.11 Genotype interactions with cell type abundance

If the abundance of a particular cell type does truly modify the eQTL effect, then an interaction term between genotype and cell type abundance is required, otherwise the regression slope of the eQTL will represent an average across the abundance range for that cell type; one can not correct for this modification just by including the main effect for cell type abundance. Given the modest sample size, I use the two-step approach used by others^{108,109,120,121}, where tests for interaction are only performed at a subset of tests, often the lead eQTL variant for each gene. The key to the two-stage approach is that if the estimates for the interaction effect are sufficiently independent from the estimates of the main effect from main-effect only models, the type I error can be controlled based on the number of interactions that are actually tested, rather the number of interactions that could have been tested for^{121,122}. It is unclear whether this assumption holds, as the size of the main effect may contribute to power for detecting interaction effects. As the main purpose of the interaction analyses is scanning for cell type effects at detected reQTLs, I chose to test for interactions only at the lead eQTL variant for each gene with a significant main eQTL, then apply the BH false discovery rate (FDR), as used by others^{120,121}.

*<https://github.com/StoreyLab/qvalue/pull/6#commitcomment-26277751>

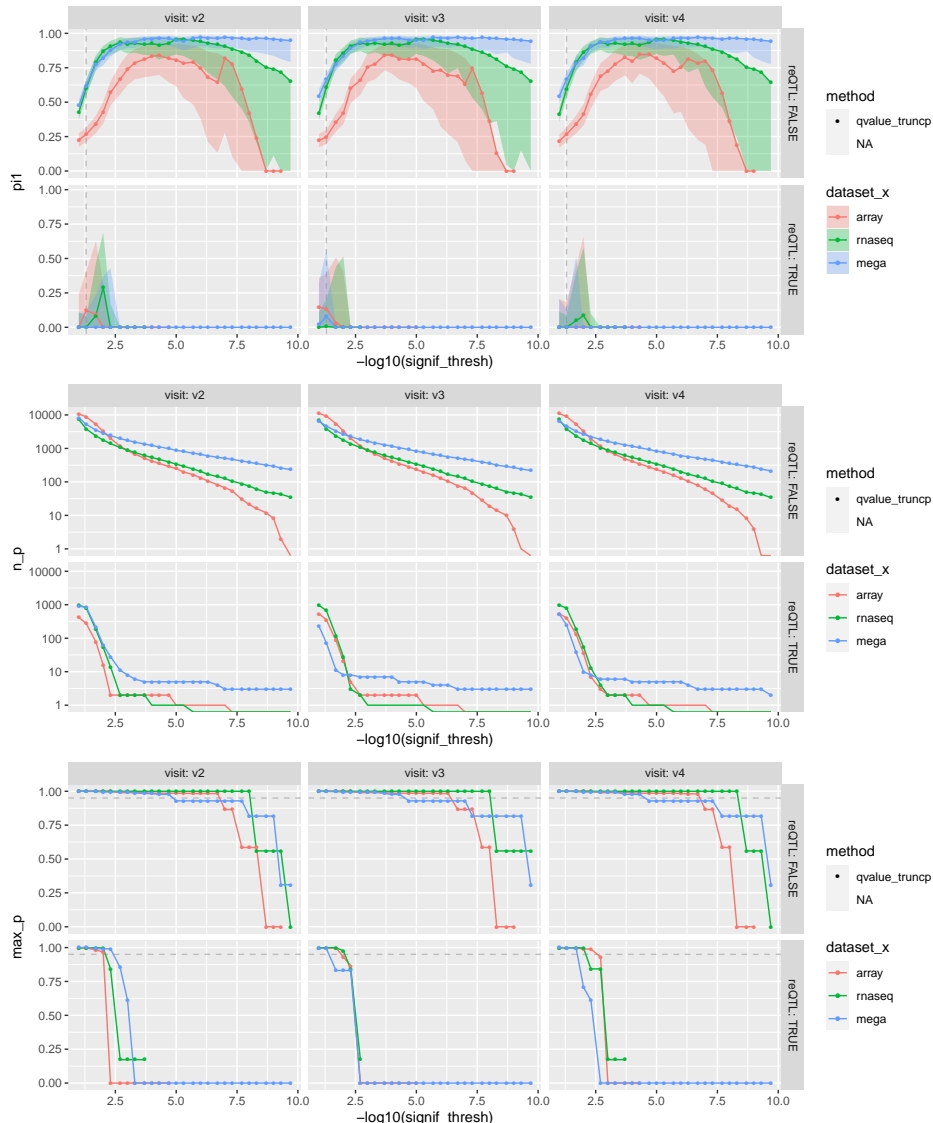


Figure 2.9: Effect of HIRD Ifsr threshold on GTEx whole blood replication rate (π_1), number of p values used to compute π_1 , and maximum p value among those p values; for shared and reQTL called from the array-only, RNA-seq-only and mega-analysis pipelines. Shaded region for π_1 represents the 5th-95th percentile range of 1000 bootstraps.

Models in interactions between genotype and other predictors were fit using `lme4qtl`. The model specification identical to [Equation 2.1](#), with the addition of three interaction terms between genotype and each xCell score. Significance is assessed using the likelihood-ratio test versus the nested model with no interaction terms.

add note here that although peer is correlated with xcell, interactions are only formed with xcell, so the interaction term can be interpreted per unit of genotype increase when xcell=0

this analysis is incomplete, and is one of the things I would suggest to round off this chapter

2.2.12 TODO Statistical colocalisation

- if adding coloc analysis, add <https://github.com/jrs95/hypocoloc> methods here

2.3 Results

2.3.1 Mapping reQTLs to Pandemix vaccination

Within each timepoint condition (day 0 pre-vaccination, day 1, and day 7), **cis-eQTLs** ($\pm 1\text{Mb}$ of the TSS) were mapped using LIMIX, then joint analysis of effects was done using `mashr` to obtain posterior effect size and standard errors. At $\text{lfsr} < 0.05$, 6887/13570 genes (50.75 %) were eGenes (genes with a significant eQTL) in at least one timepoint. To sidestep the issue of multiple tested variants per gene being in LD, the most significant eQTL variant across all timepoints was selected as the lead variant for each eGene, then **reQTLs** were defined by comparing the effect size of this lead eQTL between each pair of timepoints. Most eQTLs were shared across timepoints; 1154/6887 (16.76 %) eQTLs were classified as reQTLs between any pair of timepoints (nominal p difference < 0.05).

if it would be interesting to compare the sharing estimate condition by condition approach to mashr, then redo and pull in eigenmt-bh values

[Fig. 2.10](#) illustrates the difference between calling sharing using a significance threshold versus difference in betas approach. For instance, day 0 was the timepoint with the largest number of eGenes, reflecting the larger sample size compared to other timepoints. Although there are 1427 eGenes significant at only day 0, there are only 646/1427 reQTL among them, as the effect size at day 0 does not differ significantly when compared to day 1 or day 7 for the remainder. The strongest eQTLs with the highest proportion of variance explained (PVE)* are shared between timepoints, highlighting the power advantage for mapping shared effects granted by joint analysis.

actually, i've found that my PVE approximation is basically rescaled abs(Z), so pve is a bit pointless if we already have z, and doesn't really help with comparability between genes with diff var/MAF

*TODO: add to methods <https://journals.plos.org/plosone/article/file?type=supplementary&id=info:doi/10.1371/journal.pone.0120758.s001>

CHAPTER 2. GENETIC FACTORS AFFECTING PANDEMRIX
VACCINE RESPONSE

2.3. RESULTS

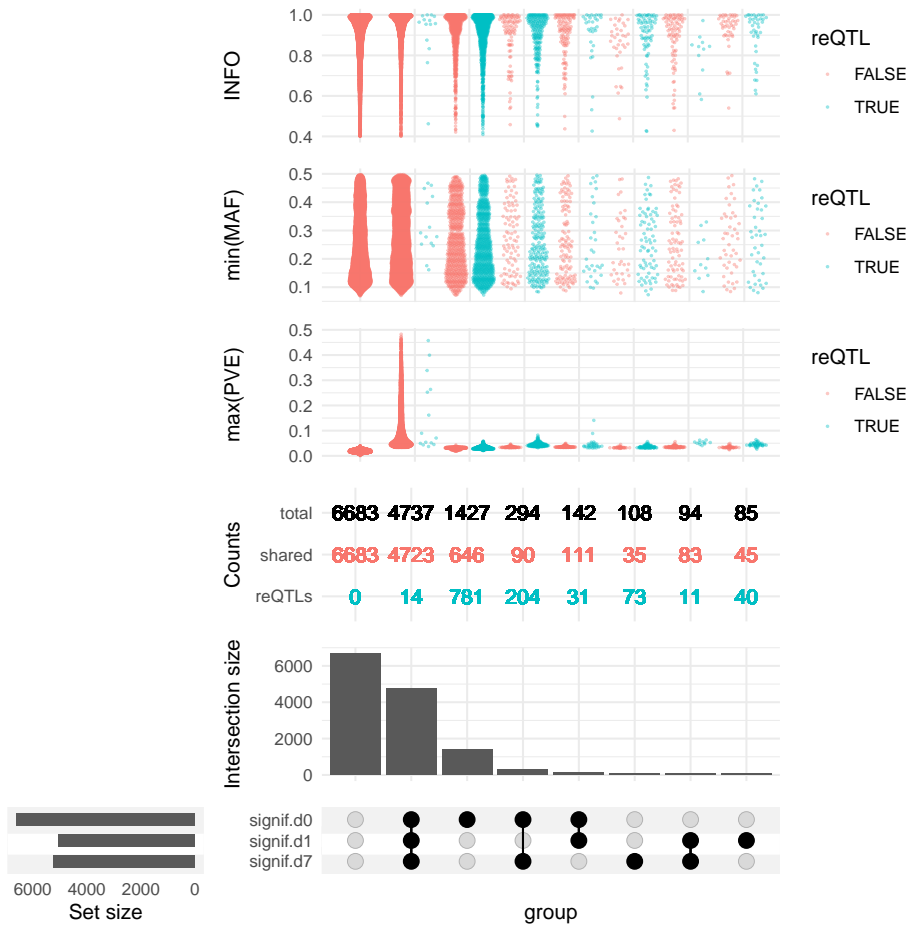


Figure 2.10: Summary of eQTL mapping results at 13570 genes-lead eQTL pairs, with intersections based on significance ($\text{lfsr} < 0.05$). Counts of shared eQTLs and reQTLs; and distribution of INFO score, min MAF across timepoints, and max PVE across timepoints for those lead variants are shown above each intersection.

2.3.2 Characterising reQTLs post-vaccination

As detection power is greatest at day 0, I focus on eQTLs that are reQTLs between day 0 and either day 1 or day 7 post-vaccination, and are significant at the corresponding timepoint: 819 reQTL between day 1 and day 0, and 1002 reQTL between day 7 and day 0 (Fig. 2.11). Gene set enrichment analysis on the eGenes targets for these sets of reQTLs did not detect any significant enrichments (gprofiler2, g:SCS adjusted $p < 0.05$). Many of the reQTL that satisfy this criteria have opposite effects pre- and post-vaccination—as lfsr quantifies uncertainty in the sign of the effect, I do not compare the sign unless the reQTL is also significant at day 0. Shared eQTLs are enriched close to the TSS, whereas reQTLs are distributed across the cis- window.

The strongest reQTL at day 1 was for *ADCY3* (p difference = 8.68×10^{-6} , BH FDR = 0.118), where the reQTL variant explained approximately 1.86 % of expression variation at day 0, increasing to 14.08 % at day 1 (Fig. 2.12). At day 7 the strongest reQTL was at *SH2D4A* (p difference = 1.37×10^{-6} , BH FDR = 0.0175). Here, the reQTL variant explained similar amounts of expression variation at day 0 (8.23 %) and day 7 (8.96 %), with opposite directions of effect (Fig. 2.13). Both *ADCY3* and *SH2D4A* have moderately high percentile expression at all timepoints, and are not differentially expressed post-vaccination. Overall, compared to genes without reQTL, reQTLs were less likely be differentially expressed post-vaccination at day 1 (26.50 % for reQTL vs. 42.27 %, Fisher's test $p < 2.20 \times 10^{-16}$), and no significant difference was observed at day 7 (2.20 % for reQTL vs. 1.37 %, Fisher's test $p = 0.0509$). Only 5/68 (13.24 %) genes with reQTLs that explain more variation at day 1 were upregulated at day 1 vs. day 0; 5/226 (2.21 %) for

day 7 vs. day 0.

requiring signif post-vaccination may not be correct, as it excludes many dampening effects

the lack of any positional enrichment makes me concerned for false positives?
check with ASE?

double check denoms

convert to subfigures

2.3.3 Genotype by cell type interaction effects

Given that many reQTLs are not explained by differential expression post-vaccination, the presence of cell type-specific eQTL effects was considered as an alternate explanation. As described in subsection 2.2.5, xCell enrichment scores were used to approximate abundance of seven PBMC cell types from the expression data. After pruning highly correlated cell types to avoid multicollinearity, standardised scores for monocytes, NK cells and plasma cells were tested for genotype interactions. Within-timepoint full eQTL

CHAPTER 2. GENETIC FACTORS AFFECTING PANDEMRIX VACCINE RESPONSE

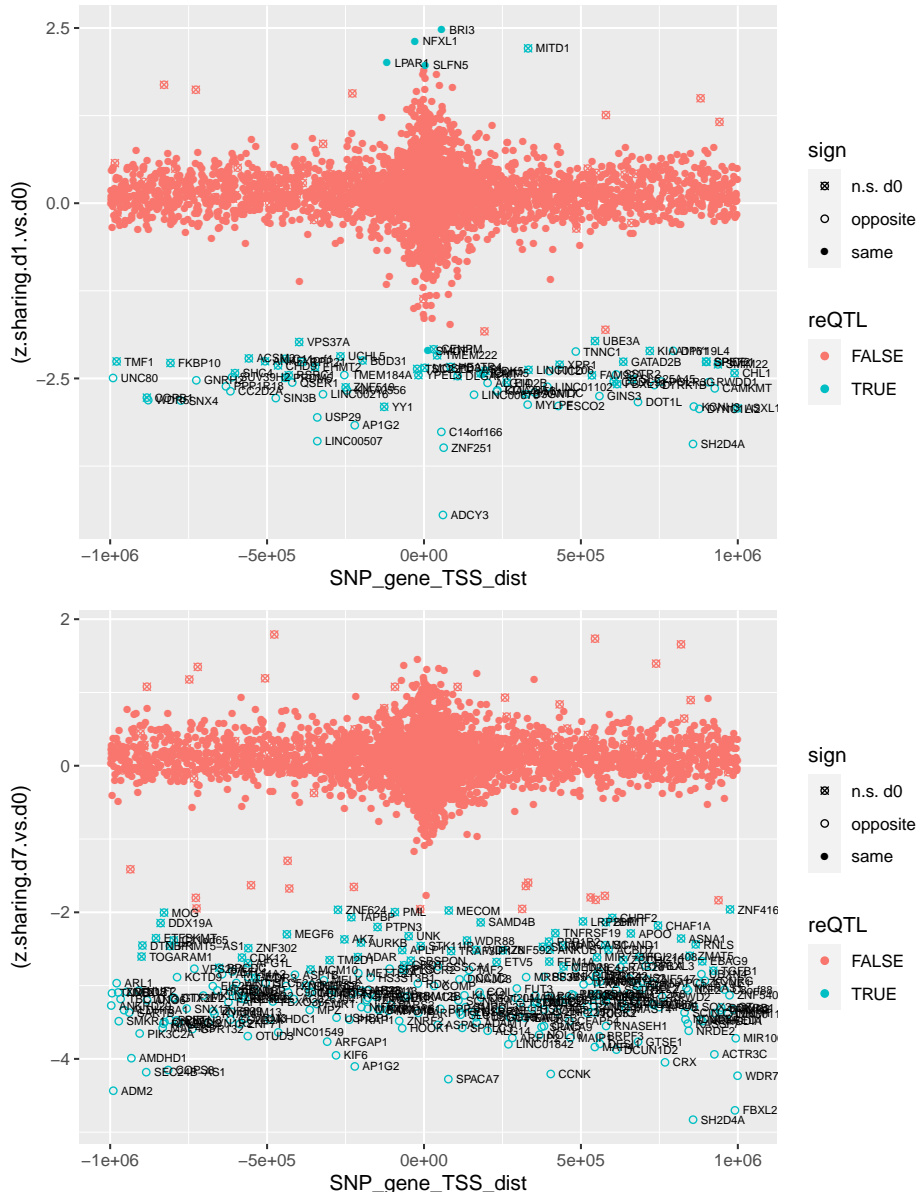


Figure 2.11: Z score for difference in effect vs. day 0, of lead eQTLs for all eGenes significant at either day 1 or day 7; versus distance of the lead SNP to the TSS. Direction of effect is aligned so that the beta at day 0 is positive. Points with positive z score are magnified effects post-vaccination, points with negative z scores are dampening and opposite sign effects.

CHAPTER 2. GENETIC FACTORS AFFECTING PANDEMRIX VACCINE RESPONSE

2.3. RESULTS

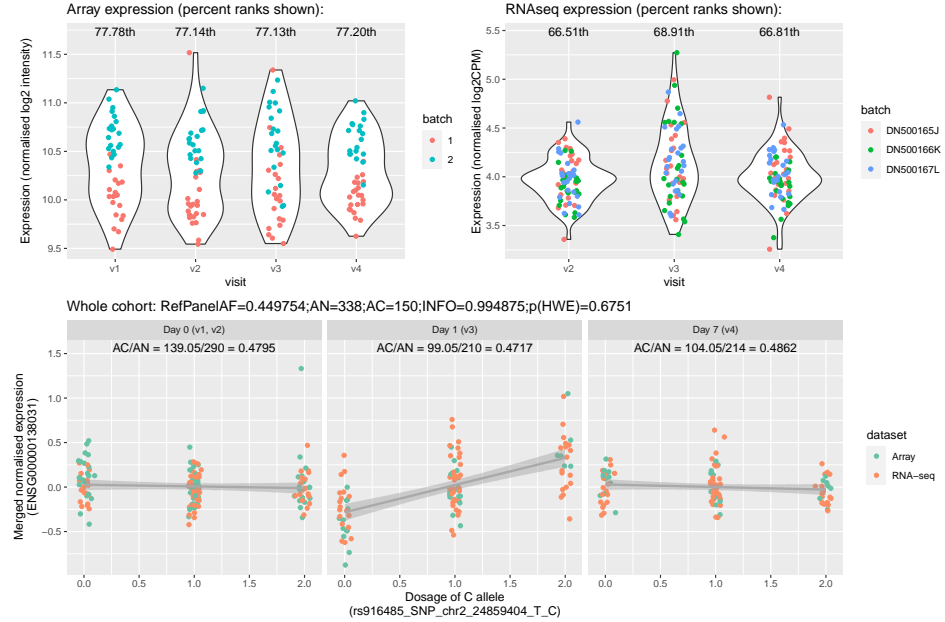


Figure 2.12: *ADCY3*, strongest reQTL at day 1.

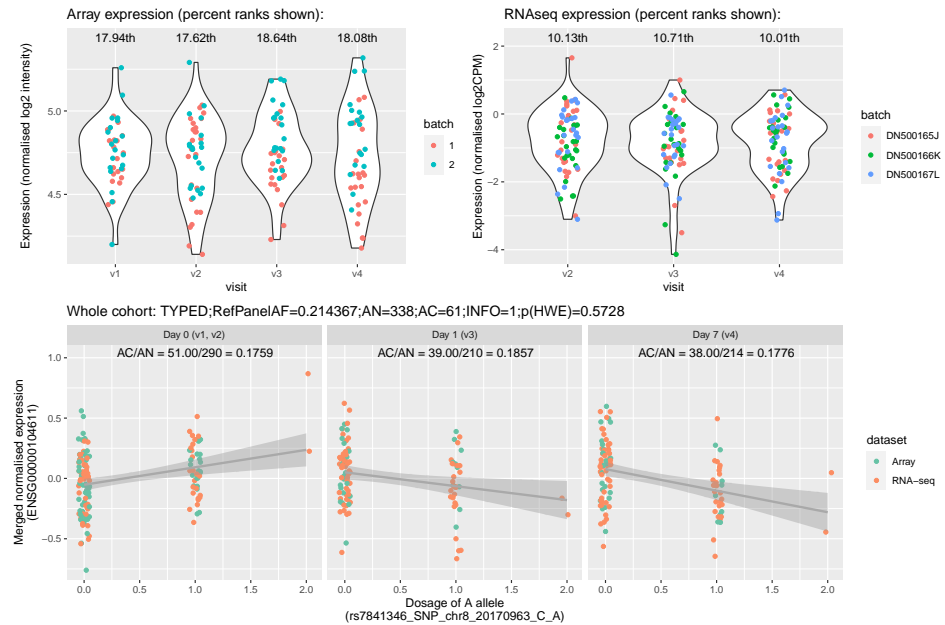
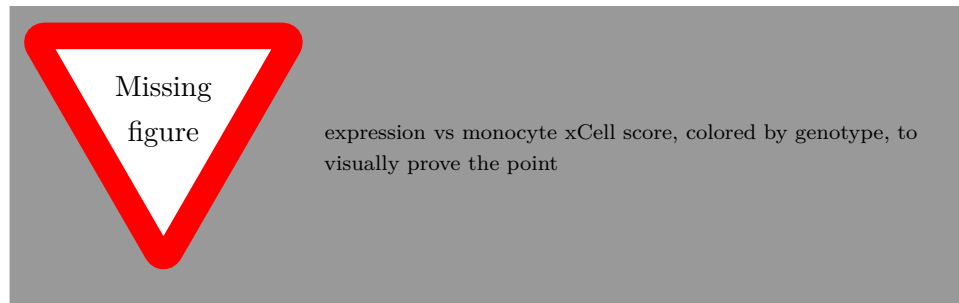


Figure 2.13: *SH2D4A*, strongest reQTL at day 7. Top: Array and RNA-seq expression before merging with ComBat for mega-analysis. Bottom: eQTL effects at each timepoint condition in the mega-analysis.

models including the genotype main effect, the three cell type abundance main effects, and three cell type-genotype interaction terms, were fit using `lme4qtl`, then compared to a nested model excluding the three interaction terms.

Significant cell type interactions were detected at 16/1154 reQTLs (BH FDR < 0.05) in any timepoint, including *ADCY3* at day 1 ($\chi^2(3) = 26.3$, likelihood ratio test (LRT) BH FDR = 9.54×10^{-5}). Although the genotype effect size was 0.256 (SE = 0.0334) in the nested model, the estimate in the full model was $-0.007\ 22$ (0.0666); with the three cell type-genotype interaction term estimates being: monocyte=0.213 (0.0490), NK cells= $-0.009\ 20$ (0.0447), and plasma cells=0.0162 (0.0663). The small magnitude of the genotype main effect in the full model vs. the nested model indicates the eQTL effect is driven largely by the monocyte score (or a cell type that is highly correlated with monocyte score, see Fig. 2.4). In the case where the monocyte score is zero (representing an average abundance across all samples, as scores are standardised), the effect of increasing genotype dosage on *ADCY3* expression is minimal.

gene set enrichment for cell type interacting genes to further validate xCell score usefulness



2.3.4 TODO Genotype by platform interaction effects

- Perhaps using platform specific effects as a filter for reQTLs.

Need to consider Nikos' comment that there are too many (1069/13570 significant BH FDR) genotype-platform interactions to use mega-analysis. Consider filtering.

2.3.5 TODO Colocalisation of reQTLs with known *in vitro* condition-specific immune eQTLs

- Colocalisation is used to understand the molecular basis of GWAS associations (of a variety of human disease traits) (Giambartolome, 2014)

this analysis is incomplete, and is one of the things I would suggest to round off this chapter

- Here the inverse: coloc is used to understand the biological relevance of observed reQTL by coloc with known immune QTL
- In a 500 Mb window around the lead *ADCY3* variant rs916485, `hyprecoloc` to colocalise with existing datasets and fine map.
- Day 1 HIRD colocs with BLUEPRINT and Fairfax monocytes (both stim and non stim), but not with Quach or Schmiedel monocytes (Fig. 2.14)
 - Biases from ethnicity-derived differences in LD?
 - Also, priors need tuning?

- `hyprecoloc` fine maps the signal to rs13407914 (credible set size=1, PP = 1), an intronic variant 45064 bp downstream of the TSS.

FYI the IBD/T cell
 coloc fine maps to
 chr2:24935139 T C
 (rs713586) with PP=1

add obesity GWAS

2.4 Discussion

In the **HIRD** cohort, **eQTL** were detected for 50.75 % of genes in at least one timepoint, day 0, day 1, or day 7. Even in a joint mapping framework, defining **reQTL** by set significance thresholds, or change in the amount of expression variation explained, will miss classifying equal but opposite effect sizes. I account for the direction and magnitude of effect sizes, defining reQTL strength as the difference in effect size between timepoints. Most **eQTL** are shared between conditions and replicate well in GTEx whole blood; 16.76 % of lead **eQTL** for each eGene were **reQTL** that differed in effect size between timepoints.

Multiple independent eQTLs are present for a large fraction of eGenes¹²³. As the lead variant for reQTL assessment for each eGene was chosen based on significance across all conditions, I can not detect reQTL that are masked by a stronger shared eQTL at that gene. This is not expected to be uncommon, as the effective sample size for shared eQTLs is usually large due to borrowing of information across conditions. Secondary **eQTL** signals tend to be weaker, more distal to the TSS, more likely to be enriched in enhancers rather than promoters, and importantly, more context-specific¹²⁴. The proportion of genes with reQTL I detect based on only the lead signal likely represents a lower bound.

CHAPTER 2. GENETIC FACTORS AFFECTING PANDEMRIX VACCINE RESPONSE

2.4. DISCUSSION

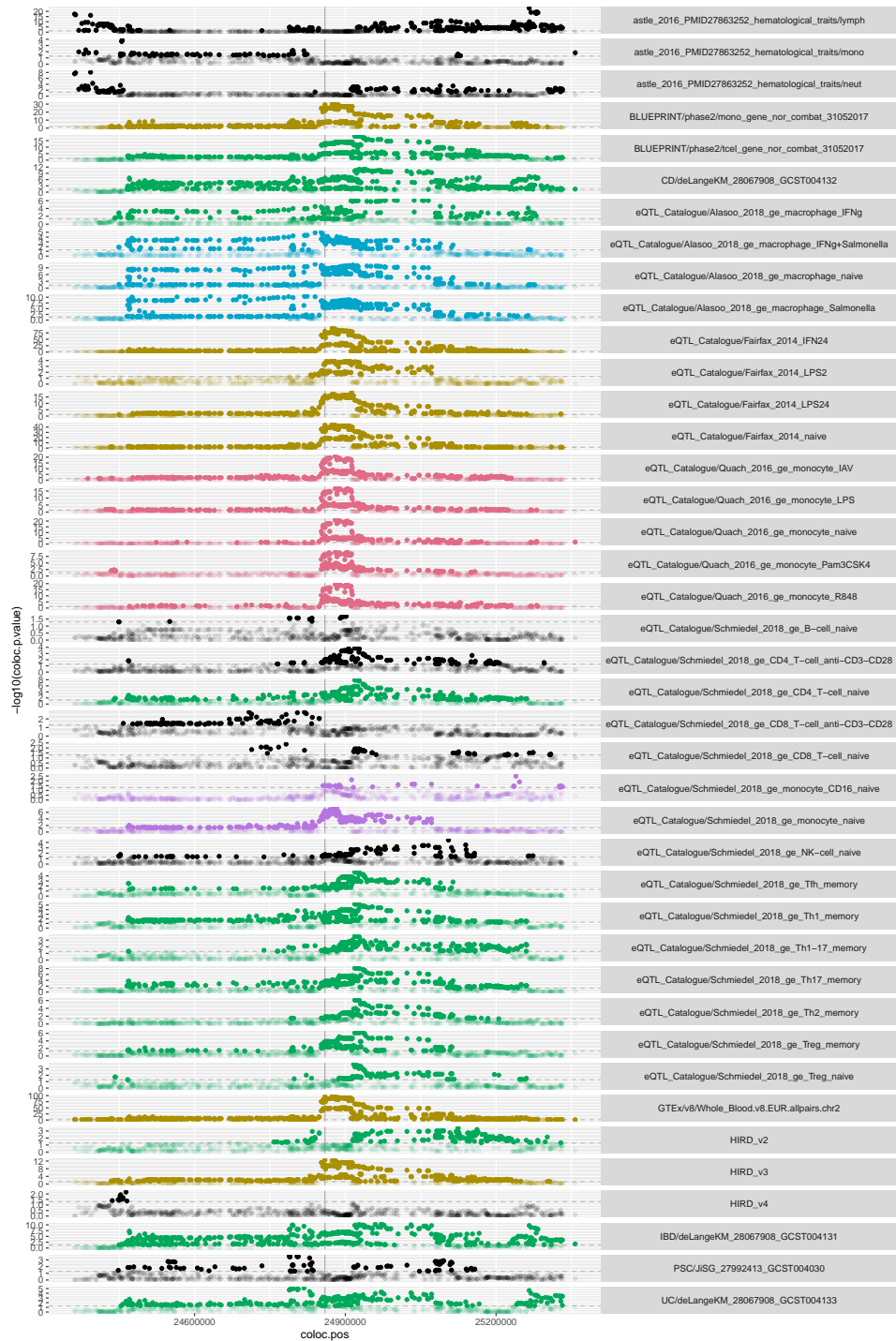


Figure 2.14: Multi-trait colocalisation of HIRD reQTL signal at ADCY3 (500 Kb window), with QTL studies from IHEC, BLUEPRINT, eQTL Catalogue, and GWAS Catalogue. Plots are colored by colocalised cluster. Black indicates non-colocalised datasets.

CHAPTER 2. GENETIC FACTORS AFFECTING PANDEMRIX
2.4. DISCUSSION

Given the larger global changes in expression vs. baseline at day 1 compared to day 7 described in chapter 1, the larger number of reQTLs detected at day 7 was unexpected (819 vs. 1002). Opposite sign effects among reQTL post-vaccination were common. Prevalance of opposite sign effects between pairs of conditions has been previously described in multi-tissue studies. In¹²⁵, the proportion of opposite sign effects as a percentage of all eGenes was 7.40% (48 tissues); in HIRD, I find 39/6887 (0.57%) at day 1, and 211/6887 (3.06%) at day 7. In¹²⁶, the proportion of opposite sign effects as percentage of all reQTLs was 4.40% (5 tissues); in HIRD, I find 39/819 (4.76%) at day 1, and 211/1002 (21.06%) at day 7. The enrichment of opposite sign effects in HIRD is also apparent at day 7. The strongest reQTL at day 7 is one such opposite sign effect; *SH2D4A* has constitutive expression in T cells, B cells, macrophages, and DCs, encoding a adapter protein involved in intracellular signal transduction*. An approach for validating these opposite sign reQTL using the existing HIRD RNA-seq data is allele-specific expression (ASE) (e.g.¹²⁷), where one would expect true opposite sign reQTL effects would also be recapitulated as opposite directions of expression imbalance.

I'm not exactly sure why at the moment. Enrichment analyses so far have not turned up much. Up regulation of cell cycle TFs is a possibility.

The strongest reQTL detected at day 1 was *ADCY3*, a membrane-bound enzyme that catalyses the conversion of ATP to the second messenger cAMP¹²⁸. Genome-wide association studies (GWAS) have identified *ADCY3* as a candidate gene for diseases such as obesity¹²⁸ and IBD¹²⁹. *ADCY3* has been identified as a target for reQTLs in multiple studies involving stimulated blood immune cells: in PBMC 24h post-infection with rhinovirus¹³⁰, in whole blood *in vivo* day 1 after vaccination with seasonal TIV⁷⁸, and in whole blood after stimulation with *M. leprae* antigen for 26-32 h¹³¹. Given the diversity of stimulations and tissue types, the effect is likely a consequence of general immune activation, rather than a Pandemrix-specific response.

Statistical colocalisation suggests that the day 1 reQTL signal identified here is likely to be a monocyte-specific effect—and independent to the IBD signal, which colocalises with T cell and macrophage datasets. The proportion of monocytes in the PBMC increase at day 1, supported by both FACS¹⁸ measurements, and an increase in monocyte xCell score. Expression of *ADCY3* is not monocyte-specific, as despite the increase in monocyte proportion, no upregulation is observed at day 1. Colocalisation is also not restricted to stimulated monocytes, hence the signal could be hypothesised

add lfsr.dge

*<https://doi.org/10.1111/j.1600-065X.2009.00829.x>

to result simply from the increased proportion of the bulk sample taken up by monocytes, rather than a upregulation-driven increase in detection power, or a vaccine-induced activation of the locus at day 1.

Changes in relative abundances for many cell types occur in the bulk PBMC samples after vaccination. I accounted for the effect of abundance on mean expression including xCell scores and PEER factors as fixed effects in the model, and also considered the effect of abundance on the genotype effect using interaction terms between xCell scores and genotype. Due to the modest sample size, and computational requirements for `lme4qt1`, I focused only whether reQTLs that have a detectable main effect may be driven by cell type interactions, testing only for interactions at significant lead reQTL. Compared to FACS measurements in a cohort subset, the xCell scores used above were only weakly correlated. Some discrepancy is expected, as the cell types as defined in the xCell signatures do not directly correspond to the combinations of surface markers used for FACS. The FACS gating strategy also meant that for some cell populations, the only available FACS measure was a proportion of the previously gated population, whereas xCell attempts to estimate scores that represent proportions of the whole mixture. The accuracy of the built-in signatures is lower when applied to the expression matrix for a stimulated state, likely because the enrichment-based method can not distinguish differential expression of signature genes due to stimulation from actual changes in cell abundance. Nevertheless, as assuming a single genotype where cell-type specific slopes are likely is inappropriate, so xCell scores were used as a best approximation. At 16/1154 reQTLs, the genotype effect was detected to interact with abundance of one or more of the tested cell types (or a correlated cell type). At the day 1 *ADCY3* reQTL, the genetic effect can be mainly attributed to the monocyte score-genotype interaction term, further supporting the hypothesis that it is monocyte-specific.

need to consider: if this kind of thing is what bulk in vivo reQTL can find, they what is the additional value over FACS?

A pressing question remains: what molecular mechanisms underlie the *ADCY3* reQTL, and indeed the remainder of the reQTLs? Power differences due to condition-specific expression are unlikely to explain a large proportion of reQTLs. As in^{109,120}, the overlap between differentially expressed genes and genes with reQTL was poor, and reQTL were not more likely to be differentially expressed compared to genes without reQTL. One mechanism by which cis-eQTL affect expression is through their impact on transcription factor (TF) binding affinity to motifs in promoters and enhancers¹³². Immune

CHAPTER 2. GENETIC FACTORS AFFECTING PANDEMRIX

2.4. DISCUSSION

harmonise terminology
for 'opposite'

cells, including monocytes, are regulated by cell type specific **TFs**¹³³. Cell type specific expression of different **TFs** have been proposed as a model for explaining magnifying, dampening and opposite reQTL effects; for example, opposite effects can result from **TFs** regulating the same gene, that are activating in one cell type and suppressive in another¹²⁶. There is evidence that **TF** activity is important for *in vivo* immune reQTL: ¹³⁰ found rhinovirus reQTLs were ENCODE ChIP-seq peaks for the **TFs** *STAT1* and *STAT2*, and¹⁰⁹ found interferon and anti-IL6 drug reQTLs likely disrupt *ISRE* and *IRF4* binding motifs. Rather than condition-specific expression of the eGene, what may be condition-specific is the expression of **TFs** whose activity is affected by the reQTL*.

Finally, I address the prospect that common genetic variation may explain some variation in antibody response to Pandemrix. I have indirectly demonstrated genotype-dependent effects on expression response by identifying reQTLs with differing effect size between timepoints, but have not yet determined resulting genotype-dependent differences in antibody phenotypes. Some of the identified reQTLs will undoubtedly affect genes whose expression or post-vaccination expression change correlates with antibody response, but a formal test such as the **causal inference test (CIT)**¹³⁴ is required to distinguish mediation of genotype-antibody associations through gene expression from competing models.⁷⁸ attempted this, but concluded that they had insufficient power with a greater sample size and comparable study design to **HIRD**. The **HIRD** cohort is also too small for a direct **GWAS** of Pandemrix antibody response. A suitable approach for prioritising reQTL that contribute to the antibody response to Pandemrix will be to leverage external genetic associations to similar phenotypes, for example, colocalisation with existing GWAS summary statistics for antibody response to a similar type of adjuvanted, inactivated vaccine.

add 1 concluding line

Overall I feel like the chapter is too descriptive, and falls short of making biological insights into Pandemrix response. Any additional analyses would hope to address that.

*A cursory scan of **TF** motifs disrupted by the location of the fine-mapped *ADCY3* reQTL intronic variant rs13407913 on <https://ccg.epfl.ch/snp2tfbs/snpviewer.php>, does indeed show several motifs (for NR2C2, HNF4A, HNF4G, NR2F1) where the PWM score is higher for the ALT allele, consistent with the direction of effect for the day 1 reQTL.

Appendix A

Supplementary Materials

A.1 Chapter 2

Lorem ipsum dolor sit amet, consectetuer adipiscing elit. Ut purus elit, vestibulum ut, placerat ac, adipiscing vitae, felis. Curabitur dictum gravida mauris. Nam arcu libero, nonummy eget, consectetuer id, vulputate a, magna. Donec vehicula augue eu neque. Pellentesque habitant morbi tristique senectus et netus et malesuada fames ac turpis egestas. Mauris ut leo. Cras viverra metus rhoncus sem. Nulla et lectus vestibulum urna fringilla ultrices. Phasellus eu tellus sit amet tortor gravida placerat. Integer sapien est, iaculis in, pretium quis, viverra ac, nunc. Praesent eget sem vel leo ultrices bibendum. Aenean faucibus. Morbi dolor nulla, malesuada eu, pulvinar at, mollis ac, nulla. Curabitur auctor semper nulla. Donec varius orci eget risus. Duis nibh mi, congue eu, accumsan eleifend, sagittis quis, diam. Duis eget orci sit amet orci dignissim rutrum.

A.2 Chapter 3

Nam dui ligula, fringilla a, euismod sodales, sollicitudin vel, wisi. Morbi auctor lorem non justo. Nam lacus libero, pretium at, lobortis vitae, ultricies et, tellus. Donec aliquet, tortor sed accumsan bibendum, erat ligula aliquet magna, vitae ornare odio metus a mi. Morbi ac orci et nisl hendrerit mollis. Suspendisse ut massa. Cras nec ante. Pellentesque a nulla. Cum sociis natoque penatibus et magnis dis parturient montes, nascetur ridiculus mus. Aliquam tincidunt urna. Nulla ullamcorper vestibulum turpis. Pellentesque cursus

luctus mauris.

A.3 Chapter 4

Nulla malesuada porttitor diam. Donec felis erat, congue non, volutpat at, tincidunt tristique, libero. Vivamus viverra fermentum felis. Donec nonummy pellentesque ante. Phasellus adipiscing semper elit. Proin fermentum massa ac quam. Sed diam turpis, molestie vitae, placerat a, molestie nec, leo. Maecenas lacinia. Nam ipsum ligula, eleifend at, accumsan nec, suscipit a, ipsum. Morbi blandit ligula feugiat magna. Nunc eleifend consequat lorem. Sed lacinia nulla vitae enim. Pellentesque tincidunt purus vel magna. Integer non enim. Praesent euismod nunc eu purus. Donec bibendum quam in tellus. Nullam cursus pulvinar lectus. Donec et mi. Nam vulputate metus eu enim. Vestibulum pellentesque felis eu massa.

Bibliography

1. Krammer, F. *et al.* Influenza. *Nature Reviews Disease Primers* **4**. doi:[10.1038/s41572-018-0002-y](https://doi.org/10.1038/s41572-018-0002-y) (Dec. 2018).
2. Houser, K. & Subbarao, K. Influenza Vaccines: Challenges and Solutions. *Cell Host & Microbe* **17**, 295–300. doi:[10.1016/j.chom.2015.02.012](https://doi.org/10.1016/j.chom.2015.02.012) (Mar. 2015).
3. Sautto, G. A., Kirchenbaum, G. A. & Ross, T. M. Towards a Universal Influenza Vaccine: Different Approaches for One Goal. *Virology Journal* **15**. doi:[10.1186/s12985-017-0918-y](https://doi.org/10.1186/s12985-017-0918-y) (Dec. 2018).
4. Broadbent, A. J. & Subbarao, K. Influenza Virus Vaccines: Lessons from the 2009 H1N1 Pandemic. *Current Opinion in Virology* **1**, 254–262. doi:[10.1016/j.coviro.2011.08.002](https://doi.org/10.1016/j.coviro.2011.08.002) (Oct. 2011).
5. Klimov, A. *et al.* in *Influenza Virus* (eds Kawaoka, Y. & Neumann, G.) 25–51 (Humana Press, Totowa, NJ, 2012). doi:[10.1007/978-1-61779-621-0_3](https://doi.org/10.1007/978-1-61779-621-0_3).
6. Plotkin, S. A. Correlates of Protection Induced by Vaccination. *Clinical and Vaccine Immunology* **17**, 1055–1065. doi:[10.1128/CVI.00131-10](https://doi.org/10.1128/CVI.00131-10) (July 2010).
7. Cox, R. Correlates of Protection to Influenza Virus, Where Do We Go from Here? *Human Vaccines & Immunotherapeutics* **9**, 405–408. doi:[10.4161/hv.22908](https://doi.org/10.4161/hv.22908) (Feb. 2013).
8. Pulendran, B. Systems Vaccinology: Probing Humanity’s Diverse Immune Systems with Vaccines. *Proceedings of the National Academy of Sciences* **111**, 12300–12306. doi:[10.1073/pnas.1400476111](https://doi.org/10.1073/pnas.1400476111) (2014).

APPENDIX A. BIBLIOGRAPHY

9. Hagan, T., Nakaya, H. I., Subramaniam, S. & Pulendran, B. Systems Vaccinology: Enabling Rational Vaccine Design with Systems Biological Approaches. *Vaccine* **33**, 5294–5301. doi:[10.1016/j.vaccine.2015.03.072](https://doi.org/10.1016/j.vaccine.2015.03.072) (2015).
10. Raeven, R. H. M., van Riet, E., Meiring, H. D., Metz, B. & Kersten, G. F. A. Systems Vaccinology and Big Data in the Vaccine Development Chain. *Immunology* **156**, 33–46. doi:[10.1111/imm.13012](https://doi.org/10.1111/imm.13012) (Jan. 2019).
11. Zhu, W. *et al.* A Whole Genome Transcriptional Analysis of the Early Immune Response Induced by Live Attenuated and Inactivated Influenza Vaccines in Young Children. *Vaccine* **28**, 2865–2876. doi:[10.1016/j.vaccine.2010.01.060](https://doi.org/10.1016/j.vaccine.2010.01.060) (Apr. 2010).
12. Bucasas, K. L. *et al.* Early Patterns of Gene Expression Correlate With the Humoral Immune Response to Influenza Vaccination in Humans. *The Journal of Infectious Diseases* **203**, 921–929. doi:[10.1093/infdis/jiq156](https://doi.org/10.1093/infdis/jiq156) (Apr. 2011).
13. Nakaya, H. I. *et al.* Systems Biology of Vaccination for Seasonal Influenza in Humans. *Nature Immunology* **12**, 786–795. doi:[10.1038/ni.2067](https://doi.org/10.1038/ni.2067) (July 10, 2011).
14. Tan, Y., Tamayo, P., Nakaya, H., Pulendran, B., Mesirov, J. P. & Haining, W. N. Gene Signatures Related to B-Cell Proliferation Predict Influenza Vaccine-Induced Antibody Response. *European Journal of Immunology* **44**, 285–295. doi:[10.1002/eji.201343657](https://doi.org/10.1002/eji.201343657) (Jan. 2014).
15. Nakaya, H. I., Li, S. & Pulendran, B. Systems Vaccinology: Learning to Compute the Behavior of Vaccine Induced Immunity. *Wiley Interdisciplinary Reviews: Systems Biology and Medicine* **4**, 193–205. doi:[10.1002/wsbm.163](https://doi.org/10.1002/wsbm.163) (Mar. 2012).
16. Wilkins, A. L. *et al.* AS03- and MF59-Adjuvanted Influenza Vaccines in Children. *Frontiers in Immunology* **8**. doi:[10.3389/fimmu.2017.01760](https://doi.org/10.3389/fimmu.2017.01760) (Dec. 13, 2017).
17. Tregoning, J. S., Russell, R. F. & Kinnear, E. Adjuvanted Influenza Vaccines. *Human Vaccines & Immunotherapeutics* **14**, 550–564. doi:[10.1080/21645515.2017.1415684](https://doi.org/10.1080/21645515.2017.1415684) (Mar. 4, 2018).

APPENDIX A. BIBLIOGRAPHY

18. Sobolev, O. *et al.* Adjuvanted Influenza-H1N1 Vaccination Reveals Lymphoid Signatures of Age-Dependent Early Responses and of Clinical Adverse Events. *Nature Immunology* **17**, 204–213. doi:[10.1038/ni.3328](https://doi.org/10.1038/ni.3328) (Jan. 4, 2016).
19. Furman, D. *et al.* Apoptosis and Other Immune Biomarkers Predict Influenza Vaccine Responsiveness. *Molecular Systems Biology* **9**, 659. doi:[10.1038/msb.2013.15](https://doi.org/10.1038/msb.2013.15) (Apr. 16, 2013).
20. Tsang, J. S. *et al.* Global Analyses of Human Immune Variation Reveal Baseline Predictors of Postvaccination Responses. *Cell* **157**, 499–513. doi:[10.1016/j.cell.2014.03.031](https://doi.org/10.1016/j.cell.2014.03.031) (Apr. 10, 2014).
21. Nakaya, H. I. *et al.* Systems Analysis of Immunity to Influenza Vaccination across Multiple Years and in Diverse Populations Reveals Shared Molecular Signatures. *Immunity* **43**, 1186–1198. doi:[10.1016/j.immuni.2015.11.012](https://doi.org/10.1016/j.immuni.2015.11.012) (Dec. 2015).
22. HIPC-CHI Signatures Project Team & HIPC-I Consortium. Multicohort Analysis Reveals Baseline Transcriptional Predictors of Influenza Vaccination Responses. *Science Immunology* **2**, eaal4656. doi:[10.1126/sciimmunol.aal4656](https://doi.org/10.1126/sciimmunol.aal4656) (Aug. 25, 2017).
23. Cohen, J. The Cost of Dichotomization. *Applied Psychological Measurement* **7**, 249–253. doi:[10.1177/014662168300700301](https://doi.org/10.1177/014662168300700301) (June 1983).
24. Senn, S. Dichotomania: An Obsessive Compulsive Disorder That Is Badly Affecting the Quality of Analysis of Pharmaceutical Trials, 14 (2005).
25. Fedorov, V., Mannino, F. & Zhang, R. Consequences of Dichotomization. *Pharmaceutical Statistics* **8**, 50–61. doi:[10.1002/pst.331](https://doi.org/10.1002/pst.331) (Jan. 2009).
26. Food and Drug Administration. *Guidance for Industry: Clinical Data Needed to Support the Licensure of Pandemic Influenza Vaccines* (Jan. 6, 2007), 20.
27. Price, A. L., Patterson, N. J., Plenge, R. M., Weinblatt, M. E., Shadick, N. A. & Reich, D. Principal Components Analysis Corrects for Stratification in Genome-Wide Association Studies. *Nature Genetics* **38**, 904–909. doi:[10.1038/ng1847](https://doi.org/10.1038/ng1847) (Aug. 2006).

APPENDIX A. BIBLIOGRAPHY

28. Eu-ahsunthornwattana, J. *et al.* Comparison of Methods to Account for Relatedness in Genome-Wide Association Studies with Family-Based Data. *PLoS Genetics* **10** (ed Abecasis, G. R.) e1004445. doi:[10.1371/journal.pgen.1004445](https://doi.org/10.1371/journal.pgen.1004445) (July 17, 2014).
29. Brown, B. C., Bray, N. L. & Pachter, L. Expression Reflects Population Structure. doi:[10.1101/364448](https://doi.org/10.1101/364448) (July 8, 2018).
30. Okonechnikov, K., Conesa, A. & García-Alcalde, F. Qualimap 2: Advanced Multi-Sample Quality Control for High-Throughput Sequencing Data. *Bioinformatics* **32**, btv566. doi:[10.1093/bioinformatics/btv566](https://doi.org/10.1093/bioinformatics/btv566) (Oct. 1, 2015).
31. Ewels, P., Magnusson, M., Lundin, S. & Käller, M. MultiQC: Summarize Analysis Results for Multiple Tools and Samples in a Single Report. *Bioinformatics* **32**, 3047–3048. doi:[10.1093/bioinformatics/btw354](https://doi.org/10.1093/bioinformatics/btw354) (Oct. 1, 2016).
32. Patro, R., Duggal, G., Love, M. I., Irizarry, R. A. & Kingsford, C. Salmon Provides Fast and Bias-Aware Quantification of Transcript Expression. *Nature Methods* **14**, 417–419. doi:[10.1038/nmeth.4197](https://doi.org/10.1038/nmeth.4197) (Apr. 6, 2017).
33. Liu, Y., Zhou, J. & White, K. P. RNA-Seq Differential Expression Studies: More Sequence or More Replication? *Bioinformatics* **30**, 301–304. doi:[10.1093/bioinformatics/btt688](https://doi.org/10.1093/bioinformatics/btt688) (Feb. 1, 2014).
34. Soneson, C., Love, M. I. & Robinson, M. D. Differential Analyses for RNA-Seq: Transcript-Level Estimates Improve Gene-Level Inferences. *F1000Research* **4**, 1521. doi:[10.12688/f1000research.7563.2](https://doi.org/10.12688/f1000research.7563.2) (Feb. 29, 2016).
35. Zhao, S., Zhang, Y., Gamin, R., Zhang, B. & von Schack, D. Evaluation of Two Main RNA-Seq Approaches for Gene Quantification in Clinical RNA Sequencing: polyA+ Selection versus rRNA Depletion. *Scientific Reports* **8**. doi:[10.1038/s41598-018-23226-4](https://doi.org/10.1038/s41598-018-23226-4) (Dec. 2018).
36. Min, J. L. *et al.* Variability of Gene Expression Profiles in Human Blood and Lymphoblastoid Cell Lines. *BMC Genomics* **11**, 96. doi:[10.1186/1471-2164-11-96](https://doi.org/10.1186/1471-2164-11-96) (2010).

APPENDIX A. BIBLIOGRAPHY

37. Chen, Y., Lun, A. T. L. & Smyth, G. K. From Reads to Genes to Pathways: Differential Expression Analysis of RNA-Seq Experiments Using Rsubread and the edgeR Quasi-Likelihood Pipeline. *F1000Research* **5**, 1438. doi:[10.12688/f1000research.8987.2](https://doi.org/10.12688/f1000research.8987.2) (Aug. 2, 2016).
38. Huber, W., von Heydebreck, A., Sultmann, H., Poustka, A. & Vingron, M. Variance Stabilization Applied to Microarray Data Calibration and to the Quantification of Differential Expression. *Bioinformatics* **18**, S96–S104. doi:[10.1093/bioinformatics/18.suppl_1.S96](https://doi.org/10.1093/bioinformatics/18.suppl_1.S96) (Suppl 1 July 1, 2002).
39. Miller, J. A. *et al.* Strategies for Aggregating Gene Expression Data: The collapseRows R Function. *BMC Bioinformatics* **12**, 322. doi:[10.1186/1471-2105-12-322](https://doi.org/10.1186/1471-2105-12-322) (2011).
40. Draghici, S., Khatri, P., Eklund, A. & Szallasi, Z. Reliability and Reproducibility Issues in DNA Microarray Measurements. *Trends in Genetics* **22**, 101–109. doi:[10.1016/j.tig.2005.12.005](https://doi.org/10.1016/j.tig.2005.12.005) (Feb. 2006).
41. Robinson, D. G., Wang, J. Y. & Storey, J. D. A Nested Parallel Experiment Demonstrates Differences in Intensity-Dependence between RNA-Seq and Microarrays. *Nucleic Acids Research*, gkv636. doi:[10.1093/nar/gkv636](https://doi.org/10.1093/nar/gkv636) (June 30, 2015).
42. Johnson, W. E., Li, C. & Rabinovic, A. Adjusting Batch Effects in Microarray Expression Data Using Empirical Bayes Methods. *Biostatistics* **8**, 118–127. doi:[10.1093/biostatistics/kxj037](https://doi.org/10.1093/biostatistics/kxj037) (Jan. 1, 2007).
43. Chen, C. *et al.* Removing Batch Effects in Analysis of Expression Microarray Data: An Evaluation of Six Batch Adjustment Methods. *PLoS ONE* **6** (ed Kliebenstein, D.) e17238. doi:[10.1371/journal.pone.0017238](https://doi.org/10.1371/journal.pone.0017238) (Feb. 28, 2011).
44. Espín-Pérez, A., Portier, C., Chadeau-Hyam, M., van Veldhoven, K., Kleinjans, J. C. S. & de Kok, T. M. C. M. Comparison of Statistical Methods and the Use of Quality Control Samples for Batch Effect Correction in Human Transcriptome Data. *PLOS ONE* **13** (ed Krishnan, V. V.) e0202947. doi:[10.1371/journal.pone.0202947](https://doi.org/10.1371/journal.pone.0202947) (Aug. 30, 2018).

APPENDIX A. BIBLIOGRAPHY

45. Zhang, Y., Jenkins, D. F., Manimaran, S. & Johnson, W. E. Alternative Empirical Bayes Models for Adjusting for Batch Effects in Genomic Studies. *BMC Bioinformatics* **19**. doi:[10.1186/s12859-018-2263-6](https://doi.org/10.1186/s12859-018-2263-6) (Dec. 2018).
46. Nygaard, V., Rødland, E. A. & Hovig, E. Methods That Remove Batch Effects While Retaining Group Differences May Lead to Exaggerated Confidence in Downstream Analyses. *Biostatistics*, kxv027. doi:[10.1093/biostatistics/kxv027](https://doi.org/10.1093/biostatistics/kxv027) (January Aug. 13, 2015).
47. Evans, C., Hardin, J. & Stoebel, D. M. Selecting Between-Sample RNA-Seq Normalization Methods from the Perspective of Their Assumptions. *Briefings in Bioinformatics* **19**, 776–792. doi:[10.1093/bib/bbx008](https://doi.org/10.1093/bib/bbx008) (Sept. 28, 2018).
48. Robinson, M. D., McCarthy, D. J. & Smyth, G. K. edgeR: A Bioconductor Package for Differential Expression Analysis of Digital Gene Expression Data. *Bioinformatics* **26**, 139–140. doi:[10.1093/bioinformatics/btp616](https://doi.org/10.1093/bioinformatics/btp616) (Jan. 1, 2010).
49. Law, C. W., Chen, Y., Shi, W. & Smyth, G. K. Voom: Precision Weights Unlock Linear Model Analysis Tools for RNA-Seq Read Counts. *Genome Biology* **15**, 1–17 (2014).
50. Ritchie, M. E. *et al.* Limma Powers Differential Expression Analyses for RNA-Sequencing and Microarray Studies. *Nucleic Acids Research* **43**, e47–e47. doi:[10.1093/nar/gkv007](https://doi.org/10.1093/nar/gkv007) (Apr. 20, 2015).
51. Soneson, C. & Delorenzi, M. A Comparison of Methods for Differential Expression Analysis of RNA-Seq Data. *BMC Bioinformatics* **14**. doi:[10.1186/1471-2105-14-91](https://doi.org/10.1186/1471-2105-14-91) (Dec. 2013).
52. Cohn, L. D. & Becker, B. J. How Meta-Analysis Increases Statistical Power. *Psychological Methods* **8**, 243–253. doi:[10.1037/1082-989X.8.3.243](https://doi.org/10.1037/1082-989X.8.3.243) (2003).
53. Borenstein, M., Hedges, L. V., Higgins, J. P. & Rothstein, H. R. A Basic Introduction to Fixed-Effect and Random-Effects Models for Meta-Analysis. *Research Synthesis Methods* **1**, 97–111. doi:[10.1002/jrsm.12](https://doi.org/10.1002/jrsm.12) (Apr. 2010).
54. Röver, C. Bayesian Random-Effects Meta-Analysis Using the Bayesmeta R Package (Nov. 23, 2017).

APPENDIX A. BIBLIOGRAPHY

55. Bender, R. *et al.* Methods for Evidence Synthesis in the Case of Very Few Studies. *Research Synthesis Methods*. doi:[10.1002/jrsm.1297](https://doi.org/10.1002/jrsm.1297) (Apr. 6, 2018).
56. Gonnermann, A., Framke, T., Großhennig, A. & Koch, A. No Solution yet for Combining Two Independent Studies in the Presence of Heterogeneity. *Statistics in Medicine* **34**, 2476–2480. doi:[10.1002/sim.6473](https://doi.org/10.1002/sim.6473) (July 20, 2015).
57. Veroniki, A. A. *et al.* Methods to Estimate the Between-Study Variance and Its Uncertainty in Meta-Analysis. *Research Synthesis Methods* **7**, 55–79. doi:[10.1002/jrsm.1164](https://doi.org/10.1002/jrsm.1164) (Mar. 2016).
58. Chung, Y., Rabe-Hesketh, S., Dorie, V., Gelman, A. & Liu, J. A Non-degenerate Penalized Likelihood Estimator for Variance Parameters in Multilevel Models. *Psychometrika* **78**, 685–709. doi:[10.1007/s11336-013-9328-2](https://doi.org/10.1007/s11336-013-9328-2) (Oct. 2013).
59. Friede, T., Röver, C., Wandel, S. & Neuenschwander, B. Meta-Analysis of Few Small Studies in Orphan Diseases. *Research Synthesis Methods* **8**, 79–91. doi:[10.1002/jrsm.1217](https://doi.org/10.1002/jrsm.1217) (Mar. 2017).
60. Seide, S. E., Röver, C. & Friede, T. Likelihood-Based Random-Effects Meta-Analysis with Few Studies: Empirical and Simulation Studies. *BMC Medical Research Methodology* **19**. doi:[10.1186/s12874-018-0618-3](https://doi.org/10.1186/s12874-018-0618-3) (Dec. 2019).
61. Gelman, A. Prior Distributions for Variance Parameters in Hierarchical Models (Comment on Article by Browne and Draper). *Bayesian Analysis* **1**, 515–534. doi:[10.1214/06-BA117A](https://doi.org/10.1214/06-BA117A) (Sept. 2006).
62. Pullenayegum, E. M. An Informed Reference Prior for Between-Study Heterogeneity in Meta-Analyses of Binary Outcomes: Prior for between-Study Heterogeneity. *Statistics in Medicine* **30**, 3082–3094. doi:[10.1002/sim.4326](https://doi.org/10.1002/sim.4326) (Nov. 20, 2011).
63. Turner, R. M., Jackson, D., Wei, Y., Thompson, S. G. & Higgins, J. P. T. Predictive Distributions for Between-Study Heterogeneity and Simple Methods for Their Application in Bayesian Meta-Analysis: R. M. TURNER ET AL. *Statistics in Medicine* **34**, 984–998. doi:[10.1002/sim.6381](https://doi.org/10.1002/sim.6381) (Mar. 15, 2015).

APPENDIX A. BIBLIOGRAPHY

64. Higgins, J. P. T. & Whitehead, A. Borrowing Strength from External Trials in a Meta-Analysis. *Statistics in Medicine* **15**, 2733–2749. doi:[10.1002/\(SICI\)1097-0258\(19961230\)15:24<2733::AID-SIM562>3.0.CO;2-0](https://doi.org/10.1002/(SICI)1097-0258(19961230)15:24<2733::AID-SIM562>3.0.CO;2-0) (Dec. 30, 1996).
65. Zhu, A., Ibrahim, J. G. & Love, M. I. Heavy-Tailed Prior Distributions for Sequence Count Data: Removing the Noise and Preserving Large Differences. *Bioinformatics* **35** (ed Stegle, O.) 2084–2092. doi:[10.1093/bioinformatics/bty895](https://doi.org/10.1093/bioinformatics/bty895) (June 1, 2019).
66. Stephens, M. False Discovery Rates: A New Deal. *Biostatistics*, kxw041. doi:[10.1093/biostatistics/kxw041](https://doi.org/10.1093/biostatistics/kxw041) (Oct. 17, 2016).
67. Weiner 3rd, J. & Domaszewska, T. Tmod: An R Package for General and Multivariate Enrichment Analysis. doi:[10.7287/peerj.preprints.2420v1](https://doi.org/10.7287/peerj.preprints.2420v1) (2016).
68. Li, S. *et al.* Molecular Signatures of Antibody Responses Derived from a Systems Biology Study of Five Human Vaccines. *Nature Immunology* **15**, 195–204. doi:[10.1038/ni.2789](https://doi.org/10.1038/ni.2789) (Dec. 15, 2013).
69. Bin, L., Li, X., Feng, J., Richers, B. & Leung, D. Y. M. Ankyrin Repeat Domain 22 Mediates Host Defense Against Viral Infection Through STING Signaling Pathway. *The Journal of Immunology* **196**, 201.4 LP –201.4 (1 Supplement May 1, 2016).
70. Schneider, W. M., Chevillotte, M. D. & Rice, C. M. Interferon-Stimulated Genes: A Complex Web of Host Defenses. *Annual Review of Immunology* **32**, 513–545. doi:[10.1146/annurev-immunol-032713-120231](https://doi.org/10.1146/annurev-immunol-032713-120231) (Mar. 21, 2014).
71. Nakaya, H. I. *et al.* Systems Biology of Immunity to MF59-Adjuvanted versus Nonadjuvanted Trivalent Seasonal Influenza Vaccines in Early Childhood. *Proceedings of the National Academy of Sciences* **113**, 1853–1858. doi:[10.1073/pnas.1519690113](https://doi.org/10.1073/pnas.1519690113) (Feb. 16, 2016).
72. Murphy, K. & Weaver, C. *Janeway's Immunobiology* 9th edition. 904 pp. (Garland Science/Taylor & Francis Group, LLC, New York, NY, 2016).

APPENDIX A. BIBLIOGRAPHY

73. Nauta, J. J., Beyer, W. E. & Osterhaus, A. D. On the Relationship between Mean Antibody Level, Seroprotection and Clinical Protection from Influenza. *Biologicals* **37**, 216–221. doi:[10.1016/j.biologicals.2009.02.002](https://doi.org/10.1016/j.biologicals.2009.02.002) (Aug. 2009).
74. Linnik, J. E. & Egli, A. Impact of Host Genetic Polymorphisms on Vaccine Induced Antibody Response. *Human Vaccines & Immunotherapy* **12**, 907–915. doi:[10.1080/21645515.2015.1119345](https://doi.org/10.1080/21645515.2015.1119345) (Apr. 2, 2016).
75. Mentzer, A. J., O'Connor, D., Pollard, A. J. & Hill, A. V. S. Searching for the Human Genetic Factors Standing in the Way of Universally Effective Vaccines. *Philosophical Transactions of the Royal Society B: Biological Sciences* **370**, 20140341–20140341. doi:[10.1098/rstb.2014.0341](https://doi.org/10.1098/rstb.2014.0341) (May 11, 2015).
76. Dhakal, S. & Klein, S. L. Host Factors Impact Vaccine Efficacy: Implications for Seasonal and Universal Influenza Vaccine Programs. *Journal of Virology* **93** (ed Coyne, C. B.) doi:[10.1128/JVI.00797-19](https://doi.org/10.1128/JVI.00797-19) (Aug. 7, 2019).
77. Poland, G. A., Ovsyannikova, I. G. & Jacobson, R. M. Immunogenetics of Seasonal Influenza Vaccine Response. *Vaccine* **26**, D35–D40. doi:[10.1016/j.vaccine.2008.07.065](https://doi.org/10.1016/j.vaccine.2008.07.065) (Sept. 2008).
78. Franco, L. M. *et al.* Integrative Genomic Analysis of the Human Immune Response to Influenza Vaccination. *eLife* **2**, e00299. doi:[10.7554/eLife.00299](https://doi.org/10.7554/eLife.00299) (July 16, 2013).
79. Avnir, Y. *et al.* IGHV1-69 Polymorphism Modulates Anti-Influenza Antibody Repertoires, Correlates with IGHV Utilization Shifts and Varies by Ethnicity. *Scientific Reports* **6**, 20842. doi:[10.1038/srep20842](https://doi.org/10.1038/srep20842) (Aug. 16, 2016).
80. Moss, A. J. *et al.* Correlation between Human Leukocyte Antigen Class II Alleles and HAI Titers Detected Post-Influenza Vaccination. *PLoS ONE* **8** (ed Sambhara, S.) e71376. doi:[10.1371/journal.pone.0071376](https://doi.org/10.1371/journal.pone.0071376) (Aug. 9, 2013).
81. Albert, F. W. & Kruglyak, L. The Role of Regulatory Variation in Complex Traits and Disease. *Nature Reviews Genetics* **16**, 197–212. doi:[10.1038/nrg3891](https://doi.org/10.1038/nrg3891) (Apr. 2015).

APPENDIX A. BIBLIOGRAPHY

82. Vandiedonck, C. Genetic Association of Molecular Traits: A Help to Identify Causative Variants in Complex Diseases. *Clinical Genetics*. doi:[10.1111/cge.13187](https://doi.org/10.1111/cge.13187) (Dec. 1, 2017).
83. Kim-Hellmuth, S. *et al.* Cell Type Specific Genetic Regulation of Gene Expression across Human Tissues. *bioRxiv*. doi:[10.1101/806117](https://doi.org/10.1101/806117) (Oct. 17, 2019).
84. Brodin, P. *et al.* Variation in the Human Immune System Is Largely Driven by Non-Heritable Influences. *Cell* **160**, 37–47. doi:[10.1016/j.cell.2014.12.020](https://doi.org/10.1016/j.cell.2014.12.020) (Jan. 2015).
85. Maranville, J. C. *et al.* Interactions between Glucocorticoid Treatment and Cis-Regulatory Polymorphisms Contribute to Cellular Response Phenotypes. *PLoS Genetics* **7** (ed Gibson, G.) e1002162. doi:[10.1371/journal.pgen.1002162](https://doi.org/10.1371/journal.pgen.1002162) (July 7, 2011).
86. Ackermann, M., Sikora-Wohlfeld, W. & Beyer, A. Impact of Natural Genetic Variation on Gene Expression Dynamics. *PLoS Genetics* **9** (ed Wells, C. A.) e1003514. doi:[10.1371/journal.pgen.1003514](https://doi.org/10.1371/journal.pgen.1003514) (June 6, 2013).
87. Shpak, M. *et al.* An eQTL Analysis of the Human Glioblastoma Multiforme Genome. *Genomics* **103**, 252–263. doi:[10.1016/j.ygeno.2014.02.005](https://doi.org/10.1016/j.ygeno.2014.02.005) (Apr. 2014).
88. Allison, P. D. Change Scores as Dependent Variables in Regression Analysis. *Sociological Methodology* **20**, 93. doi:[10.2307/271083](https://doi.org/10.2307/271083) (1990).
89. Clifton, L. & Clifton, D. A. The Correlation between Baseline Score and Post-Intervention Score, and Its Implications for Statistical Analysis. *Trials* **20**. doi:[10.1186/s13063-018-3108-3](https://doi.org/10.1186/s13063-018-3108-3) (Dec. 2019).
90. Flutre, T., Wen, X., Pritchard, J. & Stephens, M. A Statistical Framework for Joint eQTL Analysis in Multiple Tissues. *PLOS Genet* **9**, e1003486. doi:[10.1371/journal.pgen.1003486](https://doi.org/10.1371/journal.pgen.1003486) (May 9, 2013).
91. Urbut, S. M., Wang, G., Carbonetto, P. & Stephens, M. Flexible Statistical Methods for Estimating and Testing Effects in Genomic Studies with Multiple Conditions. *Nature Genetics*. doi:[10.1038/s41588-018-0268-8](https://doi.org/10.1038/s41588-018-0268-8) (Nov. 26, 2018).

APPENDIX A. BIBLIOGRAPHY

92. Li, G., Jima, D., Wright, F. A. & Nobel, A. B. HT-eQTL: Integrative Expression Quantitative Trait Loci Analysis in a Large Number of Human Tissues. *BMC Bioinformatics* **19**. doi:[10.1186/s12859-018-2088-3](https://doi.org/10.1186/s12859-018-2088-3) (Dec. 2018).
93. Stephens, M. A Unified Framework for Association Analysis with Multiple Related Phenotypes. *PLoS ONE* **8** (ed Emmert-Streib, F.) e65245. doi:[10.1371/journal.pone.0065245](https://doi.org/10.1371/journal.pone.0065245) (July 5, 2013).
94. Kim, S. *et al.* Characterizing the Genetic Basis of Innate Immune Response in TLR4-Activated Human Monocytes. *Nature Communications* **5**. doi:[10.1038/ncomms6236](https://doi.org/10.1038/ncomms6236) (Dec. 2014).
95. Sul, J. H., Han, B., Ye, C., Choi, T. & Eskin, E. Effectively Identifying eQTLs from Multiple Tissues by Combining Mixed Model and Meta-Analytic Approaches. *PLoS Genetics* **9** (ed Schork, N. J.) e1003491. doi:[10.1371/journal.pgen.1003491](https://doi.org/10.1371/journal.pgen.1003491) (June 13, 2013).
96. Duong, D. *et al.* Applying Meta-Analysis to Genotype-Tissue Expression Data from Multiple Tissues to Identify eQTLs and Increase the Number of eGenes. *Bioinformatics* **33**, i67–i74. doi:[10.1093/bioinformatics/btx227](https://doi.org/10.1093/bioinformatics/btx227) (July 15, 2017).
97. Price, A. L., Zaitlen, N. A., Reich, D. & Patterson, N. New Approaches to Population Stratification in Genome-Wide Association Studies. *Nature Reviews Genetics* **11**, 459–463. doi:[10.1038/nrg2813](https://doi.org/10.1038/nrg2813) (July 2010).
98. Golan, D., Rosset, S. & Lin, D.-Y. in Borgan, Ø., Breslow, N. E., Chatterjee, N., Gail, M. H., Scott, A. & Wild, C. J. *Handbook of Statistical Methods for Case-Control Studies* (eds Borgan, Ø., Breslow, N., Chatterjee, N., Gail, M. H., Scott, A. & Wild, C. J.) 1st ed., 495–514 (Chapman and Hall/CRC, June 27, 2018). doi:[10.1201/9781315154084-27](https://doi.org/10.1201/9781315154084-27).
99. Astle, W. & Balding, D. J. Population Structure and Cryptic Relatedness in Genetic Association Studies. *Statistical Science* **24**, 451–471. doi:[10.1214/09-STS307](https://doi.org/10.1214/09-STS307) (Nov. 2009).
100. Listgarten, J., Lippert, C., Kadie, C. M., Davidson, R. I., Eskin, E. & Heckerman, D. Improved Linear Mixed Models for Genome-Wide

APPENDIX A. BIBLIOGRAPHY

- Association Studies. *Nature Methods* **9**, 525–526. doi:[10.1038/nmeth.2037](https://doi.org/10.1038/nmeth.2037) (June 2012).
101. Lippert, C., Listgarten, J., Liu, Y., Kadie, C. M., Davidson, R. I. & Heckerman, D. FaST Linear Mixed Models for Genome-Wide Association Studies. *Nature Methods* **8**, 833–835. doi:[10.1038/nmeth.1681](https://doi.org/10.1038/nmeth.1681) (Oct. 2011).
102. Speed, D., Hemani, G., Johnson, M. R. & Balding, D. J. Improved Heritability Estimation from Genome-Wide SNPs. *The American Journal of Human Genetics* **91**, 1011–1021. doi:[10.1016/j.ajhg.2012.10.010](https://doi.org/10.1016/j.ajhg.2012.10.010) (Dec. 2012).
103. Aguet, F. *et al.* The GTEx Consortium Atlas of Genetic Regulatory Effects across Human Tissues. *bioRxiv*. doi:[10.1101/787903](https://doi.org/10.1101/787903) (Oct. 3, 2019).
104. Beasley, T. M., Erickson, S. & Allison, D. B. Rank-Based Inverse Normal Transformations Are Increasingly Used, But Are They Merited? *Behavior Genetics* **39**, 580–595. doi:[10.1007/s10519-009-9281-0](https://doi.org/10.1007/s10519-009-9281-0) (Sept. 2009).
105. Võsa, U. *et al.* Unraveling the Polygenic Architecture of Complex Traits Using Blood eQTL Meta-Analysis. *bioRxiv*. doi:[10.1101/447367](https://doi.org/10.1101/447367) (Oct. 19, 2018).
106. Qi, T. *et al.* Identifying Gene Targets for Brain-Related Traits Using Transcriptomic and Methylocomic Data from Blood. *Nature Communications* **9**. doi:[10.1038/s41467-018-04558-1](https://doi.org/10.1038/s41467-018-04558-1) (Dec. 2018).
107. Brodin, P. & Davis, M. M. Human Immune System Variation. *Nature Reviews Immunology* **17**, 21–29. doi:[10.1038/nri.2016.125](https://doi.org/10.1038/nri.2016.125) (Jan. 2017).
108. Westra, H.-J. *et al.* Cell Specific eQTL Analysis without Sorting Cells. *PLOS Genetics* **11** (ed Pastinen, T.) e1005223. doi:[10.1371/journal.pgen.1005223](https://doi.org/10.1371/journal.pgen.1005223) (May 8, 2015).
109. Davenport, E. E. *et al.* Discovering in Vivo Cytokine-eQTL Interactions from a Lupus Clinical Trial. *Genome Biology* **19**. doi:[10.1186/s13059-018-1560-8](https://doi.org/10.1186/s13059-018-1560-8) (Dec. 2018).

APPENDIX A. BIBLIOGRAPHY

110. Aran, D., Hu, Z. & Butte, A. J. xCell: Digitally Portraying the Tissue Cellular Heterogeneity Landscape. *Genome Biology* **18**. doi:[10.1186/s13059-017-1349-1](https://doi.org/10.1186/s13059-017-1349-1) (Dec. 2017).
111. Kleiveland, C. R. in *The Impact of Food Bioactives on Health* (eds Verhoeckx, K. *et al.*) 161–167 (Springer International Publishing, Cham, 2015). doi:[10.1007/978-3-319-16104-4_15](https://doi.org/10.1007/978-3-319-16104-4_15).
112. Van der Wijst, M. G. P. *et al.* Single-Cell RNA Sequencing Identifies Celltype-Specific Cis-eQTLs and Co-Expression QTLs. *Nature Genetics* **50**, 493–497. doi:[10.1038/s41588-018-0089-9](https://doi.org/10.1038/s41588-018-0089-9) (Apr. 2018).
113. Kanyongo, G. Y. The Influence of Reliability on Four Rules for Determining the Number of Components to Retain. *Journal of Modern Applied Statistical Methods* **5**, 332–343. doi:[10.22237/jmasm/1162353960](https://doi.org/10.22237/jmasm/1162353960) (Nov. 1, 2005).
114. Astle, W. J. *et al.* The Allelic Landscape of Human Blood Cell Trait Variation and Links to Common Complex Disease. *Cell* **167**, 1415–1429.e19. doi:[10.1016/j.cell.2016.10.042](https://doi.org/10.1016/j.cell.2016.10.042) (Nov. 2016).
115. Stegle, O., Parts, L., Piipari, M., Winn, J. & Durbin, R. Using Probabilistic Estimation of Expression Residuals (PEER) to Obtain Increased Power and Interpretability of Gene Expression Analyses. *Nature protocols* **7**, 500–507. doi:[10.1038/nprot.2011.457](https://doi.org/10.1038/nprot.2011.457) (Feb. 16, 2012).
116. Lippert, C., Casale, F. P., Rakitsch, B. & Stegle, O. LIMIX: Genetic Analysis of Multiple Traits. doi:[10.1101/003905](https://doi.org/10.1101/003905) (May 22, 2014).
117. Gelman, A. & Stern, H. The Difference Between “Significant” and “Not Significant” Is Not Itself Statistically Significant. *The American Statistician* **60**, 328–331. doi:[10.1198/000313006X152649](https://doi.org/10.1198/000313006X152649) (Nov. 2006).
118. Clogg, C. C., Petkova, E. & Haritou, A. Statistical Methods for Comparing Regression Coefficients Between Models. *The American Journal of Sociology* **100**, 1261–1293 (1995).
119. Schenker, N. & Gentleman, J. F. On Judging the Significance of Differences by Examining the Overlap Between Confidence Intervals. *The American Statistician* **55**, 182–186 (2001).

APPENDIX A. BIBLIOGRAPHY

120. Kim-Hellmuth, S. *et al.* Genetic Regulatory Effects Modified by Immune Activation Contribute to Autoimmune Disease Associations. *Nature Communications* **8**. doi:[10.1038/s41467-017-00366-1](https://doi.org/10.1038/s41467-017-00366-1) (Dec. 2017).
121. Peters, J. E. *et al.* Insight into Genotype-Phenotype Associations through eQTL Mapping in Multiple Cell Types in Health and Immune-Mediated Disease. *PLOS Genetics* **12** (ed Plagnol, V.) e1005908. doi:[10.1371/journal.pgen.1005908](https://doi.org/10.1371/journal.pgen.1005908) (Mar. 25, 2016).
122. Kooperberg, C. & LeBlanc, M. Increasing the Power of Identifying Gene × Gene Interactions in Genome-Wide Association Studies. *Genetic Epidemiology* **32**, 255–263. doi:[10.1002/gepi.20300](https://doi.org/10.1002/gepi.20300) (Apr. 2008).
123. Zeng, B. *et al.* Comprehensive Multiple eQTL Detection and Its Application to GWAS Interpretation. *Genetics* **212**, 905–918. doi:[10.1534/genetics.119.302091](https://doi.org/10.1534/genetics.119.302091) (July 2019).
124. Dobbyn, A. *et al.* Landscape of Conditional eQTL in Dorsolateral Prefrontal Cortex and Co-Localization with Schizophrenia GWAS. *The American Journal of Human Genetics* **102**, 1169–1184. doi:[10.1016/j.ajhg.2018.04.011](https://doi.org/10.1016/j.ajhg.2018.04.011) (June 2018).
125. Mizuno, A. & Okada, Y. Biological Characterization of Expression Quantitative Trait Loci (eQTLs) Showing Tissue-Specific Opposite Directional Effects. *European Journal of Human Genetics* **27**, 1745–1756. doi:[10.1038/s41431-019-0468-4](https://doi.org/10.1038/s41431-019-0468-4) (Nov. 2019).
126. Fu, J. *et al.* Unraveling the Regulatory Mechanisms Underlying Tissue-Dependent Genetic Variation of Gene Expression. *PLoS Genetics* **8** (ed Gibson, G.) e1002431. doi:[10.1371/journal.pgen.1002431](https://doi.org/10.1371/journal.pgen.1002431) (Jan. 19, 2012).
127. Kumasaka, N., Knights, A. J. & Gaffney, D. J. Fine-Mapping Cellular QTLs with RASQUAL and ATAC-Seq. *Nature Genetics* **48**, 206–213. doi:[10.1038/ng.3467](https://doi.org/10.1038/ng.3467) (Feb. 2016).
128. Wu, L., Shen, C., Seed Ahmed, M., Östenson, C.-G. & Gu, H. F. Adenylate Cyclase 3: A New Target for Anti-Obesity Drug Development: ADCY3 and Anti-Obesity. *Obesity Reviews* **17**, 907–914. doi:[10.1111/obr.12430](https://doi.org/10.1111/obr.12430) (Sept. 2016).

APPENDIX A. BIBLIOGRAPHY

129. McGovern, D. P., Kugathasan, S. & Cho, J. H. Genetics of Inflammatory Bowel Diseases. *Gastroenterology* **149**, 1163–1176.e2. doi:[10.1053/j.gastro.2015.08.001](https://doi.org/10.1053/j.gastro.2015.08.001) (Oct. 2015).
130. Çalışkan, M., Baker, S. W., Gilad, Y. & Ober, C. Host Genetic Variation Influences Gene Expression Response to Rhinovirus Infection. *PLOS Genetics* **11** (ed Gibson, G.) e1005111. doi:[10.1371/journal.pgen.1005111](https://doi.org/10.1371/journal.pgen.1005111) (Apr. 13, 2015).
131. Manry, J. *et al.* Deciphering the Genetic Control of Gene Expression Following *Mycobacterium Leprae* Antigen Stimulation. *PLOS Genetics* **13** (ed Sirugo, G.) e1006952. doi:[10.1371/journal.pgen.1006952](https://doi.org/10.1371/journal.pgen.1006952) (Aug. 9, 2017).
132. Pai, A. A., Pritchard, J. K. & Gilad, Y. The Genetic and Mechanistic Basis for Variation in Gene Regulation. *PLoS Genetics* **11** (ed Lapalainen, T.) e1004857. doi:[10.1371/journal.pgen.1004857](https://doi.org/10.1371/journal.pgen.1004857) (Jan. 8, 2015).
133. Choudhury, M. & Ramsey, S. A. Identifying Cell Type-Specific Transcription Factors by Integrating ChIP-Seq and eQTL Data—Application to Monocyte Gene Regulation. *Gene Regulation and Systems Biology* **10**, GRSB.S40768. doi:[10.4137/GRSB.S40768](https://doi.org/10.4137/GRSB.S40768) (Jan. 2016).
134. Millstein, J., Zhang, B., Zhu, J. & Schadt, E. E. Disentangling Molecular Relationships with a Causal Inference Test. *BMC Genetics* **10**. doi:[10.1186/1471-2156-10-23](https://doi.org/10.1186/1471-2156-10-23) (Dec. 2009).

APPENDIX A. BIBLIOGRAPHY

List of Abbreviations

AC allele count

ASE allele-specific expression

BH Benjamini-Hochberg

BTM blood transcription module

CIT causal inference test

CPM counts per million

DC dendritic cell

DGE differential gene expression

eQTL expression quantitative trait locus

FACS fluorescence-activated cell sorting

FC fold change

FDR false discovery rate

GWAS genome-wide association study

HA haemagglutinin

HAI haemagglutination inhibition

HIRD Human Immune Response Dynamics

HLA human leukocyte antigen

INT inverse normal transformation

LAIIV live attenuated influenza vaccine

LD linkage disequilibrium

lfsr local false sign rate

LMM linear mixed model

LOCO leave-one-chromosome-out

LRT likelihood ratio test

MAF minor allele frequency

MANOVA multivariate analysis of variance

MN microneutralisation

NA neuraminidase

NK natural killer

PBMC peripheral blood mononuclear cell

PC principal component

PCA principal component analysis

PVE proportion of variance explained

REML restricted maximum likelihood

reQTL response expression quantitative trait locus

RNA-seq RNA-sequencing

SD standard deviation

TF transcription factor

TIV trivalent inactivated influenza vaccine

TMM trimmed mean of M-values

TRI titre response index

TSS transcription start site